

Assessing the technical and economic viability of implementing a fuel cell-battery system in a cable-laying vessel

F.J. Verbaan

The impact of adding a methanol-fuelled SOFC and batteries to the power plant of the NEXUS on the emissions, design and performance of the ship



Thesis for the degree of MSc in Marine Technology in the specialisation of Marine Engineering

by

F.J. Verbaan

Performed at:

Van Oord

This thesis MT.23/24.047.M. is classified as confidential in accordance with the general conditions for projects performed by the TUDelft

To be publicly defended on 18 September 2023, 14:00 hr

Company supervisors

Responsible supervisor: ing. M. Burg Van Oord
Email: marco.burg@vanoord.com

Thesis exam committee:

Chair/ Responsible professor: Dr. ir. P. de Vos TU Delft
Staff member: Ir. J. Gelling TU Delft
Staff member: Dr.ir. L. van Biert TU Delft
Company member: ing. M. Burg Van Oord

Author details:

Student number: 5084768
Contact email: floris_vb@hotmail.com
Institution: Delft University of Technology
Project duration: January, 2022 – September, 2023

An electronic version of this thesis is available at <http://repository.tudelft.nl/>.



Preface

As I complete my master's journey at Delft University of Technology and pass the helm of this pioneering work to the next innovator. This journey has transformed me from a maritime officer into a maritime engineer with an even stronger passion for the industry. This thesis is the result of what I've learned both at sea and at TU Delft.

It all began when I stood beside my grandfather, who was a sailor, watching ships come and go at the Scheveningen breakwater. Little did I know that this moment would eventually lead me to where I am today.

I'd like to thank the TU Delft. The education I received here not only expanded my knowledge but also encouraged me to think critically and creatively. I want to acknowledge my daily supervisor, Mr. Jaap Gelling, whose vision and guidance greatly helped shape this research.

I want to thank to Mr. Peter de Vos for guiding me and ensuring that this thesis meets academic standards.

I want thank Van Oord, the company that not only supported me throughout my thesis but also provided practical experience. Specifically, I owe a lot to Mr. Marco Burg for his guidance and mentorship. His insights and dedication played a significant role in shaping the research in this thesis.

Lastly, I want to express my gratitude to my family, friends, and girlfriend for their support and encouragement throughout this journey.

Floris Verbaan
Delft, September 2023

Abstract

The marine industry's environmental impact is significant. The IMO aims to cut shipping emissions by 50% by 2050. Van Oord, a major player in the marine industry, plans to achieve carbon neutrality by 2050. They aim for annual emission reductions of 2.5%, an 80% decrease in sulfur and nitrogen oxide emissions, and are exploring the integration of fuel cells for emission reduction and efficiency. Fuel cells emit fewer pollutants and offer higher efficiency, but their integration requires study. This master's thesis investigates the methanol-fuelled SOFC feasibility within the context of cable layer, examining the application through a concept design.

The primary research question for this study is as follows:

- **What is the impact of adding a methanol-fuelled SOFC and batteries to the power plant of the NEXUS on the emissions, design and performance of the ship**

The study demonstrates the technical feasibility of integrating methanol-fueled SOFC and batteries into the Nexus power plant for the medium term. This integration offers acceptable operational capabilities and a notable reduction in GHG emissions compared to the reference design. Even implementing batteries alone as a level of reserve source leads to significant GHG reduction in the short term. However, the short term implementation of SOFC technology is hindered by its current limitations in power density and availability, which are not yet competitive with alternative energy conversion methods.

Looking at the economic aspect, in the medium term, the potential for lower fuel costs makes the integration of methanol-fueled SOFC and batteries financially viable. Nonetheless, in the short term, the high capital expenditure costs pose a significant economic hurdle to implementation.

The study consists of two parts: a literature review and a case study. The literature review aims to determine the optimal approach for integrating various fuel cell types and hydrogen carriers, considering cable laying operations. Hydrogen fuel cells, especially SOFCs, hold promise due to their higher efficiency and added benefits like emissions reduction and adaptability in fuel. Cable laying vessels, with modest power requirements, are suited for fuel cell technology. After evaluating options, SOFCs are identified as the most suitable choice for medium-term integration. Methanol and ammonia serve as carriers of hydrogen, with methanol being favored due to its greater energy density, including advantages in terms of tank weight and packing efficiency.

In the second section of the report, the case study, the concept design phase evaluates the feasibility of integrating a methanol-fueled SOFC and batteries into the Nexus cable layer's power plant. The Nexus cable layer's power plant is diesel-electric, powered by four diesel engines for different operating modes. To reduce GHG emissions, the solution involves integrating SOFC technology. A 1926 kW SOFC is developed to meet power requirements for various modes except transit, which has high power demand. A battery pack 1195 kWw supports the SOFC, managing fluctuating loads and reducing the number of diesel engines from four to two. This integration significantly decreases fuel consumption and emissions. Methanol's use in the SOFC system affects several aspects, such as fuel storage, weight and space requirements. The optimal location for methanol storage is the aft section, achieved by converting existing MGO bunker tanks and reusing unused ballast tanks. Trade-offs in weight and volume are balanced against emission reduction and efficiency gains. Regulatory compliance and safety standards are followed in to the design. Integrating SOFC and battery systems yields economic and environmental advantages, targeting GHG reduction in cable laying operations. The SOFC and battery system configuration, although not surpassing diesel in fuel consumption, presents a promising opportunity for efficiency improvement due to improved efficiency and reduced engine count. Similar analysis of emissions from various fuels highlights substantial reductions in CO_{2e} emissions, particularly with grey methanol. Economically, while the initial CAPEX of the SOFC-battery system is a factor 3 higher, the potential for long-term benefits from reduced fuel costs and emissions positions it as a strategic investment for sustained economic viability. The OPEX analysis demonstrates the cost-effectiveness of the SOFC-battery system compared to regular MGO.

Contents

Preface	ii
Abstract	iii
Nomenclature	xi
1 Introduction	1
1.1 Background of problem	1
I Literature Study	2
2 Literature Review Approach	3
2.1 Objective and research questions	3
2.2 Structure of the literature review.	3
3 Fuel Cells	4
3.1 Type of fuel cells	4
3.1.1 Polymer electrolyte membrane fuel cell	4
3.1.2 Molten carbonate fuel cell.	5
3.1.3 Solid oxide fuel cells.	5
3.2 Basic operation of a solid oxide fuel cell	5
3.2.1 Materials	6
3.3 Technical specifications	7
3.3.1 Electrical Efficiency	7
3.3.2 Part load performance	9
3.3.3 Dynamic behaviour	9
3.3.4 Heat recovery & combined cycles	10
3.4 SOFCs in shipping	10
3.4.1 SOFC-ICE hybrid systems	19
4 Energy carriers	20
4.1 Hydrogen	21
4.2 Ammonia	21
4.3 Methanol	21
4.3.1 Production	22
4.3.2 Future availability.	24
4.3.3 Cost	25
5 Cable layer operation and profile	27
5.1 Cable lay operation.	27
5.2 Operational profile	28
5.3 Power and propulsion plant	29
6 Conclusion literature review	30
II Object of Study	31
7 Design Approach	32
7.1 Objectives and research questions	32
7.2 Structure of the research.	32
8 Reference Design	33
8.1 Design characteristics	33
8.1.1 Deck equipment.	34
8.1.2 Engine room	34
8.1.3 Tanks	35
8.2 Dynamic Positioning	36
8.2.1 DP class	36

8.3	Power- and Energy systems	37
8.3.1	Power-plant	37
8.3.2	Power distribution	38
8.3.3	Components efficiency	39
8.3.4	Propulsion plant	41
8.3.5	Power speed curve	42
8.3.6	Power estimation per operational mode	43
8.4	Conclusion	46
9	Performance indicators	47
9.1	Fuel consumption	47
9.2	Emission Indicator	48
9.3	Conclusion	49
III	Case Study	51
10	SOFC and battery module design	53
10.1	SOFC manufacturers	53
10.1.1	Bloomenergy	53
10.1.2	Mitsubishi Hitachi Power Systems	53
10.1.3	Convion Ltd.	54
10.1.4	FuelCell Energy	54
10.2	SOFC configuration	55
10.2.1	Factors Affecting SOFC Degradation	56
10.2.2	Balance of Plant	57
10.2.3	SOFC sizing	58
10.2.4	Dimensions & Weights of SOFC configuration	59
10.3	Batteries configuration	61
10.3.1	Factors Affecting Battery Degradation	61
10.3.2	Batteries sizing	62
10.3.3	Dimensions & Weights of Batteries configuration	65
10.4	Power plant design	66
10.5	Conclusion	69
11	Ship design and Arrangement	70
11.1	General storage considerations	70
11.2	Classification rules	70
11.3	Fuel storage options	71
11.3.1	Fore ship	71
11.3.2	Mid ship	72
11.3.3	Aft ship	73
11.4	Fuel cell and battery placement	75
11.4.1	Definition of Hazardous Zones	75
11.4.2	Fuel cell placement	75
11.4.3	Battery storage	76
11.5	Conclusion	76
12	Performance indicators	78
12.1	Fuel consumption	78
12.2	Emission indicator	79
12.3	Weight and Volume	81
12.4	Conclusion	82
13	Capital- and operating expenditures	84
13.1	CAPEX	84
13.2	OPEX	85
13.3	Conclusion	86

14 Conclusion	87
14.1 Discussion	90
A Performance (6L48/60CR)	92
B Diesel Engine Test Record	93
C CDF Code	95
D Ballast Tanks	98
E ATEX zones	99
F Roadmap Offshore Wind Energy	103
G Bunker Prices	104
H Projects	105
I Fuel Consumption	106
J DP System Requirements	107

List of Figures

3.1	Fuel cells connected in series to form a stack [90]	6
3.2	Schematic of solid oxide fuel cell	6
3.3	Simplified operational characteristics of an arbitrary fuel cell system [90]	8
3.4	Distribution of fuel cell technologies	11
3.5	Distribution of fuel for fuel cell technologies	11
4.1	Energy density and specific energy of fuels with and without the tank weight and volume [51].	20
4.2	Well-to-Tank and Tank-to-Wake [15]	23
4.3	Energy carriers/Current annual production levels compared to a estimated annual demand for 50,000 ships [58]	25
4.4	Fuel production cost estimates and assumptions [74].	26
5.1	Demonstration of the most influential parameters during a cable laying process [57].	27
5.2	Operational profile	29
8.1	Principal particulars Nexus [93].	33
8.2	Nexus schematic overview deck lay-out.	34
8.3	engine room lay-out	35
8.4	DE power- and propulsion plant	37
8.5	EFD of the Nexus	38
8.6	Single line power network	39
8.7	Efficiency propulsion plant [46]	40
8.8	Power train	40
8.9	The efficiency of the generator [6]	41
8.10	Redundancy Concept	41
8.11	Power speed curve	42
8.12	Hollandse Kust Noord Operational Profile	43
8.13	Operational mode for harbour mode	44
8.14	Operational profile for transit mode	44
8.15	Operational profile for transit mode	44
8.16	Operational profile for standby mode	45
8.17	Operational profile for standby mode	45
8.18	Operational profile for DP mode	45
8.19	Operational profile for DP mode	45
9.1	SFC (g/kWh)	47
9.2	FC (kg/h)	47
9.3	CO ₂ e Emissions by Operational mode	49
10.1	Efficiency of a SOFC	56
10.2	SOFC System configuration [38]	58
10.3	Dimensions SOFC configuration	60
10.4	Capacity loss as a function of charge and discharge bandwidth [89].	62
10.5	CDF Engine power	63
10.6	Battery Capacity Full Breakdown	64
10.7	Power plant concept	66
10.8	Power plant model depicting the integration of SOFC-battery modules.	68
11.1	Storage options	71
11.2	Fore ship	72
11.3	Mid ship	73
11.4	Aft ship	74
11.5	Container slots on the aft ship	75
12.1	SFC (g/kWh)	78

12.2 FC (kg/h)	78
12.3 SOFC vs Diesel	79
12.4 Fuel consumption by Operational Profile and Fuel Type	79
12.5 CO ₂ e Emmisions by Operational Mode and Fuel Type	80
12.6 Total CO ₂ e Emissions by Operational Mode and Fuel Type	81
12.7 Comparison Weight vs. Volume	82
G.1 Methanol prices [59]	104
G.2 MGO bunker price [81]	104
H.1 Greater Changhua Power Demand	105
H.2 Brossele 1 Power Demand	105
J.1 Summary of DP System requirements [71].	107

List of Tables

3.1	Characteristics of different fuel cell types [90].	4
3.2	Technical specification SOFC [12]	7
3.3	A summary of global research initiatives focused on implementing fuel cell systems in marine applications [90][25][24].	13
3.3	A summary of global research initiatives focused on implementing fuel cell systems in marine applications [90][25][24].	14
3.3	A summary of global research initiatives focused on implementing fuel cell systems in marine applications [90][25][24].	15
3.4	Overview of maritime applications powered by fuel cell systems [90][25][24].	16
3.4	Overview of maritime applications powered by fuel cell systems [90][25][24].	17
3.4	Overview of maritime applications powered by fuel cell systems [90][25][24].	18
5.1	Operational profile [35]	28
8.1	Principal dimensions Cable laying vessel Nexus	33
8.2	Diesel Generator Identification	35
8.3	Tank specifications	35
8.4	Type of energy and energy conversion (EFD)	38
8.5	Efficiency propulsion plant	41
8.6	Thruster identification	42
8.7	The mean power per generator and total power for each operational mode	46
9.1	Fuel consumption per operation mode	48
9.2	Overview of GWP100 and GWP20 factors as in IPCC AR6 [48]	48
9.3	WTW emission MGO	49
10.1	The Bloom Energy Server 5.5 [13]	53
10.2	The Bloom Energy Server 5.5 [13]	53
10.3	MEGAMI 200kW [104]	54
10.4	MEGAMI 200kW [104]	54
10.5	Convion C60 [72]	54
10.6	Convion Ltd. [72]	54
10.7	FuelCell Energy [30]	54
10.8	FuelCell Energy [30]	54
10.9	FuelCell Energy (CSA stack) [30]	55
10.10	FuelCell Energy (CSA stack) [30]	55
10.11	Literature assumptions for SOFC module	59
10.12	Dimensions reference fuel cell [28]	60
10.13	Weights reference fuel cell [28]	60
10.14	Specifications including auxiliary systems SOFC	61
10.15	Literature assumptions for NMC Lithium-Ion Batteries	65
10.16	Dimensions reference battery system	65
10.17	Weights reference battery system	65
10.18	Specifications including auxiliary systems	65
11.1	Advantages and disadvantages for storing methanol in fore ship	72
11.2	Advantages and disadvantages for storing methano mid ship	73
11.3	Advantages and disadvantages for storing methanol aft ship	74
12.1	TTW emission grey and bio methanol	80
13.1	Engine and storage system costs	84
13.2	CAPEX SOFC-batteries system	85
13.3	CAPEX conventional system	85
13.4	OPEX Conventional vs SOFC-batteries	85

H.1	Similar projects executed by the NEXUS	105
I.1	Calculation fuel consumption	106

Nomenclature

Abbreviations

AEL Alkaline Electrolysis

AC Alternating Current

APU Auxiliary Power Unit

BOP Balance of Plant

BAT Berg Azimuth Thruster

BC Black Carbon

BTT Bow Tunnel Thruster

CCS Carbon Capture and Storage

CDF Cumulative Distribution Function

CHP Combined Heat and Power

CO_{2e} Carbon Dioxide Equivalent

CSA Compact Solid Oxide Architecture

C-Rate Charge/Discharge Rate

DAC Direct Air Capture

DC Direct Current

DG Diesel Generator

DNV-G Det Norske Veritas Germanischer Lloyd

DP Dynamic Positioning

DPS Dynamic Positioning System

DSM Demand-Side Management

E-fuel Electro-fuel

EMS Energy Management System

FC-ICE Fuel Cell - Internal Combustion Engine

FMEA Failure Mode and Effects Analysis

GDC Gadolinium-Doped Ceria

GHG Greenhouse Gases

GWh Gigawatt-hour

GWP Global Warming Potential

HT-PEMFC High Temperature Polymer Electrolyte Membrane Fuel Cell

HVDC High Voltage Direct Current

ICE Internal Combustion Engine

Kw Kilowatt

KWh Kilowatt-hour

LNG Liquefied Natural Gas

LSMGO Low Sulphur Marine Gas Oil

LPG Liquefied Petroleum Gas

LT-PEMFC Low Temperature Polymer Electrolyte Membrane Fuel Cell

MCR Maximum Continuous Rating

MCFC Molten Carbonate Fuel Cell

MeOH Methanol

MGO Marine Gas Oil

MCFC Molten Carbonate Fuel Cell

MCR Maximum Continuous Rating

MWh Megawatt-hour

MW Megawatt

NEXUS The name of the cable layer vessel being designed

NMC Nickel Manganese Cobalt

NO_x Nitrogen Oxide

NR Bureau Veritas Naval Rules

ORR Oxygen Reduction Reaction

PMS Power Management System

PV Photovoltaic

PEMEL Polymer Electrolyte Membrane Electrolysis

PEMFC Polymer Electrolyte Membrane Fuel Cell

PEMFC Proton Exchange Membrane Fuel Cell

PSCC Point Source Carbon Capture

PV Photovoltaic

Qlik Qlik Sense

REDOX Reduction-Oxidation

SAT Stern Azimuth Thruster

SDC Samarium-Doped Ceria

SFC Specific Fuel Consumption

SOEL Solid Oxide Electrolysis

SOFC Solid Oxide Fuel Cell

SRP Schottel Rudder Propeller

TPB Triple Phase Boundary

TRL Technology Readiness Level

TTW Tank-to-Wake

WTT Well-to-Tank

WTW Well-to-Wake

Wh Watt-hour

Molucular formula

CH_3OH Methanol

CH_4 Methane

CO Carbon Monoxide

CO_2 Carbon Dioxide

H_2 Hydrogen

H_2O Water

N_2 Nitrogen

NH_3 Ammonia

Introduction

The marine industry has a significant impact on the environment, particularly in terms of energy consumption and greenhouse gas (GHG) emissions [10]. With the offshore sector, including the growing wind farm industry, moving farther offshore and expanding in size, the environmental impact of the marine industry is expected to increase [45]. To address this issue, the International Maritime Organization (IMO) has established the initial strategy to reduce GHG emissions from shipping. This strategy aims to cut annual GHG emissions from international shipping by at least 50% by 2050, compared to their level in 2008, with the ultimate goal of phasing out GHG emissions entirely as soon as possible in this century. The IMO also aims to reduce the carbon intensity of international shipping, compared to the levels from 2008, by at least 40%. [9].

Van Oord, a global player in dredging, marine engineering, and offshore projects, has set an ambitious goal of achieving carbon neutrality across all three scopes of emissions (1, 2, and 3) by 2050. This means that company aims to reduce or offset the direct and indirect emissions from operations, purchased energy, and supply chain activities. To meet this goal, the company plans to reduce carbon emissions by 2.5% each year, which aligns with the Paris Agreement and the scientific consensus on the necessary levels to limit global warming to below two degrees. In addition to company carbon neutrality goal, Van Oord is dedicated to reducing sulfur oxide (SO_x) and nitrogen oxide (NO_x) emissions by at least 80% compared to the 2019 level by 2050 [65]. Furthermore, Van Oord has expressed a strong interest in exploring the use of fuel cells in their operations to reduce emissions and improve efficiency. Van Oord is actively researching the potential benefits and challenges of integrating fuel cells into it's fleet, including the use of methanol for powering ships and providing electricity on offshore projects.

1.1 Background of problem

The adoption of alternative fuels in the shipping industry is of great importance in meeting emissions reduction targets. The use of fuel cells, which generate electricity through a chemical reaction rather than combustion, offers a promising alternative to traditional fossil fuel engines. Fuel cells emit significantly lower levels of GHG and pollutants, while also offering higher efficiency and lower maintenance requirements. However, the integration of fuel cells into the propulsion systems of vessels presents certain challenges, including cost, durability, and reliability.

Van Oord, has expressed interest in the feasibility of integrating fuel cells into the propulsion systems of their cable layer vessels. Despite having information about reducing fuel consumption within Van Oord's fleet, the company's knowledge regarding fuel cells remains limited. Therefore, a thorough techno-economical feasibility study would be essential to assess the viability of integrating these aspects. This study would involve assessing the suitability of different types of fuel cells, as well as the infrastructure required to support their use, including renewable fuel storage and refueling facilities. In addition to fuel cells, Van Oord is interested in exploring alternative fuels, in particular methanol for fuel cells.



Literature Study

Literature Review Approach

The initial phase of this master's thesis involves conducting a literature review.

2.1 Objective and research questions

The objective of the literature review is to gather information, to conclude for which fuel cell and energy carrier the use of fuel cells could have an added value for a cable layer.

The main research question of the literature review of this master thesis is:

What combination of fuel cell and energy carrier is the most suitable for the implementation of a fuel cell into a power plant of a cable layer.

To be able to answer the general main question, the following sub questions will be investigated and answered in the upcoming chapters.

- What are fuel cells, their different types, and what is the current status of their usage in maritime applications along with the underlying reasons?
- What are the different types of energy carriers and what is their technology readiness for usage in maritime applications?
- What are the operations and operational profile of a cable layer?.

2.2 Structure of the literature review

The literature review aims to gather adequate information from academic sources to provide a comprehensive description of existing research and to formulate specific and solvable research questions. The literature review methodology involves analyzing each topic separately before combining them. This research covers three theoretical topics: fuel cells, energy carries and cable layers.

The first part of chapter 3 provides a theoretical explanation of fuel cells, including their working principle, various types, and required components. The second part provides previous projects that have utilized fuel cells in a maritime environment, including an analysis of the state of development.

In chapter 4 the focus is on the discussion of different energy carriers, with a particular emphasis on energy density, production, future availability and cost.

In chapter 5 the vessel operations and profile are explained.

Finally in chapter 6 the conclusion and gaps in literature are identified and proposes a revised main question for further investigation. This chapter will serve as a critical reflection on the literature presented and will provide a foundation for the subsequent stages of the research.

Fuel Cells

A fuel cell directly convert chemical energy into electrical energy, bypassing the intermediate step of converting it into thermal energy through combustion in engines, however a large proportion of ships today rely on diesel generators to generate electricity, namely by converting chemical energy into electricity through both thermal and mechanical energy. Using fuel cells has three main advantages. The first advantage is that fuel cells eliminate the need for high-temperature combustion, resulting in a reduction in the formation of NO_x , but also noise, and vibrations. But at the same time, high efficiencies can still be maintained [82]. Then, the second advantage is that fuel cells are similar to batteries in their modular structure, but then with the ability to stack multiple single cells. With a single cell having the same performance as a larger stack, because of the ability to stack multiple single cells [97]. This allows for power production to be distributed across a ship without sacrificing fuel efficiency, reducing electricity transport losses and increasing redundancy. And the last advantage is that fuel cells have excellent part-load characteristics as increased mechanical losses only affect the parasitic load of auxiliary components such as compressors, while electrochemical losses are reduced [70].

3.1 Type of fuel cells

A diverse range of fuel cells with unique features has been developed. This review will examine the low and high temperature polymer electrolyte membrane fuel cell (LT/HT-PEMFC), the molten carbonate fuel cell (MCFC), and the solid oxide fuel cell (SOFC). A brief introduction to each type of fuel cell is provided. Key characteristics are summarized in Table 3.1 [90].

Table 3.1: Characteristics of different fuel cell types [90].

Fuel cell type	Operating temperature [C]	Power [kW]	Efficiency [%]	Internal reforming
LT-PEMFC	65-85	0.01-250	40-55	No
HT-PEMFC	140-200	0.1-250	40-55	No
MCFC	650-700	200-100,000	50-60	Yes
SOFC	500-1000	0.5-2000	40-72	Yes

3.1.1 Polymer electrolyte membrane fuel cell

Reasons for using the PEMFC are that it is considered to be one of the most efficient low-temperature fuel cells, with a gross efficiency of up to 55% (converting 55% the chemical energy of the fuel into usable electrical energy) [95]. Efficiency is important, when fuel cells are added, the efficiency of a stack changes in comparison of the optimal efficiency of a single stack. which is more extensive explained in section 3.3.1. Another reason for using this type of cell is that the fuel cells are compact and perform well in dynamic conditions, which makes them a promising option for transportation. However the PEMFC has a significant drawback, which is its limited fuel flexibility. It can only operate using hydrogen, and in order to use other fuels, they must first be converted to hydrogen. Additionally, the PEMFC catalyst is highly susceptible to pollution, requiring the use of high-purity hydrogen. Furthermore, storing large quantities of pure hydrogen for long-distance operations poses a significant challenge [90]. Estimated that for voyage times exceeding 100 hours, the use of PEMFCs for ship propulsion becomes difficult due to their requirement for pure hydrogen. The use of different catalysts is possible in high-temperature fuel cells due to the higher operating temperature. In these conditions, CO_2 and CO molecules are no longer harmful, and CO can even serve as a viable fuel source.

3.1.2 Molten carbonate fuel cell

MCFC is a high temperature fuel cell that uses a molten mixture of lithium, sodium, and potassium carbonates as an electrolyte to produce electricity through an electrochemical reaction. The operating temperature of an MCFC is typically around 650-700°C. This high temperature allows for a high level of efficiency in the internal reforming of fuels, where the fuel is converted into a hydrogen-rich stream before being supplied to the cell. The power output of MCFCs depends on their size and design, but typically ranges from a few kilowatts to ten thousand of kilowatts. The efficiency of an MCFC is typically around 50-60% [44]. This is lower than other types of fuel cells, such as PEMFCs, but the high operating temperature of MCFCs allows for highly efficient internal reforming, which can increase the overall efficiency of the system. Internal reforming is the process by which the fuel (usually natural gas or biogas) is converted into a hydrogen-rich stream before being supplied to the cell. This stream contains a high concentration of hydrogen, which allows for efficient and effective operation of the fuel cell. The use of MCFCs in the maritime industry is still in the experimental phase and there are not many operational examples. However, MCFCs have the potential to offer several benefits for maritime applications, such as high energy density, quiet and vibration-free operation, and low emissions. MCFCs can also operate using a variety of fuels, including renewable fuels such as biofuels and hydrogen. In conclusion, while MCFCs have the potential to offer benefits for maritime applications, they are not yet a proven technology and have limitations that must be considered. Further research and development is needed before MCFCs can be widely adopted in the maritime industry [60].

3.1.3 Solid oxide fuel cells

In recent years, there has been an increase in research on SOFCs due to their high efficiency, ultra-low emissions, and silent operation [90]. SOFCs are high temperature fuel cells and are highly fuel flexible, accommodating various gases and liquids, such as methane, ethanol, methanol, propane, LPG, diesel, MGO, ammonia, and more [53]. They demonstrate high efficiency, availability, reliability, and durability, achieving electrical efficiency of about 60% and with combined heat and power (CHP) system efficiency up to 85-90% [34]. SOFC-GE (General Electric) hybrid systems can even reach electrical efficiencies as high as 70% [16]. While lifetime remains a consideration for SOFCs, a 40,000-hour system duration is a reasonable objective, and continuous 10-year operation has been recorded [88]. As a result, SOFCs are the most promising fuel cell technology for medium to long distance shipping applications. The advantage of the SOFC is its flexibility in fuel, which is particularly important given that future fuels are not yet known and are likely to be diverse. Although SOFC can hardly bear different loads due to slow start-up and load shifting. As such, they are typically built within a hybrid system that includes other components, such as engines, PEMFCs, and batteries, to address the dynamic energy demand. Due to the considerable potential offered by SOFC, it will be further elaborated on in the next section.

3.2 Basic operation of a solid oxide fuel cell

The SOFC operates at a high temperature range between 800°C and 1000°C, utilizing a REDOX reaction process. A REDOX reaction is a chemical reaction where electrons are transferred between atoms, causing changes in their oxidation state. This can result in substances losing or gaining electrons, which is called oxidation and reduction, respectively. These reactions play a crucial role in various chemical processes, including energy production, corrosion, and biological processes like respiration and photosynthesis. In SOFCs oxygen ions are responsible for conducting electricity. The oxygen ions are reduced at the cathode, which means they gain electrons, and then become ionized. This ionization process allows the oxygen ions to move through the SOFC towards the anode, where they react with a fuel source, such as hydrogen, to produce water and electricity.[27][102][63][79][62]. Oxygen is reduced into oxygen ions at the porous cathode and then carried to the anode through the solid electrolyte. At the anode, oxygen ions combine with hydrogen to produce water and CO₂ as can be seen in Figure 3.2. Due to the high operating temperature, SOFC components require hard and rigid materials, and must exhibit chemical and thermal stability for efficient operation over the long term. The SOFC is typically made up of many individual cells connected in series or parallel to form a stack, and other sub-units are used to support the power plant, such as a fuel processing unit, an oxygen supply unit, a DC to AC conversion unit, and a temperature control and safety unit. The anode, cathode, and electrolyte used in SOFCs are all solid, and during operation, a basic fuel cell can produce an open circuit voltage slightly above 1 V, decreasing to 0.5-0.7 V when a load is connected. To achieve higher

current and voltage output, many cells are connected together in series or parallel as can be seen in Figure 3.1. The design and fabrication of SOFCs take into account both economic and technical considerations, with a focus on cost reduction and fabrication efficiency.

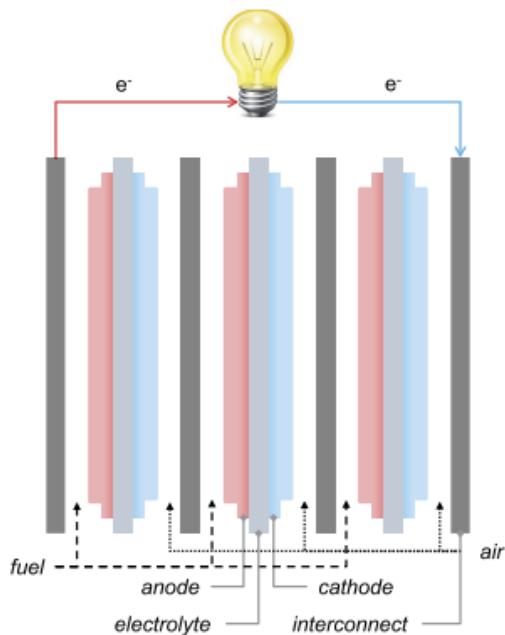


Figure 3.1: Fuel cells connected in series to form a stack [90]

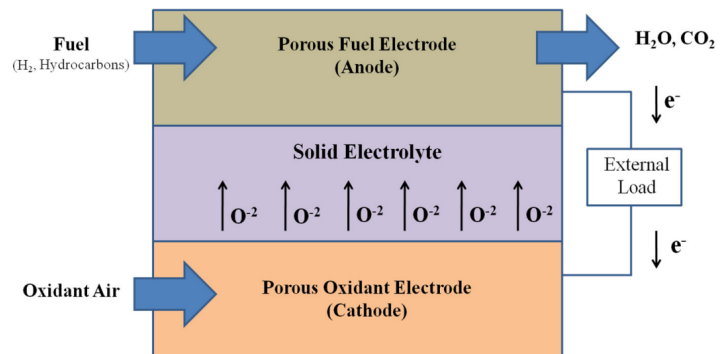


Figure 3.2: Schematic of solid oxide fuel cell

3.2.1 Materials

The materials used in SOFCs are critical for their performance and durability. According to a study by Orhan [68] and Yurum [14], materials such as ceramic electrolytes, anode catalysts, and cathode materials play key roles in the operation of SOFCs. Other materials, such as interconnects and seals, are also important for the overall performance and reliability of SOFCs.

According to a study by Cheng et al., the cathode in a SOFC is typically made of a mixed ionic-electronic conducting material, such as lanthanum strontium manganite (LSM), that facilitates the oxygen reduction reaction (ORR) [17]. The ORR occurs at the triple phase boundary (TPB) between the cathode, the electrolyte, and the gas phase. At the TPB, oxygen molecules from the air are dissociated and reduced by electrons from the cathode material, resulting in the formation of oxide ions [17]. Also note that the performance of the cathode is crucial for the overall performance of the SOFC. As such, research efforts have focused on improving the cathode properties, such as the TPB density, the catalytic activity, and the thermal stability, to enhance the cell performance, reduce the operating temperature, and increase the durability.

The electrolyte is a critical component that plays an important role in its performance, especially in conjunction with the cathode. As mentioned earlier, the cathode and electrolyte work together to enable the ORR at the TPB where oxygen molecules from the air are dissociated and reduced by electrons from the cathode material. The oxide ions generated at the TPB then migrate through the electrolyte to the anode, where they react with the fuel to produce water and electricity [80]. The electrolyte must have high ionic conductivity and be stable at the high operating temperatures of SOFCs. Ceramic materials such as Yttria-stabilized zirconia (YSZ), gadolinium-doped ceria (GDC), and samarium-doped ceria (SDC) are commonly used as electrolytes in SOFCs. According to a study by Bae et al. (2019) [7], recent research has focused on improving the properties of electrolytes to enhance the performance and durability of SOFCs. For example, research efforts have aimed to improve the TPB density, reduce the electrolyte thickness, and optimize the microstructure and interface properties of the electrolyte-cathode interface to enhance the ORR.

The anode is the last critical component of a SOFC that plays an role in the overall cell performance. The anode serves as the site for the oxidation reaction, where fuel is oxidized to produce electrons and protons. The electrons are then conducted through an external circuit to generate electricity, while the protons migrate through the electrolyte to the cathode, where they react with oxygen to produce water. The anode is typically made of a porous nickel-YSZ cermet (ceramic-metal composite) material that provides both electronic and ionic conductivity. The nickel component of the anode catalyzes the oxidation reaction, while the YSZ component conducts the oxygen ions to the cathode. However, nickel can be prone to oxidation and degradation under the high-temperature operating conditions of SOFCs. Therefore, recent research efforts have focused on developing alternative anode materials, such as ceria-based materials, that are more resistant to oxidation and provide better catalytic activity. Recent research has also focused on optimizing the microstructure and properties of anodes to enhance the cell performance and durability [98]. For example, research efforts have aimed to improve the anode-electrolyte interface to reduce the polarization losses and to develop new fabrication methods to reduce the manufacturing cost and improve the reliability of SOFCs.

3.3 Technical specifications

The technical specifications of SOFCs are crucial to understanding their performance and potential applications. These specifications include parameters such as operating temperature, cell voltage, power density, and fuel utilization efficiency.

Table 3.2: Technical specification SOFC [12]

Technical Specification	SOFC
Operating Temperature [°C]	500–1000
Electrical Efficiency [%LHV]	50–65
Hydrogen Purity	>99.98% H ₂ <3% CO <20 ppm S
Cooling Medium	Air
Specific Power [W/kg]	20–80
Power Density [W/L]	10–40
Stack Lifetime [kh]	20–90
Start-up Time (cold)	>30 minutes
Load Transients [idle-rated]	<60 minutes
Capital Cost 2021 [\$/kW]	3500–8000
Capital Cost 2030 [\$/kW]	500–2000

3.3.1 Electrical Efficiency

According to Lutz et al. (2002) [55], fuel cells have the potential to achieve the same optimal efficiencies as an ideal heat cycle. In practical applications, however, efficiencies may exceed this theoretical limit due to variations in operational principles. The efficiency of a fuel cell is influenced primarily by three parameters: operating voltage, fuel utilization, and balance of plant (BoP) losses [21]. The theoretical efficiency achievable by an electrochemical process is determined by the Gibbs energy, which characterizes the non-expansion work obtainable shown in Equation 3.1:

$$\eta_{rev} = \frac{\Delta\bar{g}_f}{\Delta\bar{h}_f} \quad (3.1)$$

Where $\Delta\bar{g}_f$ is the change in Gibbs free energy of formation during the reactions and $\Delta\bar{h}_f$ is the change in enthalpy of formation.

However, practical efficiency is lower due to various losses. Operating voltage is typically lower than the reversible voltage due to internal losses and irreversibilities. Fuel conversion or utilization is usually less than 100% to prevent fuel starvation and remove inert components and contaminants from the anode compartment. Auxiliary components such as blowers and pumps consume significant power, and power conditioning equipment, such as inverters, introduces additional losses.

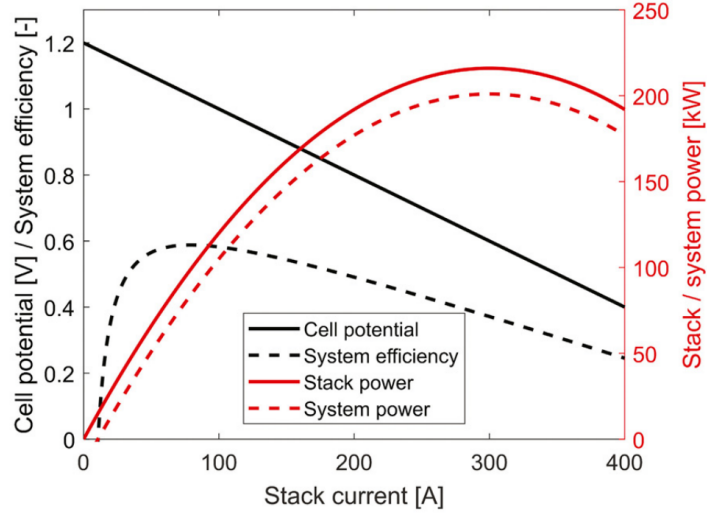


Figure 3.3: Simplified operational characteristics of an arbitrary fuel cell system [90]

Figure 3.3 shows a simplified load curve of a fuel cell system, where the open circuit voltage (OCV) is the voltage when there is no load. The actual operating voltage decreases as the current density increases due to several internal losses, including activation losses, ohmic losses, and concentration losses. Activation losses arise from the polarization potential needed to drive the electrochemical reaction. Ohmic losses result from the resistance of electrodes and electrolyte, and concentration losses occur due to mass transfer limitations at high current densities. After considering these losses, a voltage efficiency can be defined as the ratio of the fuel cell voltage to the reversible voltage as shown in Equation 3.2:

$$\eta_{voltage} = \frac{V_{cell}}{E^0} \quad (3.2)$$

With the theoretical reversible fuel cell potential E^0 which is calculated from Equation 3.3 and V_{cell} is the operating voltage.

$$E^0 = \frac{\Delta \bar{g}_f}{nF} \quad (3.3)$$

Where n is the number of electrons involved in the electrochemical reaction (2 for hydrogen) and F is the Faraday constant.

However, due to the variation in temperature and concentrations of reactants and products from inlet to outlet, the actual electrochemical process is a diverse reaction involving a variety of intermediate steps contributing to voltage losses simultaneously at various reaction sites. Different processes may dominate at different locations within the cell. There are three main losses. Ohmic losses depend on the electrode and electrolyte thicknesses, while activation losses are influenced by the catalyst surface and temperature. Concentration losses generally dominate in areas with high local reaction rates, resulting in varying current density locally. Therefore, detailed spatial models are necessary to accurately capture the individual contributions of different voltage losses. However, the behavior of the fuel cell in specific parts of the operating window may be treated linearly, and the characteristics may mimic ohmic behavior, which can be approximated using an area-specific resistance (ASR) equation [18] shown in Equation 3.4.

$$V_{cell} = V_{OCV} - 1 \cdot ASR \quad (3.4)$$

With V_{cell} for the operating voltage, V_{OCV} for Open Circuit Voltage and ASR for Area Specific Resistance.

The ASR accounts for all the internal losses in the cells and stacks, which must be determined in experiments for various conditions of interest. The ASR will change with operational conditions. In practice, fuel utilization is often less than 100% even though it is possible to fully consume all of the fuel in theory. One of the reasons for this is that contaminants, reaction products, and inert gases accumulate in the anode compartment unless part of the fuel is purged. The fraction of fuel that is effectively oxidized in a fuel cell is referred to as fuel utilization, denoted as u_f . The stack efficiency can be calculated subsequently from Equation 3.5:

$$\eta_{stack} = \eta_{rev} \cdot \eta_{voltage} \cdot u_f \quad (3.5)$$

To achieve high electrical efficiencies, maximizing fuel utilization is important. However, excessive steam concentrations can lead to reduced reversible voltage and electrode oxidation at the fuel electrode. In the case of impure hydrogen fuel, like methanol, anode off-gas purging is necessary to remove accumulated products from the reforming reaction. Additionally, supplying excess fuel and air, particularly in the outlet section, can create more uniform conditions across cells and stacks, even when using pure hydrogen [101]. The overall efficiency of a fuel cell system depends on accounting for the parasitic consumption of BoP components, such as air compressors and electrically operated actuators, represented by P_{aux} . This results in the following Equation 3.6:

$$\eta_{system} = \frac{P_{stack} - P_{aux}}{P_{stack}} \cdot \eta_{stack} \quad (3.6)$$

Where η_{stack} is the stack efficiency, P_{stack} Power stack and P_{aux} BoP components.

The extent of the auxiliary losses varies depending on the fuel cell type and BoP components, with fuel reformers contributing significantly to low-temperature fuel cell systems and air compressors being a large consumer in SOFC systems.

3.3.2 Part load performance

Fuel cells operate efficiently at part load since electrochemical losses decrease described in subsection 3.3.1 as current is reduced, improving stack efficiency. However, as load decreases, BoP losses contribute a higher proportion to the overall efficiency, resulting in lower efficiency at small loads. Figure 3.3 illustrates a typical fuel cell system load curve, where BoP consumption nullifies stack efficiency just below 50% load. As load decreases further, system efficiency drops quickly. At low loads, fuel cells are more challenging to condition correctly, requiring minimal fuel and air flows to prevent starvation. Fuel starvation happens in fuel cells when there isn't enough fuel to keep the chemical reactions going. This can cause problems like the potential rising too high and the catalyst breaking down faster [73]. Fuel cell manufacturers specify minimum load fractions to ensure reliable operation and longer lifespan, which range from 10% to 30% of rated nominal power. This must be taken into account by when designing fuel cell systems [90].

3.3.3 Dynamic behaviour

The ability to handle dynamic loads and start/stop cycling is important for a power management system (PMS), but less critical for cable layer where a part of the power plant operates uninterrupted. Electrochemical reactions in the SOFC can respond almost instantly to changes in load, but the inertia of heat, mass, and momentum in the stack and BoP components limits the actual load response [11]. Adjusting the supply of fuel, air, and coolant to the stack is necessary to accommodate changes in power, which is done using pumps and blowers. However, their response times and inertia lead to time delays before stable flow values are reached, which affects heat and mass transfer in the heat exchangers, reformers, and humidifiers, thus adding to the delayed response time of the BoP. The presence of thermal, mass, and momentum inertia can result in significant time delays when transitioning to a new stable operating

point, especially when using simple feedback control to adjust auxiliary equipment set points. This delay creates a substantial risk of exceeding acceptable limits on the stack operating conditions during load transients, including fuel starvation, overheating, or thermal stresses. To prevent such detrimental operating conditions, load transient limitations are typically specified by the system manufacturer. Low-temperature PEMFCs are constrained by the time it takes to supply reactants to the stack, allowing load transients to be performed in a couple of seconds [43]. However, high-temperature PEMFCs with reformers may take several minutes to reach a new stable operating point due to the increased thermal inertia in the BoP and fuel conversion equipment [29]. SOFC systems used in stationary power generation can take several minutes to adjust to even small load transients due to the high operating temperature and large thermal inertia of the cooling medium [18]. Slow load transients are needed for feedback controllers to react, but better a PMS can enhance transient capabilities [100]. Similar to load transients, low-temperature fuel cells have a fast start-up time compared to their high-temperature counterparts, with LT-PEMFCs able to deliver useful work already at ambient conditions. In contrast, SOFCs require a large thermal mass to be heated to relatively high temperatures before any current can be drawn, resulting in a start-up time of several hours for large stationary SOFC plants. Shut-down procedures can be complicated at a system level, but load removal is usually not restricted at the stack level and can be achieved in seconds if needed.

3.3.4 Heat recovery & combined cycles

High-temperature SOFCs can achieve high efficiencies in combined heat and power (CHP) applications. These systems recover heat generated during the electrochemical reaction to provide heat, similar to waste heat recovery in diesel engines [34]. Trigeneration systems, which combine power, heating, and cooling, can further optimize integration by utilizing additional cooling cycles. CHP is useful for ships with large heating, ventilation, and air conditioning needs, while waste heat recovery and combined cycles offer higher electrical efficiencies for ships focused on power generation. SOFC integration with gas turbines or ICE enables effective use of high-temperature heat to generate additional useful work. The unconverted fuel from the SOFC can be used in a reciprocating combustion engine, allowing for the adoption of conventional marine engine technology. Additionally, the off-gas from the SOFC can be utilized to improve combustion properties by enriching the fresh fuel, providing flexibility in selecting the appropriate fuel cell and engine powers [76]. Alternatively, conventional waste heat recovery power generation systems can be used, but with low specific power and high specific cost. Researchers have proposed using unconverted fuel from fuel cells in a reciprocating combustion engine, which allows for conventional marine engine technology to be adopted.

3.4 SOFCs in shipping

Over the past 23 years, there has been a significant increase in the number of fuel cell projects for maritime applications. To the authors knowledge, over 30 funded projects investigating various fuel cell solutions have been developed since 2000, with power ranges between 25 kW and 3 MW and utilizing technologies such as PEMFC, SOFC, and MCFC. PEMFC is the most tested technology, and hydrogen is the most commonly used fuel due to the sensitivity of PEMFCs to impurities. However, three projects have combined PEMFC with diesel and methanol, utilizing reforming technology to avoid limitations related to hydrogen storage. There are six projects based on SOFC that use LNG, diesel, methanol, and ammonia as logistics fuels, taking advantage of the high fuel flexibility of SOFC technology.

The findings from fuel cell research projects and their usage in ships were gathered from Table 3.3 and Table 3.4, and analyzed to create Figure 3.4 and Figure 3.5. The tables were generated through a review of existing literature on fuel cell research projects and fuels for fuel cells in ships. Relevant studies were identified through a search of academic databases and other reputable sources. The findings were then analyzed and synthesized to create the tables and figures presented in the study. Figure 3.4 displays the integration of PEMFC type into a hybrid system with batteries, with yachts and research vessels being used as case studies for the fuel cell system 5 and 6 times, respectively. Cruise ships and offshore support vessels have potential to be powered by fuel cell technology, whereas tug and dredgers are the less common types of ships that have implemented fuel cell systems based on past and present research projects.

In order to facilitate the transition towards zero-emission shipping, it is crucial to promote the use of

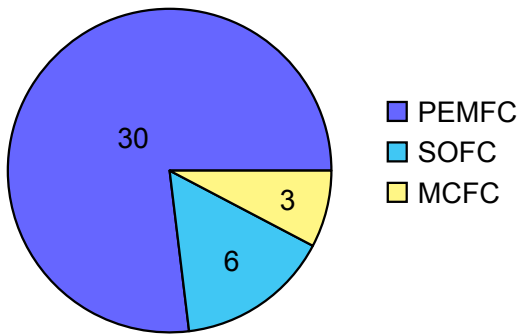


Figure 3.4: Distribution of fuel cell technologies

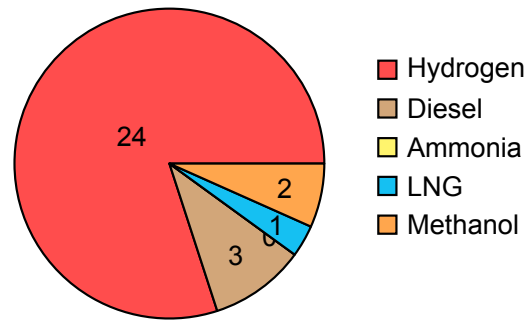


Figure 3.5: Distribution of fuel for fuel cell technologies

Fuel Cell Systems (FCS) on ships, particularly with regards to hydrogen fuel. For a potential cable layer ship, the development of FCS should take into account various factors including power capacity, size, safety, costs, durability, and reliability. While the power capacity of FCS is currently limited to tens of kW to a few MW, applications can be extended to the offshore industry through the integration of batteries as an energy storage source or with FC-ICE in hybrid propulsion systems. To increase output power, optimizing the power distribution of a hybrid system based on fuel cells and FC-ICE is recommended, while for hybrid systems based on fuel cell and batteries, optimizing the energy management system is a key consideration [78].

One important factor that will determine the future for maritime applications is its power density, taking into account both volume and weight considerations. To facilitate the commercialization of fuel cells for ships, size standardization will need to be developed. Projects such as STASHH (Standard Sized fuel cell module for Heavy Duty applications) have been launched to address this issue. STASHH aims to develop an open size standard for fuel cell modules that can be integrated into maritime applications. The project involves eight fuel cell suppliers, who are working together to develop standardized sizes for fuel cell modules and bring down their costs.

With the development of standardized sizes for fuel cell modules, the safety assessment of fuel cell power systems is crucial for their application in maritime transport, and it is largely impacted by the fuel stored onboard rather than the fuel cell system itself. While there are already regulations in place for using gases or low flash point fuels onboard ships, such as the IGF code. The IGF Code refers to the International Code of Safety for Ships using Gases or other Low-flashpoint Fuels. The integration of fuel cell systems onboard still has shortcomings. Therefore, it is necessary to include fuel cell systems in international maritime regulations and rules from a safety perspective to ensure their safe use in the maritime sector. Although the demonstration of fuel cell systems onboard ships started 25 years ago, the high capital and operating costs remain major obstacles to their widespread use in the shipping industry. However, capital costs can be reduced by increasing the demand for these systems, which could lead to economies of scale.

In addition, the use of less expensive materials in the production stage can also reduce investment costs. Recent studies have shown that the investment cost of fuel cell systems can be reduced by developing fuel-reforming technologies that enable the use of various hydrocarbon fuels like SOFC. Variable costs for fuel cell systems strongly depend on the price of the fuel and the investment in facilities and supply chain. Therefore, the development of infrastructure for renewable fuels, is critical for the future of fuel cell systems [24].

To ensure the long-term durability of fuel cell stacks for maritime applications, preventing degradation of the electrolyte, electrode, and bipolar plates is crucial. Degradation can result in decreased conductivity of the electrolyte, catalyst performance loss, and cracking or corrosion of the plates, all of which can affect the lifetime and efficiency of the fuel cell stack [36]. New materials and technologies should be implemented to address the causes of degradation and improve performance. Steady-state conditions during operation, an appropriate system design, and an optimal control strategy that takes into

account all components of the power system can help to ensure longer durability. Furthermore, care must be taken to prevent seawater mist from entering the cathode air, which can reduce the efficiency of fuel cells [77].

Table 3.3: A summary of global research initiatives focused on implementing fuel cell systems in marine applications [90][25][24].

Project	Time Period	Country	Fuel Cell Power	Fuel Cell Type	Logistic	Ship type	Ship Name	Ref
FLAGSHIPS	2019–2023	Netherlands France Norway	1200 kW 400 kW 600 kW	PEMFC	Hydrogen	Container cargo, ship/self-propelled barge/Passenger, and car ferry	FPS Waal/ Zulu/ MF Hidle	
H2PORTS	2019–2023	Spain, Valencia	70 kW	PEMFC	Hydrogen	Reach Stacker and Yard Tractor	-	
HFC MARINE	2018–2020	Denmark	200 kW	PEMFC	Hydrogen	Ferry	-	
SHIPPINGLAB	2020–2024	Denmark	N/A	PEMFC	Hydrogen	Dredger	-	
HYSEAS III	2018–2022	Scotland	600 kW	PEMFC	Hydrogen	RoPax ferry	-	
FellowSHIP	2003–2018	Norway Germany	320 kW	MCFC	LNG	Offshore supply	Viking Lady	
SchIBZ	2009–2018	Germany	100 kW	SOFC	Diesel	General cargo ship, yachts	MS Forester	
PaXell	2009–2016	Germany	60 kW	PEMFC	MeOH	Cruise ship	MS Mariella	
ZEMSHIP	2007–2014	Germany	96 kW	PEMFC	Hydrogen	Inland passenger ship	FCS Alsterwasser	
Nemo H2	2008-present	Netherlands	65 kW	PEMFC	Hydrogen	Passenger boat	Nemo H2	
PaXell 2	2019–2022	Germany	N/A	PEMFC	MeOH	Cruise ship	AIDAnova	
RiverCell	2015–2022	Germany	90 kW	PEMFC	MeOH	Inland passenger ship	-	
ELEKTRA	2017–2019	Germany	300 kW	PEMFC	Hydrogen	Canal tug	Elektra	
MC-WAP	2005–2010	Italy	150 kW	MCFC	Diesel	RoPax, RoRo/cruise vessels	-	
US SSFC	2000–2011	US	625 kW 500 kW	MCFC/ PEMFC	Diesel			
METHAPU	2006-2010	European Union	20 kW 250 kW	SOFC	MeOH	Car carrier	MV Undine	

Table 3.3: A summary of global research initiatives focused on implementing fuel cell systems in marine applications [90][25][24].

Project	Time Period	Country	Fuel Cell Power	Fuel Cell Type	Logistic	Ship type	Ship Name	Ref
FCSHIP	2002-2004	European Union	N/A	MCFC	Diesel	RoPax vessel and harbour commuting ferry.		
DESIRE	2001-2004	Germany, The Netherlands, UK, Turkey	25 kW	PEMFC	Diesel	Naval ship		
TecBIA	2018-2022	Italy	140 kW	PEMFC	Hydrogen	Research vessel	ZEUS	
TESEO	2012–2015	Italy	50 kW	PEMFC	Hydrogen	Yachts and sailing boats	-	
HI-SEA	2017–2022	Italy	250 kW	PEMFC	Hydrogen	Experimental plant	-	
HIMET	2021–2022	United Kingdom	500 kW	PEMFC	Hydrogen	Ferries	MV Shapinsay	
ShipFC	2020–2024	Norway	2 MW	SOFC	Ammonia	Offshore vessel	Viking Energy	
Nautilus	2020–2024	European Union	60 kW	SOFC	LNG	Cruise ship	-	
Maranda	2017–2022	European Union	165 kW	PEMFC	Hydrogen	Arctic research ship	Aranda	
<u>Energy Observer</u>	2017–present	France	60 kW	PEMFC	Hydrogen	Experimental vessel	Energy observer	
MF Hydra	2020-present	Norway	400 kW	PEMFC	Hydrogen	Ro-Pax ferry	MF Hydra	
HyShip	2021–2024	Norway	3 MW	PEMFC	Hydrogen	Coastal goods-carrying RoRo	Topeka	
NAVIBUS	2018–2019	France	10 kW	PEMFC	Hydrogen	River boat	Jules Verne 2	
FC-PROMATE	2019–2022	Italy Netherlands	35 kW	PEMFC	Hydrogen	Protocols for testing PEMFC for maritime applications	-	
Sea Change	2016–2022	USA	360 kW	PEMFC	Hydrogen	Passenger ferry	Sea Change	
Hydrogenia	2019–2021	South Korea	100 kW	PEMFC	Hydrogen	Small boat	Hydrogenia	

Table 3.3: A summary of global research initiatives focused on implementing fuel cell systems in marine applications [90][25][24].

Project	Time Period	Country	Fuel Cell Power	Fuel Cell Type	Logistic	Ship type	Ship Name	Ref
E4Ships – Pa-X-ell	2017-2022	Germany	60 kW	PEMFC	Methanol	passenger vessel	MS MARIELLA	
E4Ships - SchIBZ	2017-2023	Germany	100 kW	SOFC	Diesel	Comercial ship	MS Forester	
Cobalt 233 Zet	2017-present	Germany	50 kW	PEMFC	Hydrogen	Sport boats		
FELICITAS - project 1	2005-2008	European Union	N/A	N/A	N/A	Heavy duty transport system		
FELICITAS - project 2	2005-2008	European Union	250 kW	SOFC	LNG	Mobile hybrid marine version of the Rolls Royce Fuel Cell		
FELICITAS - project 3	2005-2008	European Union	80 kW	PEMFC	Hydrocarbon	PEFC-Cluster		
FELICITAS - project 4	2005-2008	European Union	N/A	PEMFC		Power management		

Table 3.4: Overview of maritime applications powered by fuel cell systems [90][25][24].

Ship Name	Ship Type	Fuel Cell Type	Specification	Power System	Power Output	Fuel	Ref.
FCS Alsterwasser	Passenger ship	PEMFC	Length: 38.5 m, Passengers:350, Speed: 22 knots.	2 × 48 kW PEMFC, 7 battery packs 234 kWh, 100 kW EM and a 20-kW bow thruster	96 kW	Hydrogen	
Nemo H2	Passenger ship	PEMFC	Length: 22.5 meters, Passengers: 100, Speed: 12 knots.	2 × 30 kW PEMFC, 55 battery packs 70 kWh, a 75-kW EM and 11-kW bow thruster	60 kW PEMFC with 3 0–50 kW battery	Hydrogen	
SF-BREEZE	Passenger ferry	PEMFC	Length: N/A, Passengers: 150, Speed: 35 knots.	41 × 120 kW PEMFC , each rack 4 × 30 kW PEMFC stacks	120 kW	Hydrogen	
Cobalt 233 Zet	Tourist Boat	PEMFC	Length: 20m , Passengers: 50, speed: N/A	2 × 28 kW PEMFC, 3 × 15.7 kWh Li-ion battery packs	50 kW	Hydrogen	
MS Mariella	Passenger ship	PEMFC	Length: 169.7 meters, Passengers: 2,800, Speed: 21 knots	2 × 30 kW PEMFC, each comprised 6 × 5 kW modules	60 kW	Methanol	
MF Vågen	Small passenger ship	PEMFC	N/A	N/A	12 kW	Hydrogen	
Viking Lady	Offshore supply vessel	MCFC	Length: 92.2m, Passengers: 25, Speed: 15.3 knots	320 kW MCFC as APU, internal reforming unit and WHR system	320 kW	LNG	
MV Undine	Car carrier	SOFC	Length: 227.9m, Passengers: N/A , Speed: 22 knots	20 kW SOFC	20 kW	Methanol	
MS Forester	General cargo ship	SOFC	N/A	50 kW SOFC with Li-ion battery packs developed for APU	50 kW	Low-sulphur diesel	
Hornblower Hybrid	Passenger ferry	PEMFC	Length: 20m, Passengers: 149 , Speed: 10 knots	Hybrid ferry with diesel generator, batteries, PV, wind and fuel cell	32 kW	Hydrogen + Diesel	

Table 3.4: Overview of maritime applications powered by fuel cell systems [90][25][24].

Ship Name	Ship Type	Fuel Cell Type	Specification	Power System	Power Output	Fuel	Ref.
Class212A/214 Submarines	Submarines	PEMFC	Length: 65m, Passengers: 27 , Speed: 12 knots	Hybrid propulsion using a fuel cell and diesel ICE	306 kW	Hydrogen	
ZEUS	Experimental research vessel	PEMFC	Length: 25.6 m, Passengers: N/A , Speed: 7.5 knots	2 × 150 kW diesel generators, 2 electric propulsion motors, 2 × 70 kW Fuel Cell plant and Battery	130 kW (FC) 160 kWh (Battery)	Hydrogen	
MTU Friedrichshafen Yacht	Yacht	PEMFC	Length: 12m, Passengers: N/A, Speed: 8 knots	4 × 1.2 kW + 9 lead-gel batteries	20 kW	Hydrogen	
Ross Barlow	Canal boat	PEMFC	N/A	5 kW PEMFC module + lead-acid battery	5 kW	Hydrogen	
Hydrogenesis	Small boat	PEMFC	N/A	12 kW PEMFC module	12 kW	Hydrogen	
MF Hydra	Ro-Pax ferry	PEMFC	Length: 82.4 m, Passengers: 292, Speed: 9 knots	2 × 200 kW PEMFC, 1.36 MWh Batteries and 2 × 440 kW diesel generators.	400 kW (FC), 880 kW (ICE), 1.36 MWh (Bat)	Hydrogen + Diesel	
Jules Verne 2	River boat	PEMFC	N/A	2 × 5 kW PEMFC + Batteries	10 kW	Hydrogen	
MV Shapinsay	Ro-Ro Ferry	PEMFC	Length: 26.6 m, Passengers: 91, Speed: 9.5 knots	Hydrogen fuel cell for auxiliary power system	-	Hydrogen	
S80 class	Submarines	PEMFC	Length: 80.8m, Passengers: 32, Speed: 28 knots		300 kW FC stacks	Hydrogen	
MF Hidle	Passenger and car ferry	PEMFC	Length: 74m, Passengers: 199, Speed: 10 knots	3 × 200 kW PEMFC modules, Battery capacity 500 kWh Biodiesel generator back-up power	600 kW	Hydrogen	
Topeka	Coastal goods-carrying RoRo	PEMFC	N/A	3 MW PEMFC and 1 MWh batteries	3 MW	Hydrogen	
Hynova Yacht		PEMFC	Length: 12.65m, Passengers: 12, Speed: 25 knots	80 kW FC, 2 battery stacks, 2 electric motor of 300 kW	80 kW	Hydrogen	
FPS Maas	Inland container vessel	PEMFC	Length: 110m, Passengers: 12, Speed: 4 knots	825 kW PEMFC, 504 kWh lithium-ion battery pack	825 kW	Hydrogen	

Table 3.4: Overview of maritime applications powered by fuel cell systems [90][25][24].

Ship Name	Ship Type	Fuel Cell Type	Specification	Power System	Power Output	Fuel	Ref.
Ulstein SX190	Offshore construction vessel	PEMFC	Length: 99m, Passengers: 90, Speed: 11 knots	2 MW PEMFC	2 MW	Hydrogen	
Zero-V	Coastal research vessel	PEMFC	Length: 51m, Passengers: 30, Speed: 12 knots	10 × 180 kW PEMFC racks	1.8 MW	Hydrogen	
Sea Change	Passenger ferry	PEMFC	Length: 22m, Passengers: 28 , Speed: 20 knots	3 × 120 Kw PEMFC, 2 × 50 Kw battery, 2 × 300 kW electric motor	360 kW	Hydrogen	
EX38A	Experimental boat	PEMFC	Length: 12m, Passengers: N/A , Speed: N/A	2 × 92 kW PEMFC and 32 kWh battery	250 kW	Hydrogen	
Xianhu 1	Passenger cruise ship	PEMFC	Length: 12m, Passengers: 30 , Speed: 22 knots	30 kW PEMFC + Battery	30 kW	Hydrogen	

3.4.1 SOFC-ICE hybrid systems

This subsection provides an overview of previous studies conducted on SOFC-ICE hybrid systems. Since the integration of SOFC-ICE technology is relatively new, there is limited research published on this topic. The studies mentioned in this section are the only relevant publications found.

Park et al. proposed a hybrid system that combines an SOFC stack with an Homogeneous Charge Compression Ignition (HCCI) internal combustion engine. In this system, the HCCI engine replaces the conventional combustor and burns the anode off-gas to generate additional power [69]. The authors conducted steady-state simulations and demonstrated an electrical efficiency of 59.5% (103.6 kWe) at a power split of 12.7% for the ICE and 87.3% for the SOFC, with a SOFC fuel utilization of 75%. While this result is promising, more detailed research is necessary to make this concept feasible. Park's work can be regarded as a preliminary study on SOFC-ICE hybrid systems.

Van Biert et al. performed a thermodynamic comparison study of SOFC-combined cycles, which included simulations of the SOFC-spark-ignited reciprocating engine bottoming cycle model [91]. Notably, this study did not include a fuel bypass to the engine. The simulation results generated interest for further research in the field. The computational simulations achieved a maximum system electrical efficiency of 64% at a SOFC fuel utilization of 90% (electric power output was not reported) and at a power split of 5%-ICE, 95%-SOFC. These findings suggest that SOFC-combined cycles have the potential to deliver high system efficiencies, although further research is required to optimize and validate the results.

Chuahy and Kokjohn developed an SOFC-ICE hybrid system and performed a system-level optimization study to determine the maximum achievable performance of the integrated system [19]. They subsequently conducted HCCI engine experiments to verify whether the ICE could operate under the predicted conditions. The authors predicted that the computational model would have an electric efficiency of 70.9% (1104.3 kWe) at a SOFC fuel utilization of 64.4% and a power split of 14.7%-ICE, 85.3%-SOFC. However, they reported practical issues with stability during HCCI combustion and even during RCCI combustion. As a result, they ultimately decided to investigate future research on spark-ignition combustion for SOFC-ICE hybrid systems.

The research believed that SI combustion would be a more stable and robust combustion mode for these systems. This final conclusion is significant for current research. The studies all investigate the use of HCCI-reciprocating engines as the bottoming cycle in SOFC-ICE hybrid systems. However, although this type of combustion has been achieved in laboratory settings, it is still far from practical application, particularly at high specific power outputs or dynamic load conditions. Therefore, it can be concluded that more research is needed before these advanced combustion strategies can be effectively integrated into marine transport applications [75].

Energy carriers

An energy carrier is a substance or phenomenon that stores and transports energy, like fuels, batteries, or fluids. They are crucial for efficient energy systems [5]. Marine vessels traditionally rely on fossil fuels for propulsion. However, due to growing concerns about the environmental impact of these fuels, there is an increasing search for alternative energy carriers. Fuel cells are a promising solution, as they offer a cleaner and more efficient means of producing energy. Fuel cells can use a range of energy carriers from now one called fuels, such as hydrogen, methanol, and ammonia, to generate electricity through an electrochemical reaction. Moreover, it is possible to retrofit conventional diesel engines to use these alternative fuels, enabling the use of existing engines with new and cleaner fuels, and facilitating an easier transition to sustainable fuels. This retrofitting of existing engines represents a significant development in the marine industry, as it reduces the costs of replacing the entire fleet while also lowering emissions. This chapter aims to provide an overview of the various alternative fuels used in fuel cells. For each fuel, their properties and characteristics will be discussed, as well as their potential to be a viable fuel for the marine industry. Additionally, for each fuel the challenges associated with storage, transport and handling will be covered. A overview of these fuels is given in Figure 4.1.

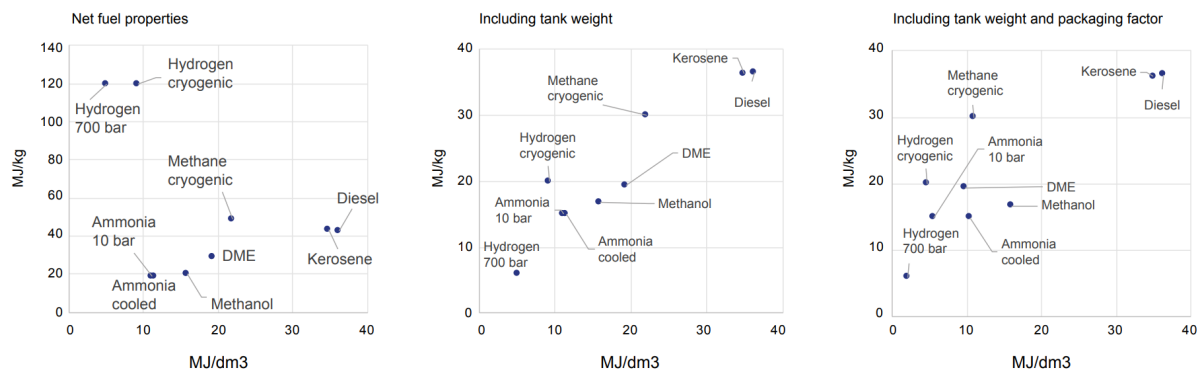


Figure 4.1: Energy density and specific energy of fuels with and without the tank weight and volume [51].

Today, heavy fuel oil (HFO), marine diesel oil (MDO), and liquefied natural gas (LNG) are the most commonly used fuels for shipping, with HFO being the most economical for long-distance shipping. Although the use of LNG as a shipping fuel has been developed over several decades, the potential emissions have not been addressed in much of the literature. While LNG has a higher hydrogen-to-carbon ratio than HFO, it does not consider the impact of methane slip, which has a stronger effect on the greenhouse effect than the equivalent amount of CO_2 , and may lead to carbon intensity of gas shipping exceeding that of oil tankers. None of HFO, LNG, or MDO are capable of providing emission-free shipping, unless there is a significant advancement in carbon capture and storage (CCS) technology. Liquefied petroleum gas (LPG) is also not a suitable fuel, as it would still produce emissions.

Nuclear-powered shipping technology is technically feasible, but the high upfront capital expenditure requirements, safety concerns, decommissioning issues, and high insurance make it unlikely to be a feasible option for commercial shipping in the near future [40].

Biofuels are a type of fuel that is a product of biomass. While their use emits carbon, they are often considered potentially carbon-neutral fuels since the carbon dioxide emitted during their use was previously absorbed during the growth of the biomass. Biofuels can be subdivided based on their level of "generation," with first-generation biofuels typically produced from edible feedstock, second-generation biofuels

primarily produced from non-edible feedstock, and third-generation biofuels made from algal biomass or potentially from CO sources. These fuels can be used both as primary fuels and drop-in fuels in various engine types, although certain engine modifications may be necessary in some cases. Due to the wide variety of biofuels available, this chapter will not go into further detail.

4.1 Hydrogen

Although hydrogen can be sourced from various means, including biomass or electrolysis, it is mostly obtained from natural gas due to its abundance. Despite being the most abundant element in the universe, pure hydrogen is rarely found in nature [61]. Hydrogen is an ideal fuel for fuel cells as it has fast electrochemical oxidation characteristics, which allows it to be used without significant pretreatment. Fuel cells that use pure hydrogen can achieve high overall power densities, making it a preferred option for converting hydrogen to electricity. In comparison to ICE, fuel cells are generally more efficient at converting hydrogen to electricity [82]. However, the low storage density of hydrogen is a significant disadvantage as a logistic fuel as can be seen in Figure 4.1. Typically, hydrogen is stored in pressurized vessels at 350 or 700 bar for automotive applications. Alternatively, hydrogen can be stored at cryogenic temperatures of -253°C at ambient pressure, or at somewhat higher temperatures and elevated pressures, which is known as cryocompressed hydrogen (LH_2). Cryocompressed hydrogen is currently considered the most energy-dense physical storage method and is the preferred storage option. Although other storage options, such as metal hydrides and chemical compounds, are being researched, they are not as developed as cryocompressed hydrogen. It is important to note that all logistic fuels discussed in this review can effectively be regarded as hydrogen carriers.

4.2 Ammonia

Ammonia is gaining interest as a potential green alternative marine fuel, and there are already some projects underway to develop ammonia-powered vessels. Like the Dutch NWO program AmmoniaDrive project that is developing a powertrain system for ICE that uses ammonia as a fuel to reduce GHG emissions and fossil fuel dependence. It involves a two-stage combustion process and aims to overcome technical and commercial barriers to adoption. Successful implementation could have significant implications for a more sustainable transportation sector [84]. Since ammonia does not contain carbon, it can be used as a fuel with zero carbon emissions. However, its nitrogen content can lead to harmful NO_x pollution [58]. Additionally, ammonia is toxic and requires additional caution when used as a fuel, although it has been transported and used (as feedstock for the production of fertilizer) in the agricultural sector already for many years [58]. Compared to hydrogen, ammonia has a higher volumetric energy density and is easier to store as a liquid at around -34°C and ambient pressure, or with a pressure of 10 bar at ambient temperatures. However, its gravimetric energy density is lower than that of hydrogen as can be seen in Figure 4.1. Ammonia can be produced by combining hydrogen and nitrogen with the Haber Bosch process, making its production pathway similar to that of hydrogen. Thus, ammonia could be a green marine fuel that requires only one additional production step compared to hydrogen. Ammonia has the potential to be used in most marine power plants, including ICE and fuel cells [103].

4.3 Methanol

Methanol is considered a leading candidate for decarbonizing the shipping industry due to its dual-fuel engine technology, wide availability and ease of handling compared to gaseous fuels such as hydrogen and ammonia [58]. It does not require cryogenic conditions as it is a liquid at room temperature and ambient pressure, allowing for easy storage in various tank shapes without losing ship volume [3] as can be seen in Figure 4.1. Methanol infrastructure is already in place globally for the chemical industry, requiring minimal modifications for use as a fuel, and early implementation can be achieved through truck-to-ship bunkering [92]. Moreover, methanol has the highest hydrogen-to-carbon ratio of any liquid fuel, resulting in up to a 10% reduction in tank-to-wake (TTW) emissions compared to diesel [8]. Combustion of methanol also produces less air pollutants and up to 60% less NO_x formation during combustion, with no sulphur and carbon-to-carbon bonds that result in 99% less SO_x and 95-99% less particulate matter, depending on the combustion principle. In the event of a spill, methanol is less harmful to the environment than heavy fuel oil or diesel as it biodegrades rapidly in water [3].

These characteristics make methanol a potential solution to meet the IMO's policy requirements. As methanol is widely considered as one of the most promising fuels for the future, it is worth providing a more comprehensive explanation of its potential.

4.3.1 Production

The emissions of GHG resulting from the production and use of fuels are categorized into two phases: Well-to-Tank (WTT) and TTW. WTT refers to the emissions from fuel production, while TTW refers to the emissions from fuel combustion. The sum of WTT and TTW emissions is referred to as WTW emissions. Figure 4.2 provides an overview of the components involved in well-to-wake GHG emissions. However, this analysis of WTW emissions only covers GHG emissions from fuel production and use, excluding emissions from the production of engines, ships, and necessary infrastructure, which are assumed to be similar for different fuel types.

For a complete analysis of the life cycle emissions of ships using different fuels, upstream and downstream emissions should also be considered. Upstream emissions from fuel production consist of emissions from extracting raw materials for building infrastructure and fuel production. Emissions from the production of e-fuels, which require a significant amount of electricity, are shown separately. For fossil-based electricity, the majority of emissions result from the operational stage of electricity generation, which involves extracting and burning fossil fuels. However, for renewable sources of electricity, the majority of emissions occur during the upstream stage. For example, wind electricity has minimal operational emissions, but still includes upstream emissions primarily from steel production for building wind turbines. Some studies only consider operational WTT emissions, where non-fossil electricity emissions are assumed to be zero, leading to significant variation in the contribution of e-fuels to WTT emissions in different studies, making comparison difficult.

This section focuses on ensuring comparable assumptions of emissions related to electricity use for e-fuels. While this does not significantly affect comparisons of fossil fuels, it is crucial for e-fuels because of their substantial electricity input. Including their energy usage and efficiencies, in order to assess their viability. As can be seen in Figure 4.2 the development of a comprehensive flowchart that accounts for the various systems and processes involved in transporting 1 tonne of cargo over a 1 km distance using a Ro-Ro vessel with different fuels. When referring to fuels that use biomass as their only feedstock, the prefix "Bio-" is used, while for fuels produced by combining captured CO₂ with H₂, the prefix "E-" is used. There are various production processes for Bio-fuels, depending on the desired fuel and available biomass. Typically, organic waste from food processing or crops is used for anaerobic processes such as fermentation or digestion, resulting in ethanol and Bio-gas, respectively. Lignocellulose feedstocks (Lignocellulose is a natural material found in plants that consists of cellulose, hemicellulose, and lignin. It is commonly used for the production of biofuels and other bio-products) are suitable for gasification, a process that converts biomass endothermically to synthesis gas without combustion. The resulting products such as ethanol, methane, and synthesis gas can be further synthesized into other fuels if required.

Vegetable oils are commonly used for the production of FAME Bio-diesel and HVO Bio-diesel through transesterification and catalytic (a reaction that converts esters into different esters and alcohols by using alcohol and a catalyst), respectively. To increase biomass production yields, H₂ can be added to the excess CO and CO₂ generated in the conversion process to fuel, resulting in additional fuel production without the need for energy-intensive carbon capture [41].

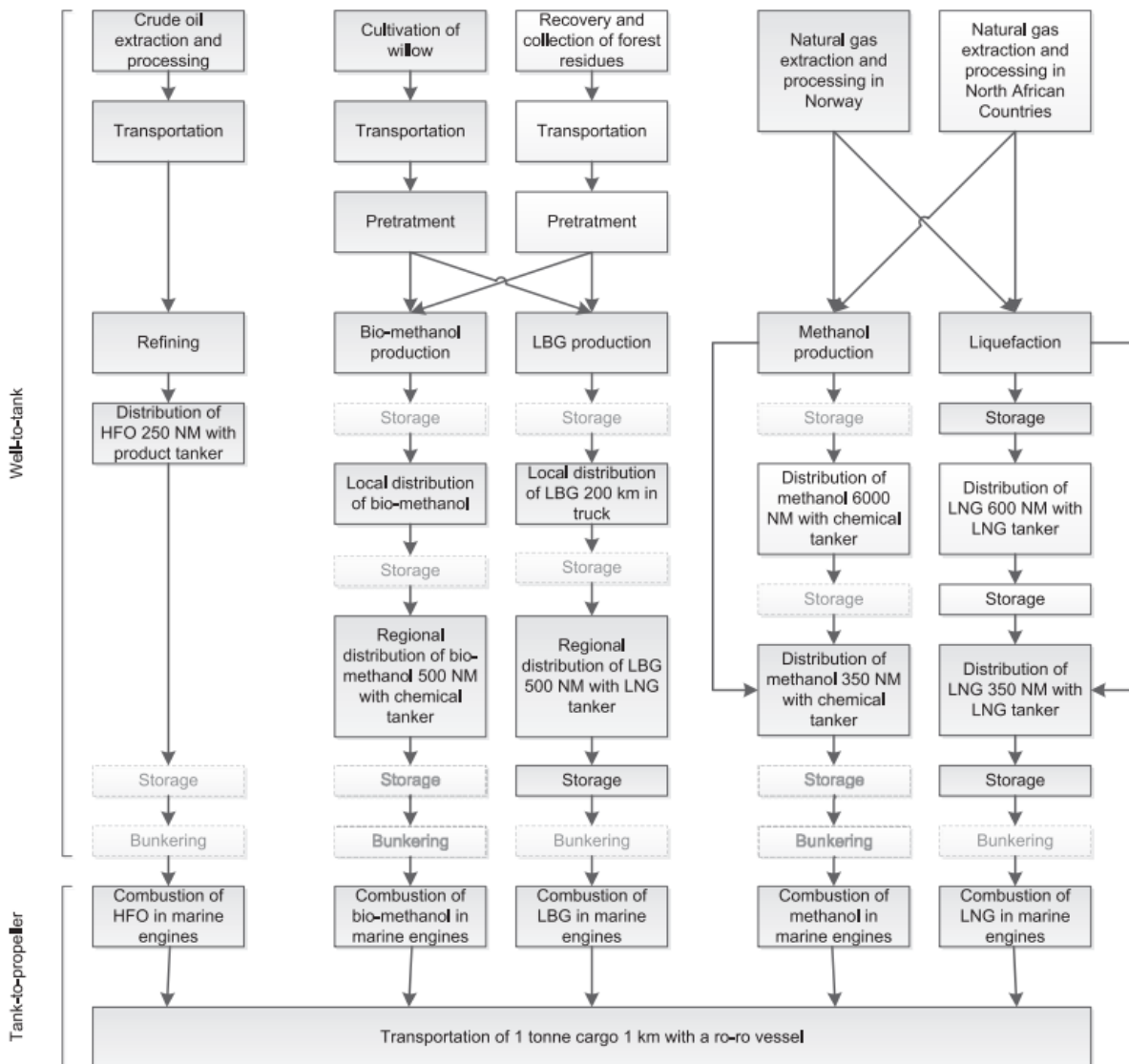


Figure 4.2: Well-to-Tank and Tank-to-Wake [15]

Estimated that the biomass-to-fuel efficiency for Bio-methanol is around 54%, while it is around 51% for Bio-diesel, by dividing the energy in the resulting fuel by the energy content in the biomass, without significant inputs or outputs of other energy [42].

Methanol can be synthesized in one or two hydrogenation steps, where synthesis gas mainly composed of CO or CO₂ and H₂ is processed to produce methanol. The composition of CO :H₂ ratio in the synthesis gas can be adjusted by the water-gas shift reaction, where CO₂ can be added or reduced by varying the steam in the reactor. Methanol can be further reacted to generate diesel if desired. The reported synthesis efficiency of synthesis gas to methanol varies between 69-89% [15], and the overall production efficiency ranges from 41-72% [33]. Fischer-Tropsch synthesis can be used to produce diesel either with synthesis gas from biomass or with captured CO₂ and hydrogen. During the process, the synthesis gas reacts to form synthetic crude, where the chain growth of the synthetic crude depends on the catalysts used, syngas stoichiometry, temperature, and reactor pressure. The reported efficiency of the Fischer-Tropsch synthesis at the process-level ranges from 59%-78% [15], and the overall production efficiency ranges from 37%-64% [33].

Renewable CO₂ can be sourced from Direct Air Capture (DAC), Point Source Carbon Capture (PSCC), or biomass. While DAC is an energy-intensive process that is not yet available on an industrial scale,

CO₂ from biomass is widely available and more affordable. However, it alone cannot provide sufficient CO₂ for large-scale production of carbon-based E-fuels in the future. Currently, CO₂ from biomass can be supplemented by PSCC as long as significant CO₂ emissions from industry are available. However, in the long term, CO₂ from industry will decrease, and upscaling of DAC will likely be required. Despite different cost estimates from various studies on DAC developments, the cost is expected to decrease in the future [20].

Three leading technologies for H₂ production are Alkaline Electrolysis (AEL), Polymer Electrolyte Membrane Electrolysis (PEMEL), and Solid Oxide Electrolysis (SOEL). Electrolysis uses electricity to separate water into hydrogen and oxygen by current between two electrodes that are separated and immersed in an electrolyte to raise ionic conductivity. The efficiency of these electrolysis methods ranges between 63-71% for AEL, 58-71% for PEMEL, and 75-83% for SOEL. In general, large amounts of hydrogen are required for E-fuel production, and therefore, the efficiency of the electrolysis primarily determines the total E-fuel production efficiency [33].

In summary the production efficiency for these fuels depends on the production process's details and the potential to combine various required feedstocks efficiently, diesel production is generally 5% to 15% less efficient than methanol production.

4.3.2 Future availability

Methanol has been gaining interest as a potential marine fuel due to its lower emissions of sulfur oxides (SO_x) and nitrogen oxides (NO_x) compared to traditional marine fuels such as heavy fuel oil. Methanol is a clear and colorless liquid that can be produced from various sources, including natural gas, coal, biomass, and renewable sources such as waste carbon dioxide. According to a report by DNV GL [32], methanol has the potential to become a significant marine fuel in the future, with the potential to replace up to 10% of the world's marine fuel demand by 2050. The report notes that methanol can be produced on a large scale and can be stored and transported easily, making it a practical option for the maritime industry [32]. However, the future availability of methanol as a marine fuel will depend on several factors, including production capacity, infrastructure, government policies, and competition with other alternative fuels. According to figure 4.3, there are significant differences between the current supply levels and the potential demand for different fuels. Despite having the lowest current production level in terms of total mass, hydrogen would only require a 171% increase to meet the potential demand, which is lower than the required increase of 391% for ammonia and 859% for methanol [58]. This is partly due to the high gravitational energy density of hydrogen, which makes it more efficient in terms of energy storage. However, it is important to note that the energy required to store each fuel has not been taken into account in these calculations. The values shown in 4.3 were calculated using specific assumptions, which include the mean annual delivered energy for the LNG tanker analyzed in the study (54.15 GWh), a deployment efficiency of 60%, and an approximation of 50,000 ships to represent the global merchant fleet [37]. Using these assumptions, the study estimated the global fleet's annual energy demand to be 4512 TWh, equivalent to 389 million metric tons (mt) of HFO. The estimate is reasonably realistic, as the IMO's 4th GHG study also calculates a total annual HFO-equivalent fuel consumption for the entire shipping industry at 339 mt [26].

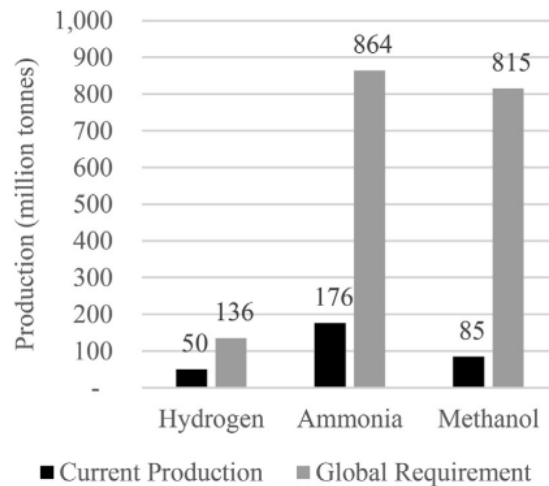


Figure 4.3: Energy carriers/Current annual production levels compared to a estimated annual demand for 50,000 ships [58]

Currently, there are a limited number of ports that offer methanol bunkering facilities, with the majority located in Northern Europe and Asia. The availability of infrastructure for methanol production, storage, and delivery will need to increase to meet potential demand. Government policies and regulations may also play a role in the adoption of methanol as a marine fuel [47]. The IMO has set a target of reducing GHG emissions from shipping by at least 50% by 2050 compared to 2008 levels. This has led to increased interest in alternative fuels such as methanol, and governments may incentives their use through regulations and incentives. Finally, methanol may face competition from other alternative fuels such as LNG, hydrogen, and ammonia. Each of these fuels has its own advantages and disadvantages, and the choice of fuel will depend on factors such as availability, cost, and infrastructure [67].

4.3.3 Cost

To accurately estimate the cost of methanol as a fuel product, it is essential to consider the additional costs that result from its transportation. Additionally, it is crucial to take into account potential reductions in cost over time due to advancements in technology and increased adoption of electro-methanol. This allows for a fair comparison with other fuel products like hydrogen. The average additional cost for transporting an electro-methanol fuel product is \$17 per tonne, based on the range of \$6 to \$38 per tonne [87]. Furthermore, the estimated cost reduction rate for the production of methanol through gasification of biomass and electrolysis of water is approximately 2.5% and 4% per year, respectively [4]. The fuel product cost estimates for the different forms of methanol production considered in this study, after taking into account additional transportation costs and applying the estimated cost reduction rates, are included in the figure.

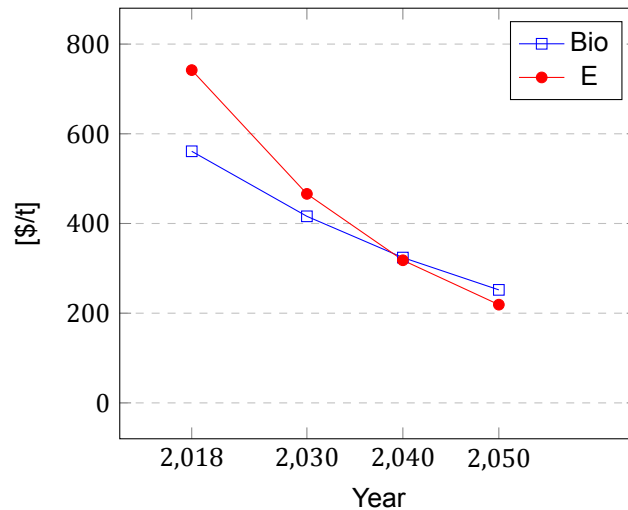


Figure 4.4: Fuel production cost estimates and assumptions [74].

A large range of uncertainty in the production costs of E-fuels was found. Various projects analyzed factors that affect the production costs and collected data on the production costs and efficiencies associated with E-fuel synthesis [15]. Most studies fall within the uncertainty range provided by Brynolf, except for the study from Lloyd's Register [74], which takes very positive assumptions. Despite this, the study from provides a helpful trend for the development of the cost of various fuels, but doesn't address uncertainty. All studies agree that the cost difference between Bio- or E-methanol and Bio- or E-diesel is only a limited percentage of the estimated cost of the fuels, ranging from 5-30% depending on the assumptions of the cost of sustainable electricity and feedstock. This is due to the lower efficiency of the production process of bio- or E-diesel, with the study from Lloyd's Register and UMAS (2019b) being a significant outlier. In conclusion, the studies agree on a 5-30% increase in price from Bio- or E-methanol and a decreasing trend in the cost of sustainable fuels as production capacity and technological readiness increase [15][74].

Cable layer operation and profile

This chapter of the literature review explores the operational profile of a cable layer. It examines the types of equipment used, the environmental conditions in which they operate, and associated risks and mitigation strategies. Through a comprehensive analysis of existing research, the review aims to identify gaps in the literature and propose a revised main question for further investigation.

5.1 Cable lay operation

To discuss the impact of cable laying activities on the vessel design, it is essential to understand the tasks that are performed on the vessel. The installation of a submarine cable is a complex and crucial operation that involves connecting onshore and offshore topside facilities with equipment located on the seabed. It requires careful planning, specialized equipment, and highly skilled personnel. The installation process typically involves laying the cable along the seafloor, burying it to protect it from damage, and connecting it to shore. Once installed, the cable provides critical infrastructure for communication, power transmission, and other important services. Due to the complexity and cost of installation, submarine cables are often designed to last for several decades, and their maintenance and repair require specialized expertise and equipment. As can be seen in Figure 5.1, the cable is composed to both a dynamic and static forces during the installation period. The static part is laid by the cable layer and is located on the seabed under stable environmental conditions, while the dynamic part hangs freely from the onboard vessel's equipment, including a tensioner and overboard chutes. The dynamic part is subjected to loading due to vessel motions and environmental loads [57].

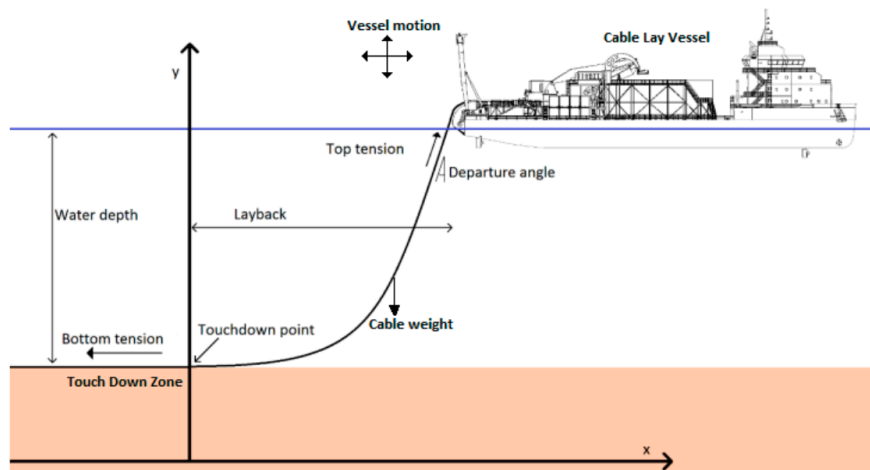


Figure 5.1: Demonstration of the most influential parameters during a cable laying process [57].

The touch down zone (TDZ) is the critical region where the cable first hits the seabed. This zone may be exposed to severe curvature and axial compression, which may result in local buckling inside the cross-section that causes the cross-section to be unstable in torsion, global loop formation, or a combination of those that may finally result in capacity failure. Therefore, it is crucial to prevent such conditions at all times, as failure to do so could have significant financial implications due to the high cost of the cable. Current practice is to avoid the occurrence of compression at the TDZ to eliminate any possibility of the cable failure. However, this restricts the weather window for the laying operation since the dynamic responses of cable layer, especially the motions along the cable axis, significantly

affect the axial force applied to the cable during installation. The current operation involves several complex variables, and ensuring a stable energy supply is of importance for the dynamic positioning (DP) and auxiliary systems [57].

5.2 Operational profile

Assessing the operational profile is crucial in determining the appropriate fuel and power plant. In the case of Van Oord, this section will delve into an analyse of operational profile for a cable layer. Various factors such as the operational area and design speed will be discussed to determine the profile. While the operational profile can be analyzed in great detail, this section will focus on the most pertinent aspects.

To determine an operational profile for a vessel, one must simulate the vessel's operation in its intended mission, as defined by the mission requirements. This involves estimating the time spent on various tasks, such as sailing, dynamic positioning, and port-stay, while taking into account environmental factors such as sea state, wind condition, and sea/air temperature. The operational profile is the result of these estimates and provides information on the time consumption in different tasks, modes, and weather profiles. Unlike traditional weather routing tools that mainly focus on optimizing the route with respect to a weather forecast, this approach allows for the calculation of key performance indicators, such as time spent for different tasks, modes applied to accomplish tasks, weather encountered while accomplishing tasks, and power consumed. A typical operational profile is presented in Table 5.1 and includes tasks such as harbour, transit, standby, and DP operations. The latter three tasks are divided into two weather conditions. Each task is specified with loads for individual thrusters, heavy consumers, hotel load, as well as relative allocated time. Furthermore, each task has a set of requirements and can only operate in certain predefined modes [35].

Table 5.1: Operational profile [35]

Operational profile	Relative Time
Harbour	20%
Transit at 11 knots	10%
Transit at 13 knots	10%
Standby in calm weather**	20%
Standby in harsh weather***	10%
DP2 in calm weather**	20%
DP2 in harsh weather***	10%
Full power to main thrusters	0
DP2 failure with max crane load	0

** Calm weather is defined as sea state 0-3 and wind speed below 15 knots

*** Harsh weather is defined as sea state greater than or equal to 4 or wind speed above 15 knots.

Based on an analysis of the cable laying vessels, the distribution of their operational status was determined. Four types of operations were defined: harbour, transit, standby, and DP. As can be seen in Figure 5.2 presents a pie chart that visualizes the time distribution of the four operations of a cable layer. It is noteworthy that the chart reveals an almost equal distribution between sailing and standstill (waiting and (un)loading), indicating that the vessels spend nearly half of their operational time not sailing.

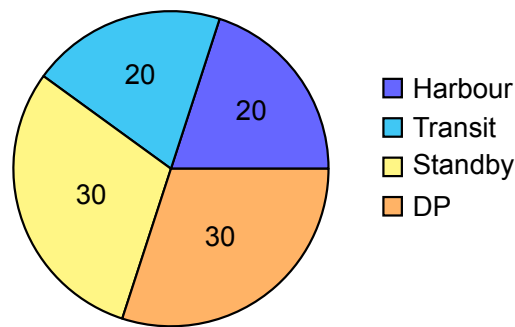


Figure 5.2: Operational profile

5.3 Power and propulsion plant

To fulfill a ship's mission, two important functions that need to be performed are propulsion and power supply. The majority of the offshore fleet, is equipped with a Diesel electric power and propulsion plant. This system utilizes diesel engines to drive electric generators, which produce electrical power for the ship's various systems. Van Biert et al [90]. conducted a literature review to assess the suitability of fuel cells for marine applications and compared fuel cell systems to conventional marine power plant solutions based on various criteria. These criteria should be considered when designing SOFC ICE hybrid system configurations. The criteria include:

1. Power and energy density.

This criterion is essential in determining the feasibility of a fuel cell system for marine applications. The power and energy density of the system affect the space and weight required for the installation of the fuel cell system. SOFCs have higher power density compared to other fuel cells, but their energy density is relatively low. This criterion needs to be taken into consideration to achieve a balance between the system's power and energy

2. Load transients and system start-up.

Load transients are an essential factor to consider when designing a fuel cell system for marine applications. In the maritime industry, ships' loads are highly dynamic and vary with time, depending on the ship's operation. The fuel cell system must be capable of handling these load transients effectively. The system start-up is also crucial, as the fuel cell must be able to start up quickly to meet the energy demand of the ship.

3. Environmental impact.

The environmental impact of the fuel cell system is an essential factor to consider in the maritime industry. The marine environment is sensitive to pollution, and the fuel cell system must have minimal impact on the environment. The use of hydrogen as a fuel for the SOFC system has zero emissions, which makes it an environmentally friendly alternative to conventional marine power plants.

4. Safety and reliability.

Safety and reliability are critical factors to consider when designing a fuel cell system for marine applications. The fuel cell system must be safe to operate, and the risk of any potential hazards must be minimized. The system must also be reliable and capable of operating under various conditions, including extreme weather conditions and harsh environments.

5. Economics.

The economics of the fuel cell system are essential to consider when designing a fuel cell system for marine applications. The initial cost of the system and the operating costs must be taken into account to ensure that the system is economically viable. The fuel cell system must be cost-effective, and the benefits of the system must outweigh the initial investment and operating costs over the system's lifetime.

Conclusion literature review

In conclusion, this research has investigated the suitability of fuel cells and energy carriers for the implementation of a fuel cell into a power plant of a cable layer. The following research questions were addressed:

- What are fuel cells, their different types, and what is the current status of their usage in maritime applications along with the underlying reasons?
Fuel cells are electrochemical devices that convert chemical energy into electrical energy. They come in different types, such as PEMFCs and SOFCs. While the usage of fuel cells in maritime applications is not yet common, there are documented cases of successful implementation due to their potential to provide cleaner and more efficient ship energy systems. The SOFCs are a promising fuel cell, but their combination with the thermodynamic cycle is not yet fully developed for this purpose.
- What are the different types of energy carriers, and what is their technology readiness for usage in maritime applications?
There are various types of energy carriers, such as hydrogen, methanol, and ammonia, that have the potential to be used in maritime applications. Among them, methanol is a highly suitable option for decarbonizing the shipping industry due to its wide availability, ease of handling, and existing infrastructure.
- What are the operations and operational profile of a cable layer?
The operational profile of a cable layer involves different modes of operation, such as transit, harbour, and DP. It requires different power demands, which makes the optimal sizing and integration of batteries with fuel cells necessary to ensure reliability and safety.

Overall, the use of fuel cells, particularly SOFCs, in combination with energy carriers such as methanol, has the potential to significantly contribute to the development of cleaner and more efficient ship energy systems. Further research is needed to determine the optimal sizing and integration of fuel cells and batteries with the operational profile of a cable layer to ensure reliability and safety.



Object of Study

Design Approach

7.1 Objectives and research questions

To accomplish the objectives of this thesis, research questions have been revised and formulated with the info of the literature review. The primary research question is stated as follows:

- **What is the impact of adding a methanol-fuelled SOFC and batteries to the power plant of the NEXUS on the emissions, design and performance of the ship?**

In order to address the main research question several sub-questions are formulated to address the main research questions and thus filling the gaps identified in the literature review:

- What is the energy demand of the cable layer and how can methanol-fuelled SOFC and batteries technology be integrated into its power plant?
- How does the use of a methanol-fuelled SOFC and batteries affect the design and performance of the cable layer?
- What are the economic and environmental benefits of using a methanol-fuelled SOFC and batteries?

7.2 Structure of the research

The research study is divided into two main sections: the object of study and the case study, each containing multiple chapters.

In chapter 8, an analysis of the reference design is conducted. The current design is examined, and specific requirements related to various aspects are explained. This process sets up the basic structure for the later parts of the research.

chapter 9 involves the definition and formulation of performance indicators, which will serve as benchmarks for evaluating the operational efficacy of the vessel. These indicators are carefully chosen to facilitate the assessment of the ship's operational efficiency and effectiveness across different scenarios.

In the context of the case study, the following aspects will be addressed:

chapter 10 delves into the individual manufacturers of SOFC modules and their corresponding support systems. The analysis also examines additional power sources, conducting a detailed examination of their characteristics and specifications. Furthermore, a thorough comparison of configurations of battery modules is undertaken.

In chapter 11, the placement of the methanol bunkertank, fuel cells, and battery modules is investigated. chapter 12 involves a comparison of performance indicators of the reference design with the concept design. Finally, chapter 13 provides an financial overview, including both Capital Expenditures and Operating Expenditures associated with the proposed new system.

Reference Design

To determine the feasibility of using fuel cells as a replacement for the current ICE-based power plant, a reference design is necessary for comparison. The chosen design for this master's thesis is the Nexus provided by Van Oord. As it aligns with the conclusions of the literature review, indicating that fuel cells could be viable for use on cable layers. The cable layer load profile makes it suitable for fuel cells to provide a base load, while another power source would be necessary more fluctuating load profiles and to compensate for SOFCs' long start-up times. The existing design serves as a benchmark for the research, and the new configuration should match its performance and maintain capabilities as closely as possible.

8.1 Design characteristics

The vessel known as the Nexus (Yard No. 553014) is a cable-laying ship that utilizes DP technology. It is designed based on the Damen Offshore Carrier 7500 design showed in Figure 8.1. For this study, the original design and specifications of the vessel will be used, which are shown in Table 8.1

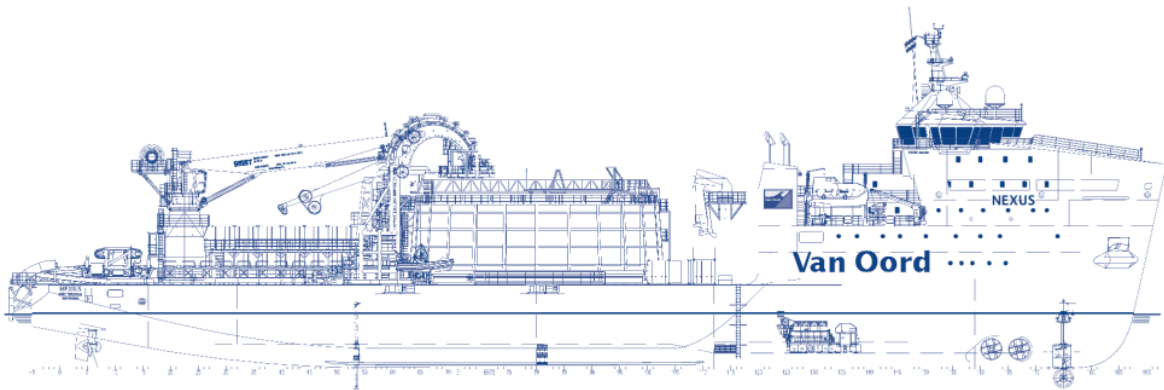


Figure 8.1: Principal particulars Nexus [93].

Table 8.1: Principal dimensions Cable laying vessel Nexus

Vessel Parameter	Nexus	Unit
Length over all:	122,68	m
breadth moulded	27,45	m
Draught moulded	5,82	m
Deadweight	8.398	tons
Displacement	13.585	tons
Total power installed	10.948	kW

The vessel has a length of 122.68 meters and a width of 27.45 meters, and it is intended to accommodate a deadweight of 8398 tonnes. The deadweight of a vessel refers to its total weight-carrying capacity, excluding its own weight. The vessel's length-to-beam ratio (L/B) can also be calculated by dividing the length of the vessel by its maximum beam. In this case, the L/B ratio would be approximately 4.47, which falls within the typical range for vessels of this size. The L/B ratio is an important design consideration as it affects the vessel's stability, maneuverability, and performance in various sea conditions.

8.1.1 Deck equipment

Now that the general dimensions of the Nexus have been established, it is necessary to define the specifications of other relevant structures on the weatherdeck. The weatherdeck is the uppermost, exposed deck of a ship that provides access to various areas of the vessel. Structures on the weatherdeck include the list described in Figure 8.2.

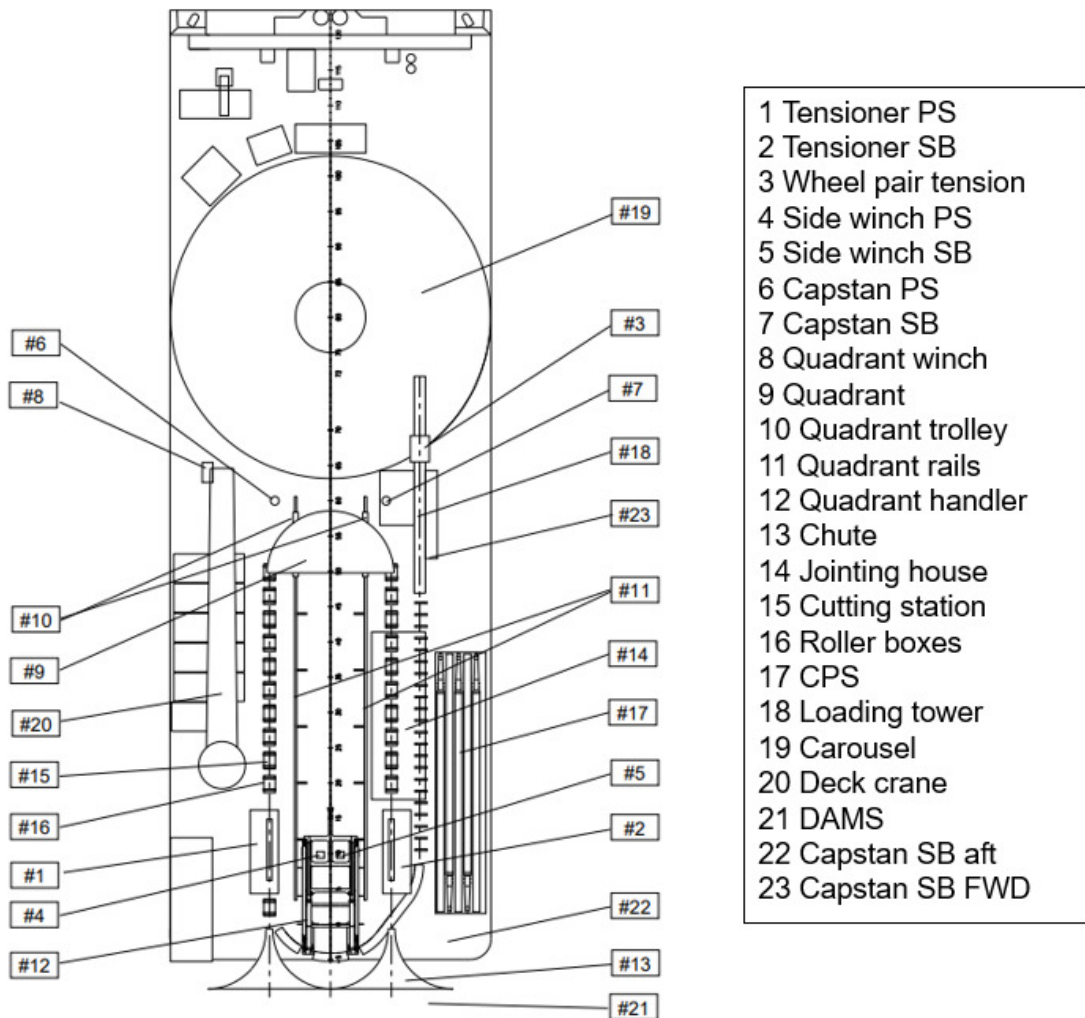


Figure 8.2: Nexus schematic overview deck lay-out.

The above devices are a mix of different equipment used in cable lay operation, they are used for tasks such as tension control, winching, loading, and handling of cable. It can be challenging to determine their power consumption in real-world scenarios. This is because the operation of cable laying is often a dynamic process that can vary based on factors such as usage patterns, environmental conditions, and other variables. However, it's safe to assume that the larger equipment such as the loading tower, carousel, and deck crane likely consume more power than the smaller devices like the tensioners and winches. This need to keep in mind during the process.

8.1.2 Engine room

The engine room is situated beneath the accommodation at the front of the ship, as illustrated in Figure 8.3. The vessel utilizes a diesel-electric design and is equipped with three thrusters located at the bow (one retractable azimuth thruster and two tunnel thrusters), as well as two azimuth thrusters at the stern. All thrusters have variable speed fixed pitch propellers. The vessel is powered by four main diesel generators, one auxiliary diesel generator, and an emergency diesel generator as can be

seen in Table 8.2. The main and auxiliary diesel generators are situated in the single engine room, while the emergency diesel generator is located in a separate space. Automation and power management systems for the vessel are provided by 'Alewijnse Marine Systems' and feature distributed control hardware connected through a single ring network located in the switchboard room.

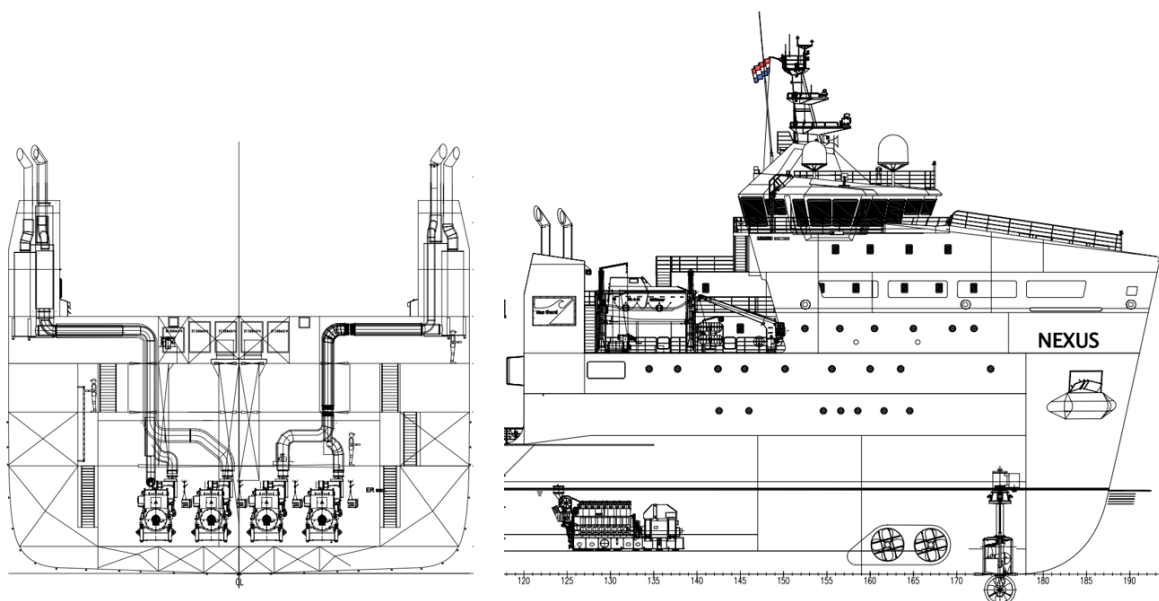


Figure 8.3: engine room lay-out

Table 8.2: Diesel Generator Identification

DG	Engine	Alternator	Speed	Output Rating
DG1	MaK 6M25 AEM	SE710SA10	720rpm	1910kW, 2390kVA, 690V, 3ph, 50Hz
DG2	MaK 8M25 AEM	SE710S10	720rpm	2560kW, 3200kVA, 690V, 3ph, 50Hz
DG3	MaK 8M25 AEM	SE710S10	720rpm	2560kW, 3200kVA, 690V, 3ph, 50Hz
DG4	MaK 6M25 AEM	SE710SA10	720rpm	1910kW, 2390kVA, 690V, 3ph, 50Hz
DG5	Caterpillar 3512C	LSA 51.2 S55	720rpm	1300kW, 1500kVA, 690V, 3ph, 50Hz

8.1.3 Tanks

The previous section presented a series of technical drawings illustrating the weatherdeck and engine room. The side and top views of these drawings revealed multiple tanks, which are the focus of this chapter's analysis. Table 8.3 outlines the various tanks constructed within the Nexus and their respective storage capacities.

Table 8.3: Tank specifications

Tank	Quantity	Volume [m^3]	ρ [kg/m^3]
Ballast water	15	8166.7	1.025
Fresh water	13	4447.0	1.000
Marine Gas Oil	13	1768.2	0.890
Void	25	3016.6	-

The MGO tanks and other storage tanks, such as fresh and ballast water tanks, are relevant tanks onboard of the Nexus. In addition, the study includes the "void" tanks, which are empty spaces within the ship's structure designed for structural support and not for storage and transport purposes. However, the Nexus is a special case. The Nexus is from origin an submersible ship that includes a moonpool in its design. While both functionalities are not currently in use, the technical layout for them still exists.

Due to its submersible functionality, the ship contains a considerable number of ballast tanks. These tanks serve the purpose of maintaining the ship's stability and maneuverability both when surfaced and submerged. The water ballast tanks are distributed throughout the length of the ship, with the largest storage capacity found in the mid-ship region in the double bottoms and side tanks. The remaining water ballast tanks are located in both the fore and aft ship,

According to Table 8.3, the Nexus ship has a significantly larger storage volume for fresh water than a general cargo ship with a similar. This large capacity is necessary to support the accommodation of up to 90 crew members and allow the ship to operate independently for up to 21 days.

The MGO tanks on the Nexus are placed in the middle section of the ship before the moonpool. The total fuel capacity of the vessel, including both the bunker and day tanks, amounts to 1768 cubic meters. For the purposes of analysis, the overflow and emergency tanks will be excluded from consideration, as the former is intended to remain empty to accommodate any potential overflow of the bunkertanks, and the latter is only utilized in emergency situations when the primary generators are not operational. The MGO service tanks, on the other hand, are situated towards the fore section of the ship in the engine room.

Lastly, it should be noted that the ship also features a void space with a total volume of 3016 cubic meters. While the majority of this space is not designated for storage purposes, the moonpool could potentially be utilized as a suitable storage tank for methanol.

8.2 Dynamic Positioning

To gain an understanding of the requirements for the engine room of a cable laying vessel, it is important to consider the role of DP. DP is technology for cable laying operations and has a significant impact on the load of the grid. As such, a comprehensive understanding of DP technology and its associated requirements is essential for the safe and efficient operation of the engine room and so for this thesis. In Appendix I a summary is shown with all requirements for different classes.

8.2.1 DP class

The IMO defines three primary DP Equipment Classes as follows:

- Equipment Class 1: Loss of position may occur in the event of a single fault.
- Equipment Class 2: Loss of position should not occur in the event of a single fault in any active component or system. Normally static components will not be considered to fail where protection from damage is demonstrated and reliability meets Administration standards. Single failure criteria include any active component or system and any normally static component that is not properly documented with respect to protection and reliability.
- Equipment Class 3: For this class, a single failure includes items listed above for class 2, and any normally static component is assumed to fail, as well as all components in any one watertight compartment from fire or flooding, and all components in any one fire sub-division from fire or flooding.

Additional considerations may be required to achieve a DP class notation with certain classification societies, such as an independent joystick, which some societies require for class 2 or 3. The decision on which class of vessel is appropriate for a particular task is addressed in section 2.1 of 113 IMO – Guidelines for vessels with DP systems [66]. This section suggests that the equipment class of the vessel required for a particular operation should be agreed upon between the owner of the vessel and the customer based on a risk analysis of the consequence of a loss of position. Alternatively, the Administration or coastal State may decide the equipment class for the particular operation. All DP vessels should comply to this principle, regardless of when they were built or what DP notation or class they have. The risk analysis that is called for need not be extensive, but it has to adequately reflect the consequences that a loss of position can reasonably cause or lead to. The best time to carry out a risk analysis is when the work scope is known, and experienced personnel from the vessel are available.

The Nexus has Equipment Class 2 DNV-G classification, equivalent to IMO DP Class 2, requires that all power, control, and thruster systems, as well as any other systems that could potentially affect the DP system's correct functioning, must be configured and provided so that a fault in any active component or system will not lead to a loss of position. This includes components such as prime movers, generators, and their excitation equipment, gearing, pumps, fans, switchboard and control gear, thrusters, and power-actuated valves. Additionally, systems that are not a part of the DP system but could impact its proper functioning in the event of a fault, like fire suppression systems, engine ventilation systems, and shutdown systems, are incorporated into the Failure mode and effects analysis (FMEA). To meet the mentioned criteria, the ship operates with an open bus system, which involves two separate grids, each powered by two diesel engines, later on explained in subsection 8.3.4.

8.3 Power- and Energy systems

In this section, the analysis focuses on the layout and specifications of the current power plant to determine the performance of the existing vessel. This performance will be considered the reference value for any methanol-fueled SOFC power and energy systems in the future, based on the results of this analysis.

8.3.1 Power-plant

To analyze the power plant layout for the Nexus Figure 8.3 and Figure 8.10 are used as resources. The schematic layout of the power plant is shown in Figure 8.4, the engine and propulsion room on the Nexus are separated due to the implementation of a diesel-electric concept. The four diesel engines with generators are located on the tank top. Further specifications of the azimuths and diesel engines will be discussed later.

As mentioned briefly in subsection 8.1.2 the Nexus uses a diesel-electric drive with four energy converters that produce electricity for the main propulsion (two azimuths), board net, and other users. This is illustrated in more detail in figure Figure 8.5. The diesel-electric drive is advantageous in that it can match the energy demand with supply, operating in a more efficient manner. For every operational mode, the number of operating engines can be adjusted to operate at their peak efficiency, providing redundancy for the power supply, which benefits the system's reliability. As mentioned this different if the ship is sailing in DP mode.

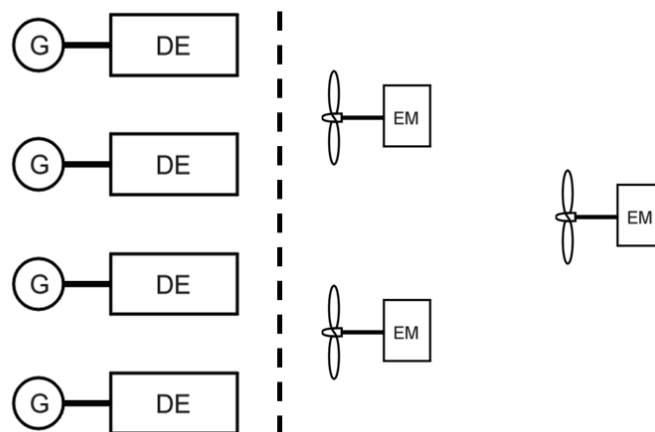


Figure 8.4: DE power- and propulsion plant

To provide a more detailed and complete view of the energy flow on board of the Nexus, an energy flow diagram (EFD) has been created. Figure 8.4 did not fully display the energy demand, hence the need for the EFD which includes additional electrical consumers. The energy flow in figure Figure 8.5 starts with an energy source (ES) located at the top left corner of the diagram. MGO is the energy source and is transferred to the energy converters, which are the main and emergency engines. These

engines convert the chemical energy into mechanical energy, with the emergency generator remaining inactive during normal operations. The mechanical energy is then converted directly to electrical energy by the generator the created AC is fed to the 690V bus. The AC switchboard then distributes the electric power among the main propulsion, transversal propulsion (bow thruster), and other electrical consumers. Using an AC switchboard simplifies the electrical system since many electrical devices and motors on board are designed to operate on AC power and AC power can be transmitted over long distances with less power loss compared to DC power. However, it's worth noting that there are certain disadvantages to using an AC switchboard. For example, AC power requires additional components such as transformers and inverters to convert it to DC power, which can add complexity and weight to the electrical system. Additionally, electrical synchronization when power is supplied by the generators may be slower with an AC switchboard. Despite these disadvantages, the Nexus cable layer uses an AC switchboard since it is a proven and reliable technology for distributing electrical power on board.

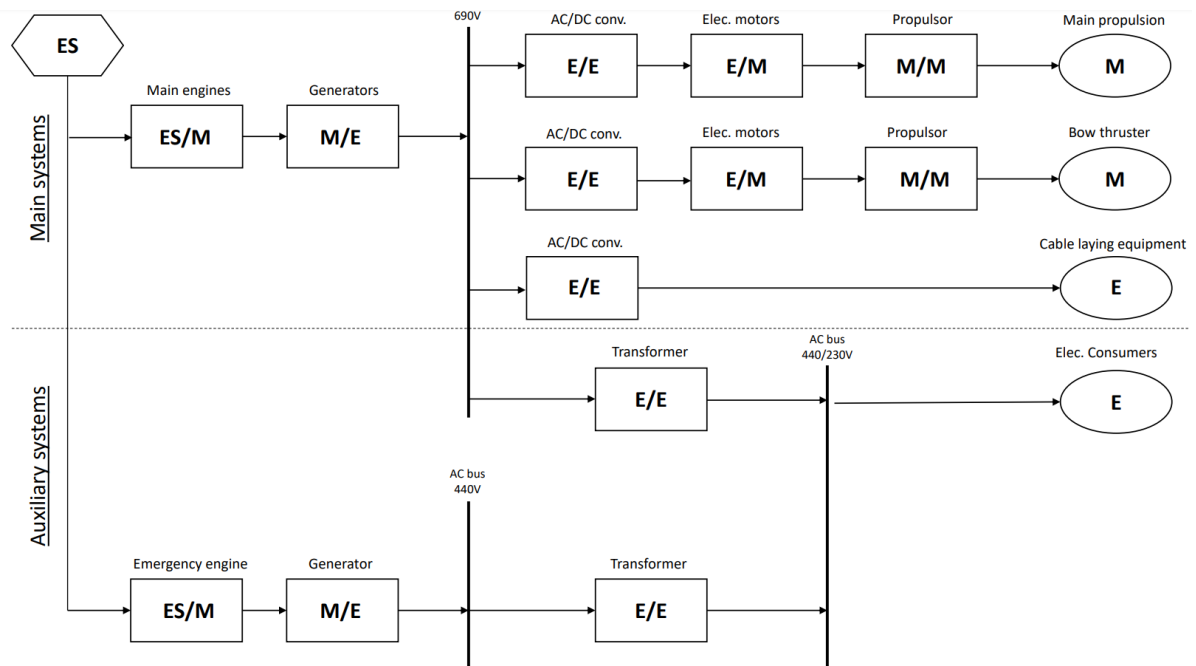


Figure 8.5: EFD of the Nexus

Table 8.4: Type of energy and energy conversion (EFD)

Energy Source	Energy Conversion, Storage & Distribution	Energy Use
ES:	X/Y:	EU:
Chemical	M: Mechanical	M: Mechanical
Solar	E: Electrical	E: Electrical
Wind	H: Hydraulic	Q: Heat/Cold
Nuclear	A: Pneumatic	
	Q: Heat/Cold	

8.3.2 Power distribution

The vessel's primary distribution is 690VAC, 3Ph, 50Hz and is divided into three sections: Port, Centre, and Starboard. The 690V Main Switchboard DP is designed to operate in a split bus configuration with the 690V switchboard bus ties open. The power distribution design follows the DP Redundancy Concept, with distribution boards and consumers segregated per redundancy group through the use of a split bus configuration and consumer segregation. Each 690V switchboard supports one 440V main switchboard and (Port and Starboard only) one 230V switchboard for low voltage distributions. The Starboard 440V Main Switchboard typically powers the 440V Emergency Switchboard. Additionally,

there are five 230V UPS and seven 24VDC systems that are charged from the low voltage distributions.

The principle power distribution of the vessel is illustrated in the following figure:

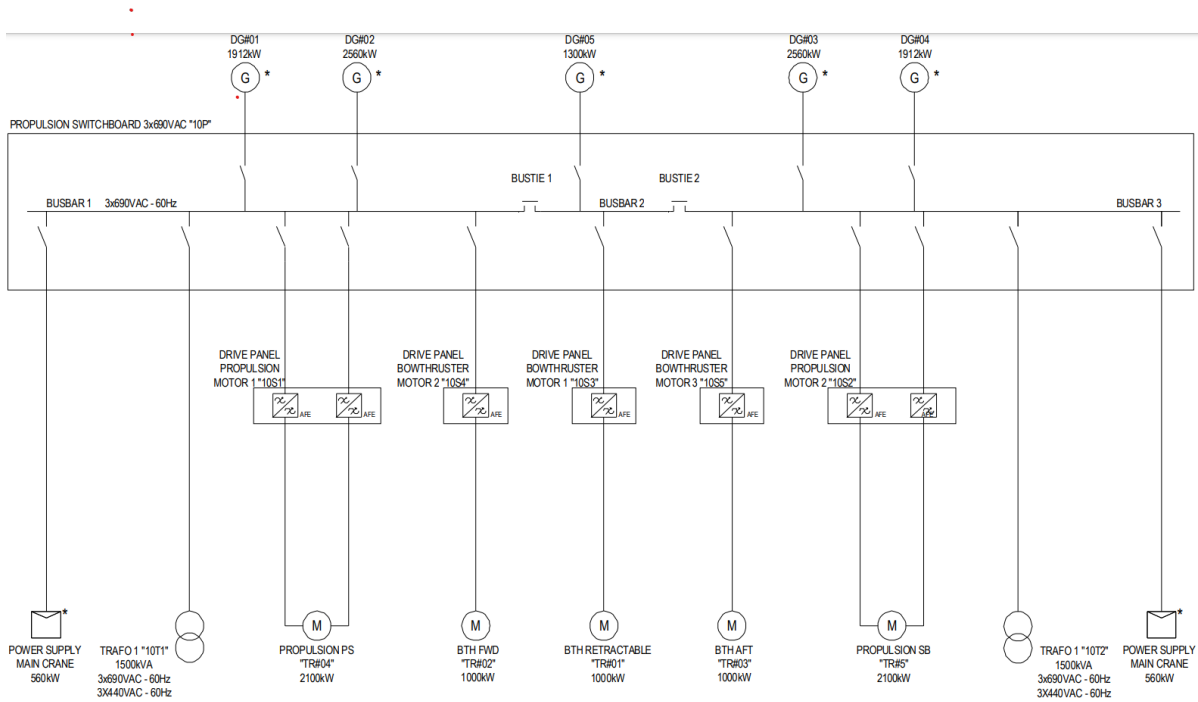


Figure 8.6: Single line power network

Additional details regarding the single power line network mentioned earlier reveal that it includes a main crane supply with a capacity of 560 kW, as well as cable laying installations that require approximately 300 kW of power. These power requirements are important factors to consider for operation of the network.

8.3.3 Components efficiency

To investigate the performance of the power plant on the Nexus, it's important to consider the efficiencies of the various components that make up the power chain. Figure 8.7 provides information on the efficiencies of the total power chain, which can help in assessing the overall performance of the power plant. By analyzing the efficiencies of each component, it is possible to identify areas where improvements can be made to optimize the performance of the power plant.

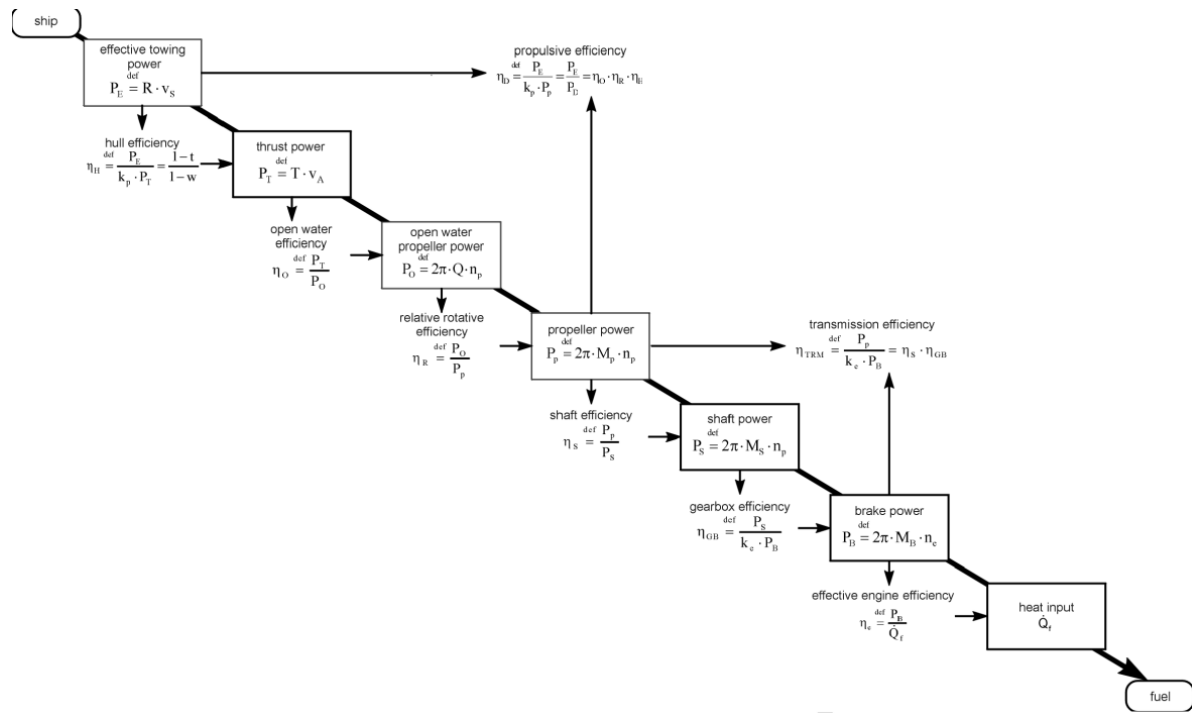


Figure 8.7: Efficiency propulsion plant [46]

Figure 8.8 illustrates the power train of the propulsion system, with efficiencies shown in Table 8.5. The manufacturer MaK calculates the efficiency at maximum rpm or MCR using the Specific Fuel Consumption (sfc). In a conventional mechanical power train, losses occur at the gearbox (η_{GB}) and shaft (η_s), resulting in a transmission efficiency (η_{TRM}) of 98.0%. However, in an all-electric ship concept, electrical losses also play a significant role.

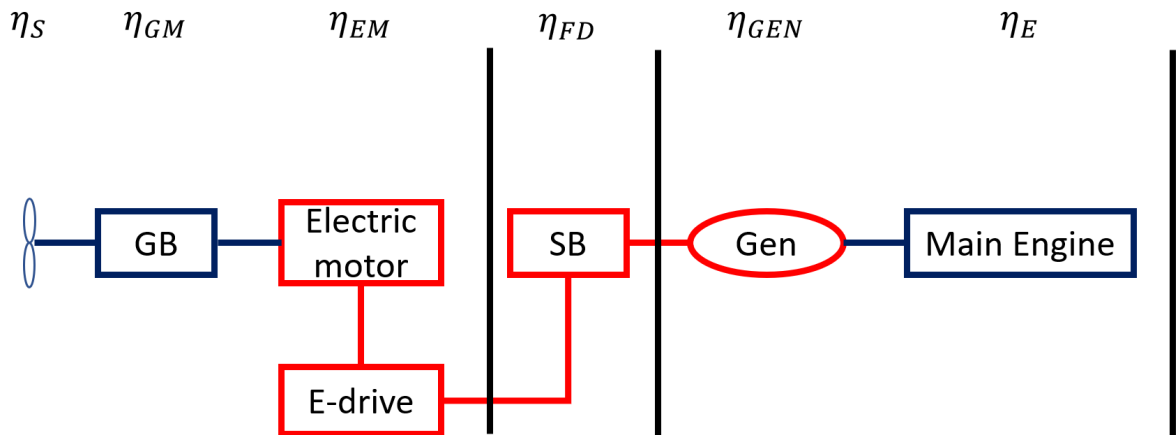


Figure 8.8: Power train

For a diesel-electric drive, there are additional electrical losses at the electric motor (η_{EM}), generator (η_{GEN}), and the variable frequency drive (η_{FD}), resulting in an additional electrical system efficiency of 88.8%. Therefore, the diesel-electric power configuration loses an additional 11.2% of energy compared to the mechanical system. In total, the efficiency from the engine output shaft to the propeller shaft is reduced by 13% in the diesel-electric configuration.

Table 8.5: Efficiency propulsion plant

Component	Parameter	Unit	Ref.
Effective engine	η_E	-	0.45
Generator	η_{GEN}	-	0.95
Switchboard	η_{FD}	-	0.97
Electric motor	η_{EM}	-	0.96
Gearbox	η_{GB}	-	0.99
Shaft	η_S	-	0.99

It should be noted that the electrical efficiency values for the electric motor, generator, and variable frequency drive in a diesel-electric drive may vary with the operating conditions, such as speed and load. For instance, the generator efficiency may decrease at low loads or high speeds. Thus, the efficiency values mentioned are typical or nominal values, and the actual efficiency may deviate from these values depending on the specific operating conditions as can be seen in figure Figure 8.9

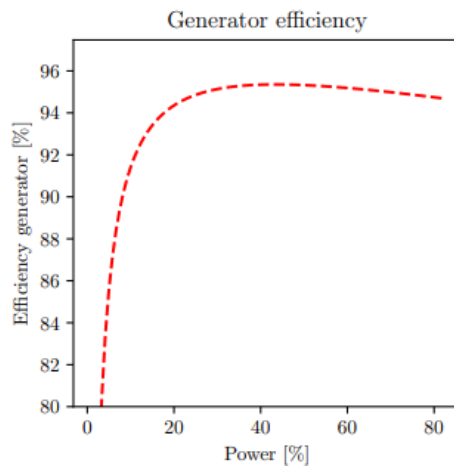


Figure 8.9: The efficiency of the generator [6]

8.3.4 Propulsion plant

The power generation and distribution on the cable laying vessel is divided into three redundancy groups: Port, Centre, and Starboard. This can be seen in Figure 8.10.

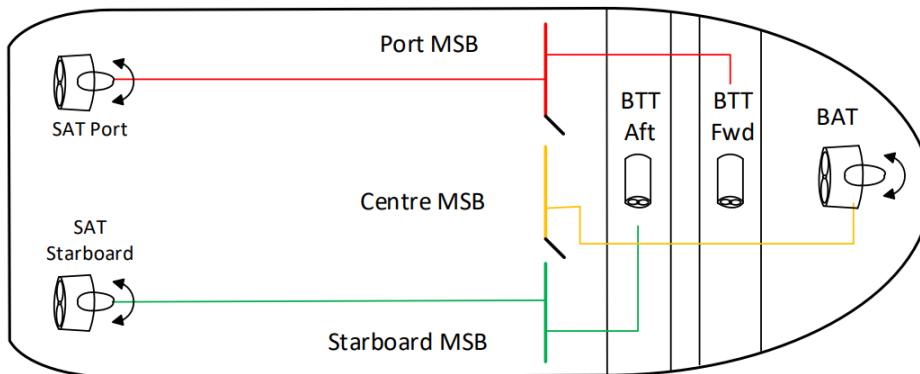


Figure 8.10: Redundancy Concept

Table 8.6: Thruster identification

Thruster	Type	Rating (kW)
Bow Azimuth Thruster	Schottel SRP 1012	1000 kW
Bow Tunnel Thruster Forward	Berg BTT 552	1000 kW
Bow Tunnel Thruster Aft	Berg BTT 552	1000 kW
Stern Azimuth Thruster Port	Berg BAT 626	2100 kW
Stern Azimuth Thruster Starboard	Berg BAT 626	2100 kW

The Port 690V Switchboard is powered by two diesel generators (DG1 & DG2), which supply power to one bow tunnel thruster (BTT Forward) and one stern azimuth thruster (SAT Port). The Port 690V Switchboard also powers the Port 440V switchboards and Port 230V switchboards.

The Centre 690V Switchboard is powered by a single diesel generator (DG5), which supplies power to the Bow Azimuth Thruster (BAT). The BAT is considered the most efficient type of thruster. If this particular thruster fails, it would have the same level of importance as the failure of both a BTT and a stern azimuth thruster combined. The Centre 690V Switchboard also powers a single Centre 440V Switchboard, with no Centre 230V distribution.

The Starboard 690V Switchboard is powered by two diesel generators (DG3 & DG4), which supply power to one bow tunnel thruster (BTT Aft) and one stern azimuth thruster (SAT Starboard). The Starboard 690V Switchboard also powers the Starboard 440V switchboards and Starboard 230V switchboards.

The three redundancy groups are designed to be independent, meaning that when operating in OPEN BUS mode, no single failure will result in the loss of more than two thrusters. Therefore, failures affecting the Port, Centre, or Starboard sections cannot affect any other section. This is also called the 'island' concept.

8.3.5 Power speed curve

The power curve obtained from Damen shipbuilding the data provides important insights into the performance of the ship's engines and their efficiency. It indicates the amount of power required to maintain a certain speed and is a key parameter in determining the fuel consumption and overall operating costs of the vessel. By analyzing the power curve, one can identify the optimal operating conditions for the ship's engines and determine the most fuel-efficient speed. This information is important for a power plant configuration.

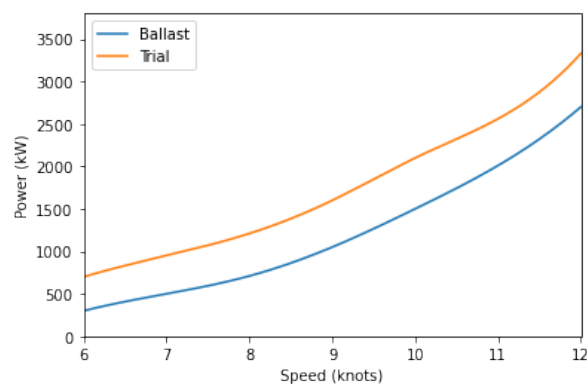


Figure 8.11: Power speed curve

Based on the Figure 8.11, it can be observed that the curve obtained from the trial condition data differs slightly from the predicted ballast curve. This variation may be due to several factors, such as differences in the weight and distribution of the load or environmental factors like wind and current. It is pertinent to note that the speed measurements were conducted with both main engines operating at the specified engine settings. Additionally, the actual consumed power and engine speed were measured directly on the output shaft of the electric motor using strain gauges, ensuring a high degree of accuracy and reliability.

8.3.6 Power estimation per operational mode

In order to conduct a comparative analysis of performance and emissions between the reference and concept designs for cable layer operations, it is important to consider the various tasks involved in a cable lay operation. These tasks can be obtained from data provided by tools like 'Qlik' which provide insights and analytics based on operational data. 'Qlik' is a powerful business intelligence and data visualization platform that can be used to gather and analyze operational data to understand the specific modes of cable layer operations. However, it is worth noting that finding a suitable fit for the modes was quite challenging due to the inherent variety of tasks that cable layers must carry out. The complexities involved in cable laying operations make it essential to carefully analyze and interpret the operational data to ensure a meaningful and accurate comparative analysis.

An analysis has been conducted for the 'Hollandse Kust Noord' project to gain insights into the operational profiles of a cable layer. The 'Hollandse Kust Noord' project is an offshore wind farm located off the coast of the Netherlands shown in Appendix F. The analysis aimed to compare and evaluate the performance and emissions of different designs. To evaluate the comparability of the projects executed by the Nexus, Appendix H showcases the results of other logged projects. A thorough analysis of these projects highlights significant similarities in their outcomes.

As shown in Figure 8.12, a pie chart was generated to illustrate the distribution of operational modes. It was observed that the chart differed slightly from the one presented in Figure 5.2. Notably, the time spent operating in DP mode was found to be significantly higher than initially anticipated. This was likely due to specific operational requirements and conditions. On the other hand, transit time was shorter than expected, owing to the relatively close proximity of the field to the port. The duration of time spent in the harbor aligned with the initial expectations.

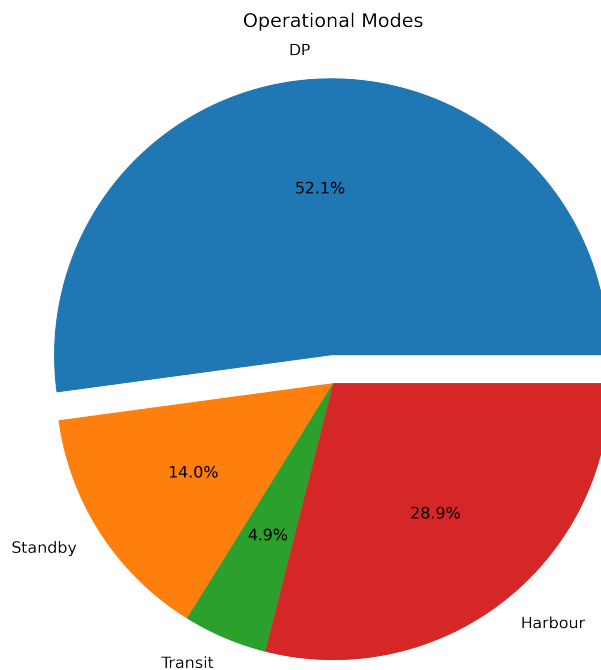


Figure 8.12: Hollandse Kust Noord Operational Profile

Harbour

In the harbor mode, the cable laying ship is stationed at a port or harbor. It is not actively engaged in cable laying operations but is instead moored or anchored. The DP system may be turned off or set to

a low-power mode to conserve energy. The ship is usually prepared for upcoming operations, which may involve loading or unloading cable, equipment maintenance, or personnel transfers.

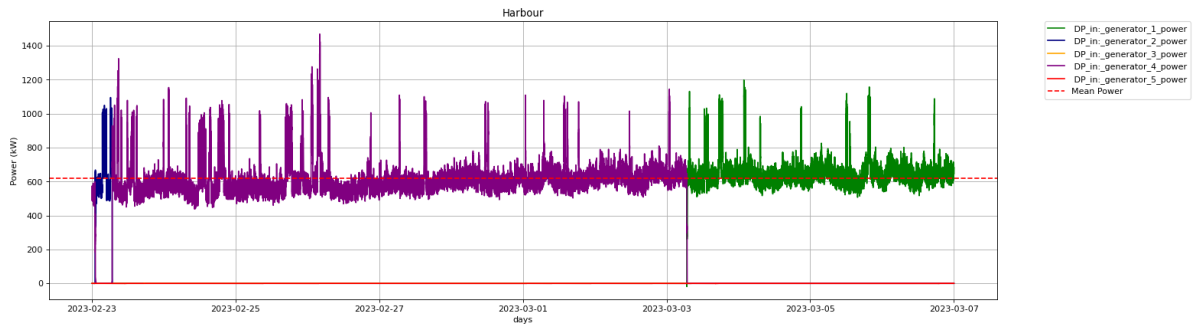


Figure 8.13: Operational mode for harbour mode

Transit

During transit, the cable laying ship is moving between different locations, such as from one cable installation site to another or from a harbor to the cable laying area. The ship’s DP system is typically non-active, continuously adjusting the ship’s position and heading to maintain a desired course and speed is done by the the two Stern Azimuth Thrusters (SAT).



Figure 8.14: Operational profile for transit mode



Figure 8.15: Operational profile for transit mode

Standby

The standby profile refers to a state where the cable laying ship is on standby mode near the cable installation area. This could be while waiting for favorable weather conditions, coordinating with other vessels, or addressing any unexpected issues before commencing or resuming cable laying operations. In standby mode, The DP system may be turned off or set to a low-power mode to conserve energy, maintaining a fixed position or following a predefined pattern to remain within the designated operational area.

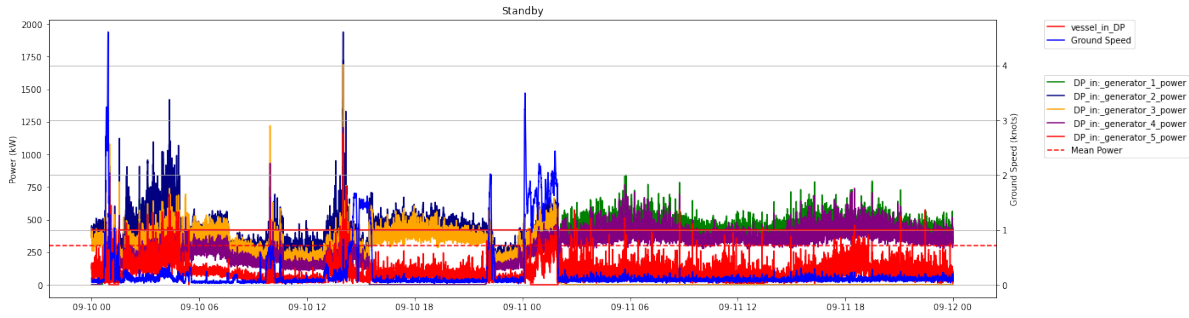


Figure 8.16: Operational profile for standby mode

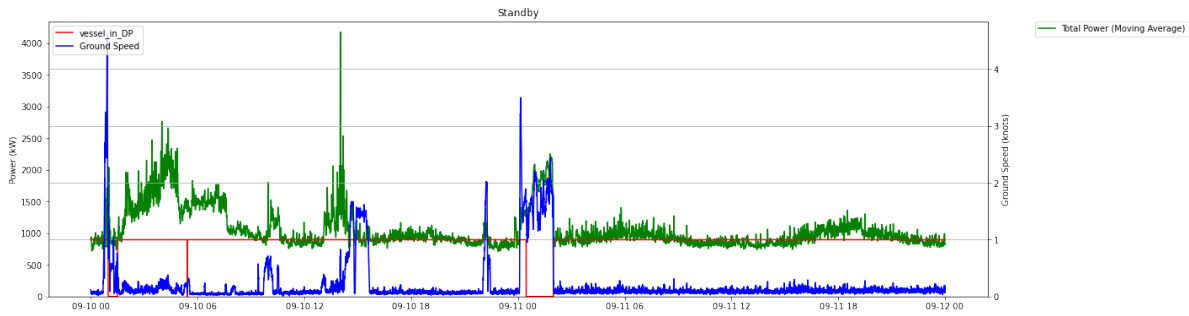


Figure 8.17: Operational profile for standby mode

DP operations

DP operation is the primary operational mode for a cable laying ship. During cable laying operations, the ship uses its DP system to maintain a precise position and heading while laying the submarine cables on the seabed.

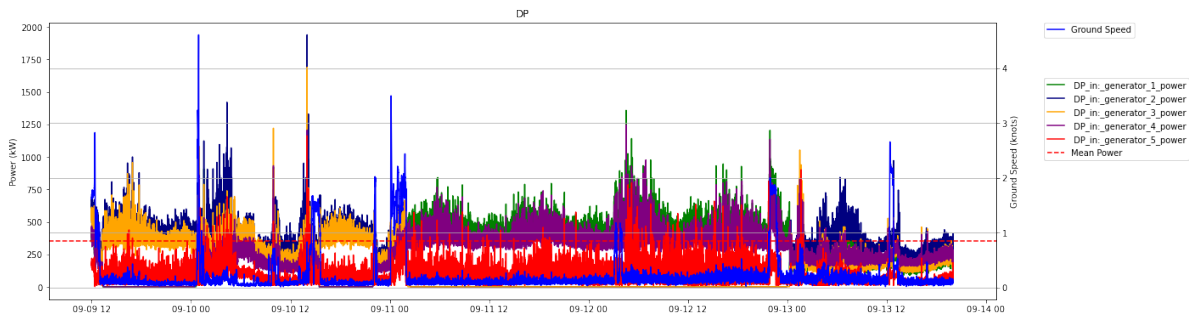


Figure 8.18: Operational profile for DP mode

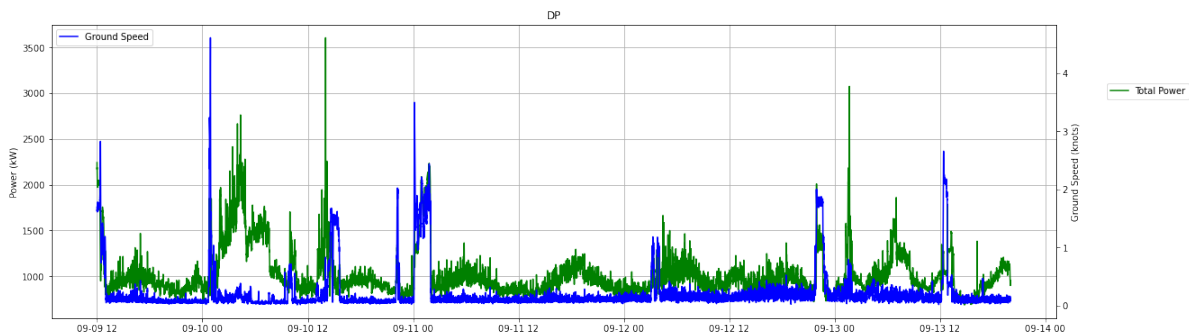


Figure 8.19: Operational profile for DP mode

Table 8.7 summarizes the mean power per generator and total power for each operational mode. The DP mode has a mean power of 353 kW, resulting in a total power of 1059 kW. The Waiting mode has a mean power of 541 kW, with a total power of 1082 kW. The Transit mode has a mean power of 1526 kW, contributing to a total power of 4578 kW. Finally, the Harbour mode has a mean power of 638 kW, matching the total power of 638 kW.

Table 8.7: The mean power per generator and total power for each operational mode

Operational modes	Power per generator [kW]	Total power [kW]
DP	353	1059
Standby	541	1082
Transit	1526	4578
Harbour	638	638

8.4 Conclusion

In this chapter, the focus lies on introducing the reference design for the Nexus cable layer vessel. The design incorporates purpose-built deck equipment to facilitate cable laying activities. These components are strategically integrated to optimize the vessel's agility and speed, aligning with specific operational demands. The power plant configuration of the reference design adopts a diesel-electric layout, accommodated within a dedicated engine room featuring three distinct bus bars. Two out of the three buses powered by a pair of engines and one bus powered by a single engine resulting in a total of five diesel engines. Additionally, a higher-positioned emergency diesel generator, complete with its switchboard, is part of the design. Notably, this overall setup provides an adaptable foundation for the potential SOFC and battery system. Propulsion is managed through two azimuth stern thrusters, two bow thrusters, and a single azimuth bow thruster, effectively creating three redundant groups. This arrangement ensures that a failure in one group does not compromise the vessel's DP capabilities. It's noteworthy that the stern azimuth thrusters also serve transit functions, achieving a maximum speed of 12.4 knots, while the designated cruising speed is set at 11 knots. Lastly, a comprehensive evaluation of the Nexus's power requirements has been conducted, considering an operational profile derived from a specific project. The analysis identifies four distinct modes: DP, harbor, standby, and transit. For each mode, calculations have been carried out to determine total power consumption and power distribution per generator. A finding is that transit mode exhibits a power demand approximately three times higher compared to other operational modes. However, the engine loads are well-suited to the engine's design in this scenario. Conversely, during DP and standby modes, the engines operate with notably lower loads.

Performance indicators

This chapter compares emissions for the four operational modes presented in subsection 8.3.6. It discusses how the amount of CO₂ emissions is dependent on fuel usage and the sulfur content in the fuel, with MGO producing SO_x emissions while methanol does not. MGO also contains particulate matter, while methanol does not. The level of NO_x emissions is uncertain, but it is assumed that NO_x emits the amount that is designed to comply with Tier II regulations. Additionally, this section mentions that fuel consumption and emissions are performance aspects used to determine performance indicators. The results of this analysis will be used as reference points for comparing the power plant configurations.

9.1 Fuel consumption

Fuel consumption serves as a crucial parameter that is analyzed based on the ship's operational mode and data from engine manufacture Appendix B . It directly affects the vessel's profitability and the emission of pollutant gases such as CO₂, NO_x, SO_x, and others. One of the key performance indicators used is SFC, which measures the amount of fuel consumed per unit of generated energy in kilowatt-hours (kWh).

Figure 9.2 illustrates the SFC for various loading conditions. Figure 9.1 trend line is included in the figure to illustrate the extent of the increase or decrease in SFC as the load varies. Notably, there is a significant increase in SFC when the engine operates below 50% of its maximum power, and this increase becomes even more pronounced below 25% of the load, following the trend line. Another noteworthy characteristic of the engine is the relatively constant SFC between 50% and 100% of the Maximum Continuous Rating (MCR).

On the other hand, Figure 9.2 displays the FC in kg/h, which appears to be almost a linear line. This observation may seem contradictory when compared to the previous figure. However, this phenomenon can be explained by considering that at low loads, a lower amount of power (in kW) is delivered, resulting in a relatively smaller total fuel consumption. Nevertheless, operating at low rates decreases efficiency and leads to an increase in unnecessary running hours.

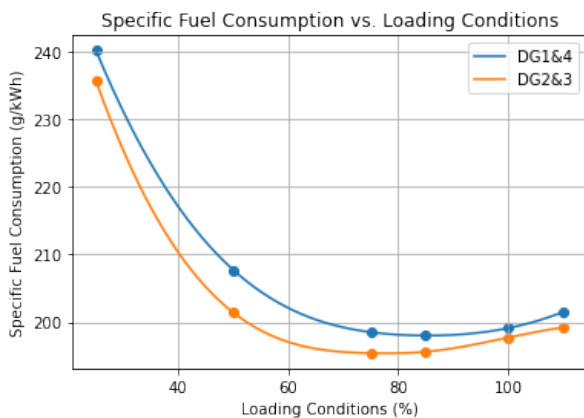


Figure 9.1: SFC (g/kWh)

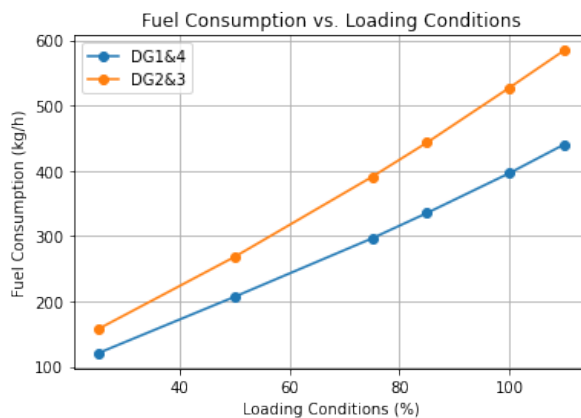


Figure 9.2: FC (kg/h)

The combination of both figures provides insights into the relationship between SFC, engine load, and total fuel consumption, allowing for a analysis of the engine's performance under different operational conditions.

The fuel consumption per operational mode is presented in Table 9.1. calculation is shown in Appendix I.

Table 9.1: Fuel consumption per operation mode

Operational mode	Fuel consumption	
	g/kWh	kg/h
DP operations	262,86	318,46
Standby	239,58	273,16
Transit	197,47	943,53
Harbour	225,73	235,88

9.2 Emission Indicator

In this section, a overview is provided regarding the various emissions linked to MGO. The primary emphasis is on the emissions generated onboard the vessel (tank-to-wake emissions). Nevertheless, it's essential to highlight that the research scope contains emissions origin from the fuel extraction or generation process (well-to-tank emissions). The significance of well-to-wake emissions lies in their role as a robust method for assessing GHG emissions equitably. Furthermore, these emissions play a crucial role in calculating project emissions from a performance perspective [22].

This research will not use Energy Efficiency eXisting ship Index (EEXI) as indicator , simply because it is not suitable for assessing the energy efficiency of offshore vessels due to their different goals and regulations.

In the analysis conducted, the emissions will be expressed in CO₂e, which refers to carbon dioxide equivalent. CO₂e is a widely used metric in environmental assessments to quantify and compare the global warming potential of various GHG in relation to carbon dioxide (CO₂). GHG, such as methane (CH₄) and nitrous oxide (N₂O), have different capacities to trap heat in the atmosphere compared to CO₂. To facilitate meaningful comparisons, emissions of these gases are converted into CO₂e by multiplying them by their respective global warming potential factors. This allows for a standardized assessment of the overall warming impact of different GHG over a specific time frame, typically 20 years (*GWP₂₀*) or 100 years (*GWP₁₀₀*). As can be seen in Table 9.2

Table 9.2: Overview of GWP100 and GWP20 factors as in IPCC AR6 [48]

Greenhouse gas	Formula	CO ₂ e <i>GWP₁₀₀</i>	CO ₂ e <i>GWP₂₀</i>
Carbon dioxide	CO ₂	1 (ref)	1 (ref)
Methane	CH ₄	29.8	82.5
Nitrous oxide	N ₂ O	273	273
Black Carbon	BC	900	3200

The concept of GWP takes into account two key properties of a GHG. The first property is the GHGs capacity to trap heat radiated from the earths' surface (i.e.: its instantaneous warming potential). The second property is the GHGs longevity (the time that is stays in the atmosphere before degrading or being absorbed). Combining the two properties yields the aggregate warming potential of the GHG over a defined time horizon when compared to the reference GWP factor of 1 for CO₂. Box 1 contains the GWP factors for a time horizon of 20 years and for 100 years:

- CH₄ has a higher GWP factors over 20 years than over 100 years. This due to the fact that CH₄ degrades quite rapidly leading to lower GWP factor over 100 years than over 20 years.
- N₂O is very persistent leading to equal GWP factors for 20-years and 100-year time horizons.
- BC has a high GWP factor (also box 1) especially for the shorter time horizon of 20 years, since it is relative short-lived.

For the fuel type MGO 0.1%S (Marine Gas Oil with sulfur content of 0.1%), the emissions associated with its combustion can be assessed in terms of CO₂e are show in Table 9.3.

Table 9.3: WTW emission MGO

Fuel type	Emission type	Factor	Unit
MGO	TTW CO ₂	3,206	t/t
	TTW CH ₄	0,002	t/t
	TTW N ₂ O	0,044	t/t
	TTW CO ₂ e	3,252	t/t
	WTW CO ₂ e	3.967	t/t

By combining the tables for fuel consumption per operational mode (Table 9.1) and emissions of MGO (Table 9.3), the CO₂e emissions can be derived for each specific operational mode. This analysis quantifies the GHG emissions associated with each mode and provides valuable insights into their environmental impact. This information enables the evaluation of emissions performance across various operational scenarios and facilitates the identification of potential strategies for emission reduction and optimization.

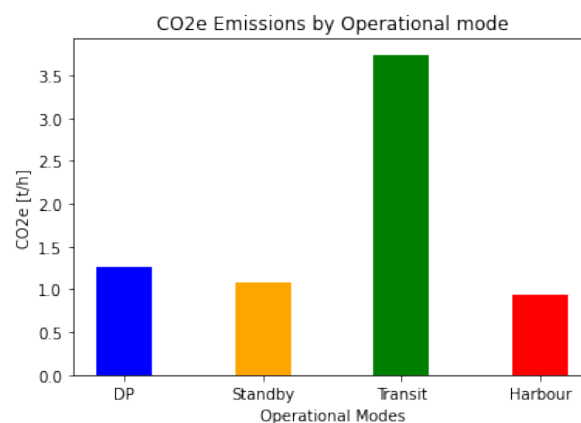


Figure 9.3: CO₂e Emissions by Operational mode

The provided CO₂e values correspond to different operational modes: DP, Standby, Transit, and Harbour. The Standby and Harbour modes have relatively lower CO₂e values, indicating lower associated emissions. On the other hand, the DP and Transit modes have higher CO₂e values, suggesting relatively higher emissions during dynamic operations and vessel transit. These values provide an initial indication of the emissions associated with each operational mode.

9.3 Conclusion

In this chapter, a performance analysis has been conducted, focusing on fuel consumption and emissions as key indicators. The assessment begins by examining fuel consumption, particularly with regard to the four diesel engines. A comparison is made between fuel consumption measured in g/kWh and kg/h. These metrics serve as the basis for calculating fuel consumption across the four distinct operational modes. The findings reveal that g/kWh values, indicative of efficiency, demonstrate favorable results for the Transit mode, whereas other modes exhibit less advantageous figures. The main reason for this difference is that, as per class requirements, the DP and standby modes involve using power

from two engines for the bus. These engines run at relatively lower loads during these modes, and so less efficient. Conversely, kg/h values, representing actual consumption, are relatively moderate across the three modes (DP, Harbor, and Standby), with the highest consumption observed during Transit. Transitioning to emission indicators, the analysis focuses on expressing emissions in terms of CO₂e for the WTW emissions. This metric offers a more basis for comparison. The analysis underscores that CO₂e emissions in t/h (tons per hour) exhibit similar levels across DP, Transit, and Harbor modes, with Transit mode registering approximately three times higher emissions. This difference is primarily attributed to the heightened power demand during Transit and, consequently, increased fuel consumption.



Case Study

Case study approach

The objective of this chapter is to create a power plant layout for a cable laying vessel. This layout employs SOFCs and batteries to meet the power requirements for three out of the four operational modes. The SOFCs need to be engineered to provide a consistent load output, while the battery pack is designed to manage loads beyond the SOFC capacity and serve as a reserve power source.

The chosen power plant design must maintain to the specific requirements outlined in previous chapters for the cable layer. These requirements consist of:

- Cable carousel of 5000 tons
- Top speed of 12,4 kn
- Cruise speed of 11 kn
- Accommodation for 90 persons
- Self-sufficient for 21 days

The overall system design for the cable layer vessel commences with the integration of SOFCs and their associated support systems. These components, contains the fuel cell stacks, BoP equipment, and peak load shaving batteries, are shared among all configurations of power plants.

After finalizing the power plant configuration, attention is redirected to the design of the vessel's storage capability integration.

SOFC and battery module design

This chapter takes look into a detailed study focused on creating a SOFC and battery module design. The cable laying activities has unique requirements for power and flexibility, needing a power system that can handle changing power needs during cable laying tasks.

10.1 SOFC manufacturers

This section provides an overview of the current fuel cells available in the market, with a focus on their application in the marine environment for main propulsion of vessels. Only the promising types of fuel cells and manufacturers offering higher power ranges are included, as ship propulsion typically requires megawatts of power. Other manufacturers that produce smaller fuel cell modules for household use are not considered in this research due to the challenges in scaling them for higher power demands and the limited experience of the manufacturers. Additionally can be concluded that there are currently SOFCs available on the market at this power output for marine applications. However, based on the information regarding existing SOFC designs and the prospects of the companies manufacturing them, assumptions can be made regarding the parameters of a SOFC system at a megawatt scale for use in the power plant of a vessel.

10.1.1 Bloomenergy

Bloom Energy is a leading provider of SOFC technology, offering innovative Energy Servers that convert various fuels into clean and efficient electricity. Their solutions are scalable, reliable, and help accelerate the transition to a zero-carbon future. Bloom Energy is committed to delivering sustainable energy solutions for commercial, industrial, and residential customers, while reducing carbon emissions and improving energy resiliency.

The Bloom Energy Server 5.5	
Load output [kW]	330
Weight [tons]	17.3
Dimensions LxBxH [m]	10.21x1.32x2.21
Cumulative electrical efficiency [%]	65-53

Table 10.1: The Bloom Energy Server 5.5 [13]



Table 10.2: The Bloom Energy Server 5.5 [13]

10.1.2 Mitsubishi Hitachi Power Systems

Mitsubishi Hitachi Power Systems (MHPS) has developed a pressurized hybrid power generation system that integrates SOFC stacks with micro gas turbines (MGT). The system uses hydrogen and operates at high temperatures of around 900 °C. It achieves high efficiency by generating electricity through the chemical reaction between oxygen, hydrogen, and carbon monoxide extracted from the gas. The system's combined efficiency can exceed 65% by recovering exhaust heat as steam or hot water. Compared to conventional power generation, this hybrid system reduces CO₂ emissions by approximately 47%.

MEGAMI 200kW	
Load output [kW]	200
Weight [tons]	33
Dimensions LxBxH [m]	11.4x3.30x3.20
Cumulative electrical efficiency [%]	73

Table 10.3: MEGAMI 200kW [104]

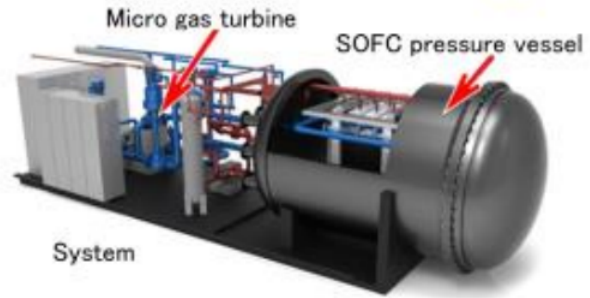


Table 10.4: MEGAMI 200kW [104]

10.1.3 Convion Ltd.

Convion Ltd. is a fuel cell system developer that was established in 2012. In January 2013, the company acquired Wärtsilä’s fuel cell program and continued the development and commercialization of products based on SOFC technology as an independent entity. With a focus on distributed power generation fueled by natural gas or biogas, Convion aims to be a leading provider of SOFC systems in the power range of 50-300 kW. The company’s shareholders include VNT Management and Wärtsilä. Convion is dedicated to offering power generation solutions based on SOFC technology.

Convion C60	
Load output [kW]	60
Weight [tons]	-
Dimensions LxBxH [m]	3.5x1.9x2.3
Cumulative electrical efficiency [%]	60

Table 10.5: Convion C60 [72]



Table 10.6: Convion Ltd. [72]

10.1.4 FuelCell Energy

FuelCell Energy is a leading company that specializes in fuel cell technology and clean energy solutions. They offer a reliable, efficient, and ultra-clean power generation solution. One of their existing fuel cell systems has a capacity of 250 kW and is designed to be fuel flexible. It is capable of running on natural gas, renewable biogas, or hydrogen.

FuelCell Energy	
Load output [kW]	250
Weight [tons]	-
Dimensions LxBxH [m]	10.66x2.43x3.04
Cumulative electrical efficiency [%]	65 +/-2

Table 10.7: FuelCell Energy [30]

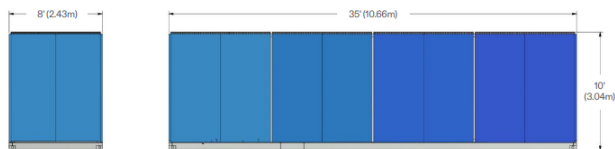


Table 10.8: FuelCell Energy [30]

In addition to their existing fuel cell technology, FuelCell Energy has also presented a new ambition to scale up SOFC modules to form a megawatt power plant. This technology utilizes a Compact Solid Oxide Architecture (CSA) stack. The CSA stack is a promising advancement in fuel cell technology that offers potential for increased power output and efficiency as can be seen in Table 10.10.

CSA Stack is an advanced design approach that incorporates several key features to achieve optimal performance and efficiency. One of its core aspects is the use of thinned components, specifically in the cell and interconnect, which allows for a significant reduction in stack material content. This reduction aims to achieve a high power-to-weight ratio, targeting approximately 0.5 kW/kg. By minimizing the amount of material used, the CSA Stack becomes more compact and lightweight, making it ideal for applications with limited space and weight restrictions.

FuelCell Energy (CSA stack)	
Load output [kW]	322
Weight [tons]	0.72
Dimensions LxBxH [m]	approx. 6x2x2
Cumulative electrical efficiency [%]	57

Table 10.9: FuelCell Energy (CSA stack) [30]

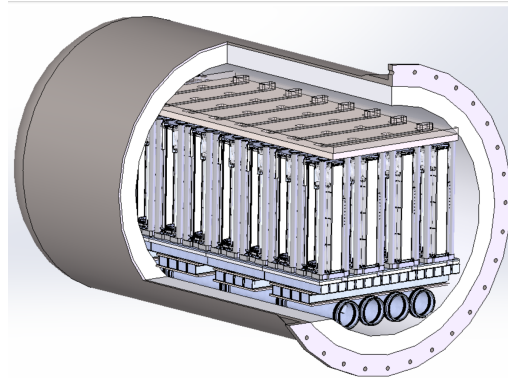


Table 10.10: FuelCell Energy (CSA stack) [30]

In addition to thinned components, the CSA Stack incorporates a simplified unit cell with fewer components. This design streamlining not only simplifies the manufacturing process but also enables automated assembly. By reducing the number of individual parts, the stack becomes easier to produce, resulting in improved efficiency, reduced costs, and enhanced scalability. Effective thermal and flow design is another crucial aspect of the CSA Stack. Temperature control within the module is achieved through meticulous engineering of the thermal properties of the components and the implementation of optimized cooling mechanisms. These measures ensure that temperature variations are minimized and that there is a uniform distribution of temperature throughout the stack. This is essential for maintaining consistent performance and reliability.

Despite the promising features of the CSA Stack, including thinned components, a simplified unit cell, automated assembly, and advanced thermal and flow design, its current TRL prevents its widespread use. The stack's TRL indicates that it is still in the early stages of development and has not yet undergone sufficient testing and validation for commercial deployment. Therefore, while the CSA Stack shows potential, further research and development are needed to enhance its reliability and performance before it can be considered for practical applications.

10.2 SOFC configuration

The design and sizing of the power system are dependent on the operational mode analysis presented in subsection 8.3.6. Due to a multitude of factors, sizing the SOFC 1:1 is not feasible. Several assumptions need to be established to accurately determine its appropriate size.

The efficiency curve is a crucial aspect to consider in this research; however, the availability of options in the SOFC market is currently limited, and manufacturers are hesitant to disclose detailed information due to the ongoing investigation of this technology. Based on the data presented in section 10.1 and the insights provided by Dr. ir. L. van Biert, the assumed efficiency curve for a SOFC module in this

research is depicted in Figure 10.1. The curve illustrates that below a 20% load, the fuel cells are unable to generate any power. At 20% load, the efficiency is estimated to be approximately 53%, reaching its maximum value of 67% at a 60% load, before decreasing back to 53% at 100% load. Figure 10.1 demonstrates the polynomial fit of the efficiency values, representing a second-degree polynomial that can be utilized to calculate efficiencies at different load levels.

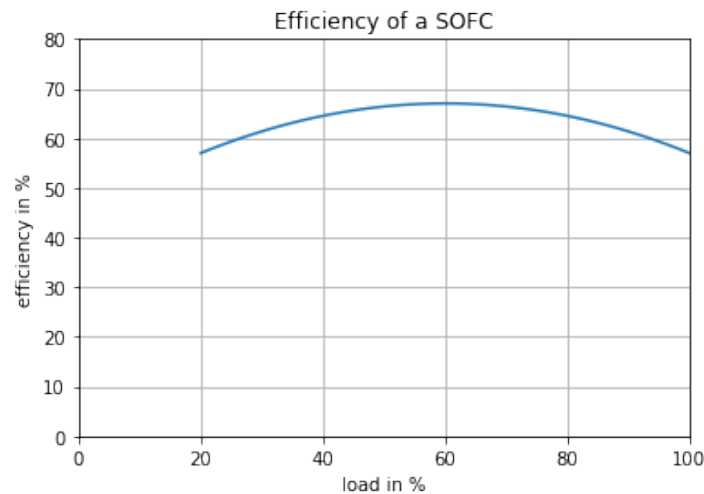


Figure 10.1: Efficiency of a SOFC

10.2.1 Factors Affecting SOFC Degradation

Like any energy conversion technology, SOFC can experience degradation over time. Here are some key factors influencing SOFC degradation:

- **Operating Temperature:** High temperatures accelerate material degradation.
- **Thermal Cycling:** Frequent temperature changes induce stress and microstructural alterations.
- **Redox Cycling:** Changes in fuel/air composition cause chemical and structural changes.
- **Contaminants:** Small impurities catalyze reactions and degrade performance.
- **Material Degradation:** Electrodes and electrolytes degrade over time.
- **Operating Conditions:** Extreme conditions accelerate degradation.

In the context of performance decay and the limited replacement opportunity for SOFC after five years, adopting an "end-of-life" design approach becomes crucial for the SOFC system. This approach involves initially over-powering the system to ensure it meets power demands throughout its operational lifespan.

Currently verified long-term SOFC stack endurance, operating for more than 1.5 years with 3% cathode air humidity, shows a degradation rate of 0.26% per 1000 hours [31]. Another study mentions a degradation rate of <0.5%/1000 hours [99]. The US Department of Energy has set targets of <0.2% per 1000 hours by 2025/30; however, for now, a rate of 1% per 1000 hours is considered [96].

Therefore, the latter value is used to overpower the SOFC plant, considering desired system longevity. It's important to note that SOFC performance decay also depends on usage patterns, especially cooling-down frequency. Extended periods of idle operation without power production can negatively affect decay. Thus, these factors must be carefully considered in the end-of-life design of the SOFC system.

10.2.2 Balance of Plant

The BoP for the SOFC system contains various auxiliary components and subsystems that play a crucial role in supporting the overall functionality of the SOFC stack. The BoP ensures the efficient operation and integration of the fuel processing system, stack operation, and heat management processes. By optimizing the performance of these auxiliary systems, the BoP enhances the overall efficiency, stability, and safety of the SOFC system.

One of the central components within the BoP is the methanol fuel processing system. This system entails the treatment of liquid methanol, which is then directed to the fuel processor (not shown in Figure 10.2). Within the fuel processor, a series of steps are employed to convert the methanol into a hydrogen-rich gas mixture, commonly known as syngas. This syngas is subsequently heated and conveyed to the anode of the SOFC stack, where it undergoes electrochemical reactions to generate electricity.

Concurrently, an air blower supplies atmospheric air to the cathode of the SOFC stack. Prior to entering the fuel cell, this air is preheated in a heat exchanger. The generated electricity is a product of the electrochemical reactions occurring within the SOFC stack. Moreover, surplus hydrogen, which may result from the fuel processing process, is managed within the BoP. It is partially recycled and reintroduced into the system, while the excess is combusted in a catalytic burner. This controlled combustion not only prevents the accumulation of excessive hydrogen, which poses a flammability risk, but also supports the reforming process in the fuel processor.

In parallel to the fuel processing system, the SOFC stack operation involves the effective management of methanol and air feeds. Methanol, initially stored as a liquid at ambient conditions, is depressurized and its flow rate is regulated through a valve to match the operational pressure of the SOFC stack. Accompanied by the required airflow provided by the air blower, both the methanol and air streams are preheated using dedicated anodic and cathodic heat exchangers. This preheating process is crucial to avoid thermal stress on the stack and ensure its optimal performance.

The interaction of the anode and cathode recirculation streams with the methanol and air feeds, respectively, further demonstrates the intricate nature of the BoP. The unrecirculated anode off-gas and cathode off-gas are effectively managed by combining them and subjecting them to combustion in an afterburner. This controlled combustion ensures the complete utilization of any unreacted hydrogen, leading to efficient resource utilization.

For a visual representation of the SOFC propulsion system utilizing methanol as fuel, refer to Figure 10.2. In terms of the air requirements, it is assumed that a SOFC container in this system would require an air-to-fuel ratio (λ) of 2.5. This ratio, which determines the stoichiometric balance between air and fuel for efficient combustion, has been used in previous research and confirmed with experts in the field of SOFCs. [38].

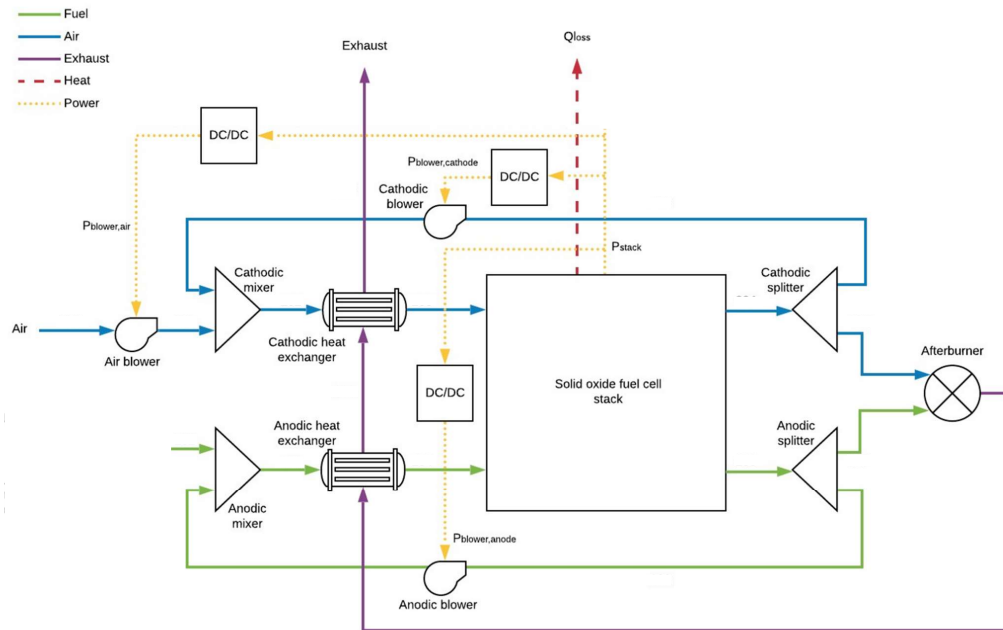


Figure 10.2: SOFC System configuration [38]

10.2.3 SOFC sizing

To appropriately size the SOFC, it's important to estimate the necessary quantity of both SOFC modules and battery modules during the initial conceptual design phase. The ultimate goal of this design process is to minimize emissions across different operational modes, DP, waiting, and harbor operations. To effectively manage the varying load demands associated with these modes, the approach involves selecting the mode with the highest demand as the basis for sizing calculations.

Based on the data presented in subsection 8.3.6, an estimate can be derived for the quantity of SOFC modules required to accommodate an average power output of 1082 kW.

To accurately determine the size requirements of a SOFC module throughout its lifespan (5 years), including degradation, the following calculation is employed:

$$\text{Effective Capacity} = \frac{\text{Required Power}}{1 - \left(\frac{\text{Degradation Rate}}{100} \right) \times \left(\frac{\text{Total Time Period}}{1,000} \right)} \quad (10.1)$$

Plugging in the values:

$$\begin{aligned}
 &= \frac{1,082}{1 - \left(\frac{1}{100}\right) \times \left(\frac{43,825}{1,000}\right)} \\
 &= \frac{1,082}{1 - 0.43825} \\
 &\approx \frac{1,082}{0.56175} \\
 &\approx 1926\text{kW}
 \end{aligned}$$

Therefore, considering the degradation rate and total time period, a power pack with an effective capacity of approximately 1926 units would be required to meet the power demand of 1082 units over the specified duration.

10.2.4 Dimensions & Weights of SOFC configuration

To accurately estimate the weight of a SOFC configuration, it is necessary to consider more than just the weight of the fuel cell stacks. Since SOFC systems are not yet widely used on a large scale, specific information about the weight of such systems is limited. However, existing literature provides valuable insights into various components and their associated weights, as shown in Table 10.11.

Table 10.11: Literature assumptions for SOFC module

Performance Specification	Values	Unit
Nominal electrical power output (kW)	1925,0	kW
Voltage output	690,0	V
Cell Gravimetric Energy Density	20,0	W/kg
Cell Volumetric Energy Density	12,0	W/L
Electric efficiency	65-53	%
Fuel consumption	0,4	kg/kwh
Fuel mass flow rate	3×10^{-2}	kg/s
Degradation per 1.000hr	1,0	%

When estimating the weight of a SOFC configuration, consider the following factors:

1. Fuel cell stacks: Include the weight of the ceramic electrolyte, anode, cathode, and interconnects.
2. BoP : Account for components like fuel and air supply systems, reformers, gas purification systems, heat exchangers, pumps, fans, compressors, and control systems.
3. Enclosure and housing: Consider the weight of the structure that protects and supports the SOFC system.
4. Thermal management systems: Account for insulation materials, cooling systems, and heat sinks.
5. Ancillary components: Consider sensors, monitoring systems, electrical wiring, connectors, and safety devices.
6. System integration: Include the weight of structural supports, frames, and other elements for assembly and installation.

The total weight of a SOFC configuration can be estimated by combining the weights of these various components as can be seen in .

Table 10.12: Dimensions reference fuel cell [28]

Dimensions		
Fuel Cell Module and Mechanical Balance of Plant	total length:	7.69 m
	wideness:	3.06 m
	height:	3.90 m
Electrical Balance of Plant	total length:	4.90 m
	wideness:	0.6 m
	height:	2.2 m

Table 10.13: Weights reference fuel cell [28]

Weights		
Mechanical Balance of Plant	6,5	t
Electrical Balance of Plant	2,5	t
Fuel Cell Module	16	t

It is important to note that the weight estimation is based on scaling from existing examples, such as similar-sized power plants utilizing MCFC. The weight of the support systems for a SOFC container is estimated by scaling the BOP component weights of a 250kW plant [28]. The weight of the cylinder housing the stacks (the SOFC module) is assumed to be proportionate to the area of a 20-foot container as can be seen in .

This example is chosen because it provides the most detailed information in comparison with other manufacturers' data, allowing for a more accurate estimation of the weight distribution within the SOFC configuration. The scaling approach based on a well-documented MCFC reference system aids in bridging the knowledge gap and obtaining reasonable weight approximations for the various components involved in a SOFC setup

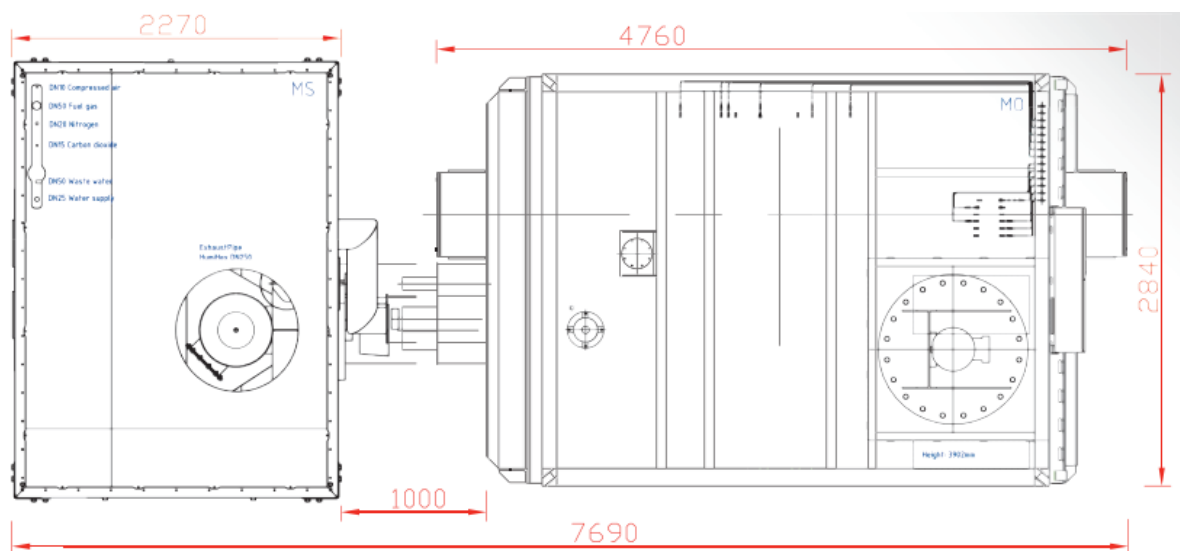


Figure 10.3: Dimensions SOFC configuration

The decrease in gravimetric and volumetric energy densities is primarily attributed to the impact of auxiliary systems, particularly the BoP components. These necessary systems contribute to a notable increase in the overall weight and volume of the SOFC configuration. This effect is clearly demonstrated in the following Table 10.14.

Table 10.14: Specifications including auxiliary systems SOFC

Performance Specifications	Values	Unit
Cell Gravimetric Energy Density	20 → 15.6	W/kg
Cell Volumetric Energy Density	42 → 2.5	W/L

10.3 Batteries configuration

SOFCs exhibit poor dynamic response characteristics, making them unable to rapidly react to sudden changes in load. Consequently, the inclusion of batteries is necessary to handle peak loads effectively. Based on information obtained from manufacturers and experts, it is anticipated that SOFCs can respond to a load change within fifteen minutes when maintained in an idle state. This implies that it takes approximately fifteen minutes for them to transition from an idle mode to operating at 100% load.

During idle periods, the fuel cells are kept at a static power output, whereby they can charge the battery pack. Because when the fuel cells are cold, they require a longer period of time to warm up before they can operate efficiently and prevent cell damage. The specific warm-up time varies depending on the manufacturer, but it typically takes at least a couple of hours. As a result, to avoid damaging the cells. This approach ensures that the cells are ready to respond promptly to load demands and minimizes the risk of thermal stress or other potential damage associated with frequent heating and cooling cycles.

During the time it takes for a vessel to transition from idling to full load, it needs to source additional energy from another power source. In this case, batteries are being proposed as the solution to provide the required power. The advantage of using batteries is that they can immediately supply the necessary energy, and their usage is limited to a specific timeframe of 20 minutes. This makes batteries a suitable choice for meeting the vessel's power needs during this transitional period.

10.3.1 Factors Affecting Battery Degradation

A focused literature review was conducted to assess and compare different battery manufacturers with a specific focus on battery degradation, as outlined in the study by [39]. This review aimed to provide insights that remain relevant in the medium term, considering the swift and ongoing advancements in battery technology.

Among the various battery chemistries considered, NMC (nickel manganese cobalt) lithium-ion batteries were selected as a primary focus due to their notable characteristics, including high energy densities and promising performance outcomes. NMC batteries have demonstrated the potential to deliver efficient energy storage solutions, making them a prominent choice for various applications. However, it is noteworthy that the review also examined another prominent battery chemistry known as LFP (lithium iron phosphate). Despite its strengths and advantages, current findings suggest that, at the present moment, NMC batteries still maintain a competitive edge over LFP batteries in terms of energy density and overall performance. This is likely to influence the selection of NMC batteries as the preferred choice for certain applications, especially when considering medium-term requirement

Manufacturers are already producing these batteries for automotive applications, reaching energy densities of 250 Wh/kg [39]. When the cells are grouped into a module, the total energy density of the module is calculated using a packing factor. In the study [54] stands at 1.3 for the gravimetric energy density and 1.6 for the volumetric energy density. As a result, the effective gravimetric energy density of a battery module decreases to 192.3 Wh/kg.

When sizing a battery system, the following degradation's needs to be considered.

- Capacity degradation: Batteries lose their total capacity over time due to chemical reactions and aging.

- Cycle life: Charging and discharging cycles contribute to battery degradation and reduce its overall capacity.
- Temperature sensitivity: Extreme temperatures can accelerate battery aging and degrade its capacity.
- Depth of Discharge (DoD): Battery lifespan can be extended by not fully discharging it during each cycle.
- C-rate: High-frequency cycling and rapid charging/discharging can accelerate degradation.

In Figure 10.4 the graph shows that batteries last longer when charged up to 75% and discharged to 10-75% capacity (orange points). In contrast, batteries used more intensely, charged to 100% and discharged to 25% (black points), like in smartphones, deplete faster and endure fewer cycles.

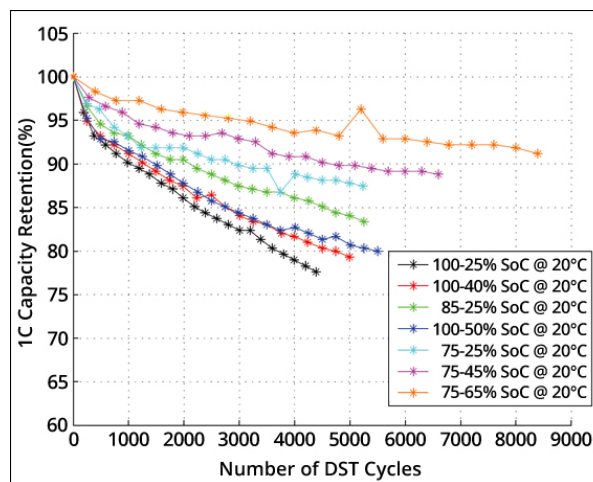


Figure 10.4: Capacity loss as a function of charge and discharge bandwidth [89].

As said batteries will inevitably degrade over time. For instance, an NMC lithium-ion battery charged at a 3C rate has been shown to lose 21% performance after 2000 full cycles [83]. Consequently, it is reasonable to anticipate similar degradation for a battery discharged at a 3C rate with a 90% DoD after the same number of cycles. In this context, 2000 full cycles would correspond to more than one full cycle per day if the vessel operates continuously. However, the batteries would only be fully charged in extreme cases, suggesting that the assumption of 2000 full cycles is a conservative estimate for a cable layer that operates for 10 years.

10.3.2 Batteries sizing

To determine the appropriate size of a battery system for a given application, an analysis is conducted involving the calculation of Cumulative Distribution Functions (CDFs) for each generator set. A CDF represents the probability distribution of a random variable, in this case, the rate of change of power (dP/dt) for each generator. The CDF provides insights into the distribution of power changes over time for a particular generator set. It allows to understand the likelihood of observing different power change values. By examining the CDF, one can determine the proportion of time that the power change falls below or above specific thresholds.

In the analysis conducted to calculate the size of the battery system, the most demanding operational mode is selected as the dataset for generating the CDF. This operational mode represents the scenario with the highest power demand or consumption, excluding transit-related data. By selecting the most

demanding operational mode, the analysis focuses on capturing the maximum power fluctuations and ensuring that the battery system is appropriately sized to handle these demanding conditions. Transit-related data, which may not reflect the peak power demands of the system, is excluded to ensure a more accurate representation of the operational requirements.

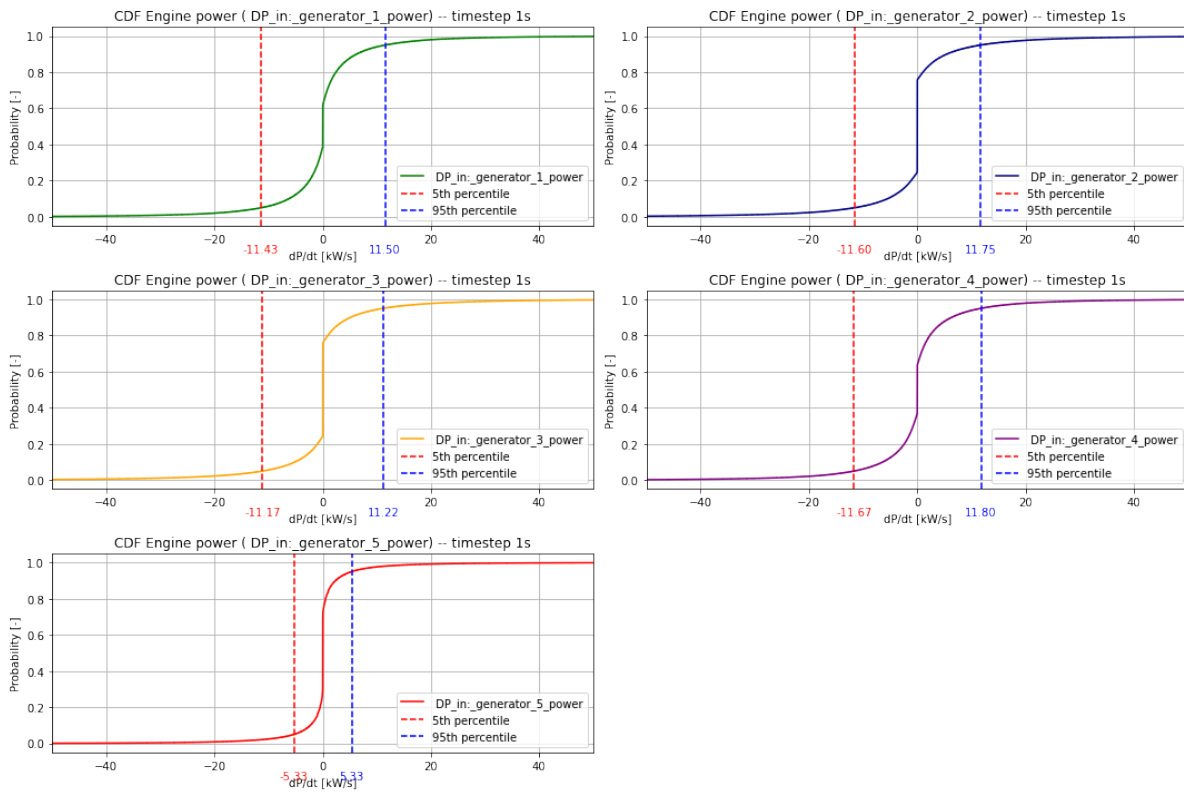


Figure 10.5: CDF Engine power

In this analysis shown in Figure 10.5, the 5th and 95th percentiles are of particular interest. The 5th percentile represents the threshold below which only 5% of power changes fall, while the 95th percentile represents the threshold below which 95% of power changes fall. These percentiles act as boundaries for the acceptable power change range. By examining the portions of the CDF beyond the 5th and 95th percentiles, it becomes possible to identify instances where the power change exceeds the expected range. This information is crucial in designing a battery system since it helps determine the capacity required to accommodate the excess power demand or supply beyond the normal operating range of the generators.

The required technical battery capacity to cope with loads outside the 5th and 95th percentiles is: **606.0kWh** . Calculation shown in Appendix C.

In the case of a DP 2 ship, there are additional class requirements to consider, particularly the inclusion of a spinning reserve. The spinning reserve refers to the surplus power capacity available in the battery system, which can be utilized to address sudden changes in power demands or failures. This ensures uninterrupted position maintenance for the ship.

The level of redundancy or reserve is determined by the degree of separation and independence of systems related to propulsion and steering, both mechanically, electrically, and spatially. This level is represented by an additional index denoted as x%, which in the case of Nexus, means that 40% of the gensets' power must be available for a duration of 20 minutes.

In Equation 10.2, a calculation is provided to determine the required capacity of a battery acting as spinning reserve. As previously mentioned, there are two different outputs for the gensets: 1910 kW and 2560 kW. For safety reasons, the higher output is considered in the calculation.

$$\begin{aligned}\text{Level of reserve} &= \text{Power output} \cdot \text{Level of redundancy} \cdot \text{Time} & (10.2) \\ &= 2560\text{kW} \cdot 40\% \cdot 0.33\text{hr} \\ &\approx 338\text{kWh}\end{aligned}$$

The required class battery capacity is **338 kWh**, this capacity should always available in cause of a failure.

The netto capacity is calculated as follows:

$$\begin{aligned}\text{Total battery capacity} &= \text{Technical capacity} + \text{Level of reserve} & (10.3) \\ &= 606.0\text{kWh} + 338\text{kWh} \\ &= \mathbf{944\text{kWh}}\end{aligned}$$

To accurately determine the size requirements of a battery module throughout its 10-year lifespan, taking into account the degradations discussed in the previous subsection 10.3.1, an end-of-life calculation is conducted. This calculation aids in assessing the appropriate size and capacity needed to maintain optimal performance and efficiency over the module's operational period.

$$\begin{aligned}\text{Effective Capacity} &= \frac{\text{Required Power}}{1 - \left(\frac{\text{Degradation Rate}}{100}\right)} & (10.4) \\ &= \frac{944}{1 - \left(\frac{21}{100}\right)} \\ &= \frac{944}{1 - .21} \\ &\approx \frac{944}{0.79} \\ &\approx \mathbf{1195 \text{ kWh}}\end{aligned}$$

Based on the degradation rate and the total time period, it is determined that a power pack with an effective capacity of approximately 1195 kWh is required to meet the power demand of 944 kWh over the specified duration, as shown in Figure 10.6. Furthermore, it is evident that the installed capacity is almost double of what is actually needed, which will prove beneficial in mitigating the effects of degradation over time.

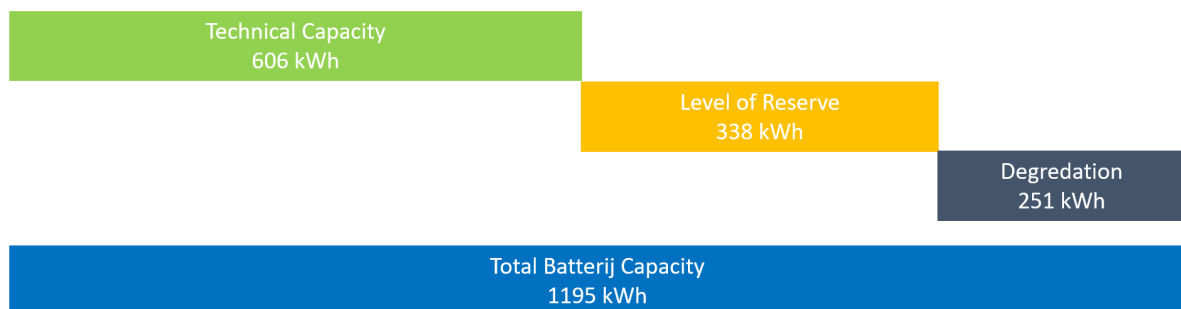


Figure 10.6: Battery Capacity Full Breakdown

10.3.3 Dimensions & Weights of Batteries configuration

Table 10.15 presents the specifications utilized for calculating the batteries required for the Nexus. Corvus Energy [2] was selected as manufacture as it delivers class proved battery systems. To determine the realistic C-rate of NMC lithium-ion cells, . The company offers batteries that can handle a discharge rate of up to 3C at temperatures between 10-25°C. Not charging batteries to full capacity can extend their lifespan, so the DoD was limited to 90%.

Table 10.15: Literature assumptions for NMC Lithium-Ion Batteries

Performance Specifications	Values	Unit
Cell Gravimetric Energy Density	250	Wh/kg
Cell Volumetric Energy Density	468	Wh/L
Gravimetric Packing Factor	1.3	
Volumetric Packing Factor	1.6	
C-Rate for 10-25°C	up to 3	
Depth of Discharge	90	%
Degradation at 2,000 Full Cycles	21	%

In addition to the batteries themselves, the power distribution systems for the Nexus project require modifications in several components, including the main switchboard, intermediate switchboard, LV transformers, and drive systems. The weights and dimensions of these components are provided below:

Table 10.16: Dimensions reference battery system

Dimensions			
Battery and Mechanical	total length:	5.91	m
	wideness:	0.74	m
Balance of Plant	height:	2.24	m
Electrical	total length:	5.6	m
Balance of Plant	wideness:	0.6	m
	height:	2.23	m

Table 10.17: Weights reference battery system

Weights		
Mechanical Balance of Plant	9.4	t
Electrical Balance of Plant	4.5	t
Battery system	13.9	t

The Table 10.18 provide revised performance values for the NMC Lithium-Ion Batteries, considering the impact of additional components. The gravimetric and volumetric energy densities are lower due to the inclusion of auxiliary systems, especially the cooling system, which significantly contributes to the decrease in the volumetric energy density. These auxiliary components, such as switchboards and transformers, are essential for the proper functioning and safety of the battery system but also affect its overall energy density and physical dimensions.

Table 10.18: Specifications including auxiliary systems

Performance Specifications	Values	Unit
Cell Gravimetric Energy Density	250 →77	Wh/kg
Cell Volumetric Energy Density	468 →88	Wh/L

10.4 Power plant design

The analysis of the new power and energy system involves examining its mechanical, electrical, and heat aspects. In relation to the propulsion system, the mechanical components are deemed less important since they retain their identical structure from the current power plant.

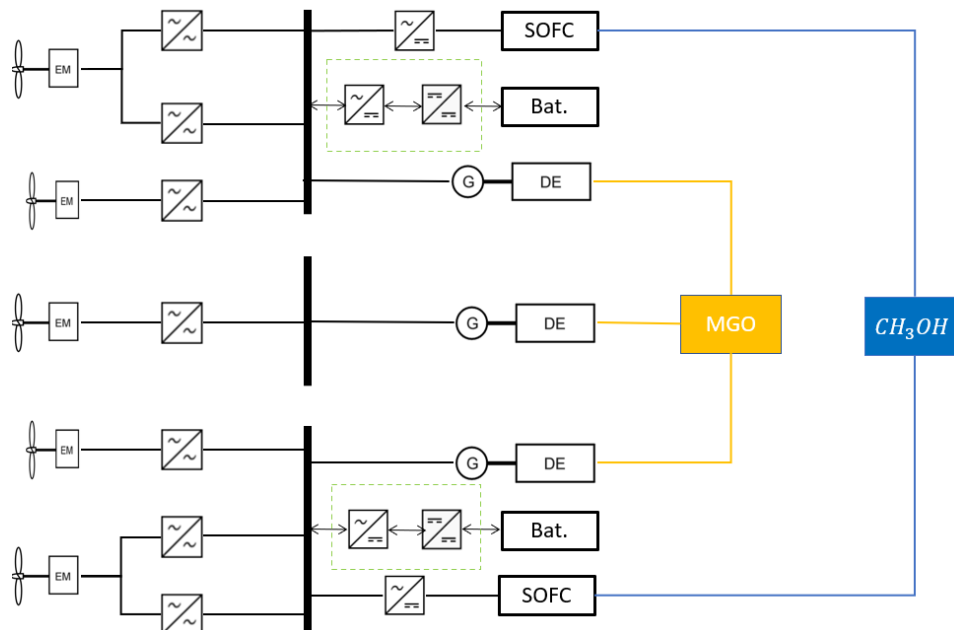


Figure 10.7: Power plant concept

The concept depicted in Figure 10.7 showcases a significant transformation on the power plant side, while the propulsion system remains unaltered. Specifically, the illustration highlights the replacement of two main engines (DG 1 & 4) with SOFC-battery modules. Unlike the main engines that rely on MGO, these modules are fueled using methanol. A notable addition visible in the figure is the green square symbolizing the directional converter. This converter plays a crucial role in maintaining a balanced and stable power supply. It facilitates a seamless transition between different operational scenarios: firstly, in instances where there is a surplus demand for power, the excess energy stored in the batteries can be channeled back into the grid. Conversely, during periods of inadequate power demand, the batteries can be recharged using the available energy sources. This dynamic approach helps optimize the utilization of energy resources and ensures that the power distribution remains reliable.

To enhance the coordination and effectiveness of this modified power plant setup, an Energy Management System (EMS) has been introduced into the power management system. The EMS serves as a sophisticated control system designed to optimize energy generation, distribution, and consumption. It plays a vital role in maintaining a harmonious balance between power generation, storage, and supply. By continuously monitoring various factors such as demand, availability of fuel, state of charge of batteries, and overall system efficiency, the EMS makes real-time decisions to ensure optimal operation and minimal wastage. It essentially acts as the "brain" behind the entire power plant concept, enabling intelligent decision-making and efficient energy usage.

The model depicted in Figure 10.8 provides a visual representation of how the Power Management System (PMS) is integrated into the broader power plant setup. While this model could potentially be utilized to estimate fuel consumption and emissions, it's important to note that the creation and detailed design of such a model are beyond the scope of the current research or study. Instead, the focus is on illustrating the integration of SOFC-battery modules, highlighting the role of the directional converter, and emphasizing the importance of the Energy Management System in optimizing the overall energy

ecosystem.

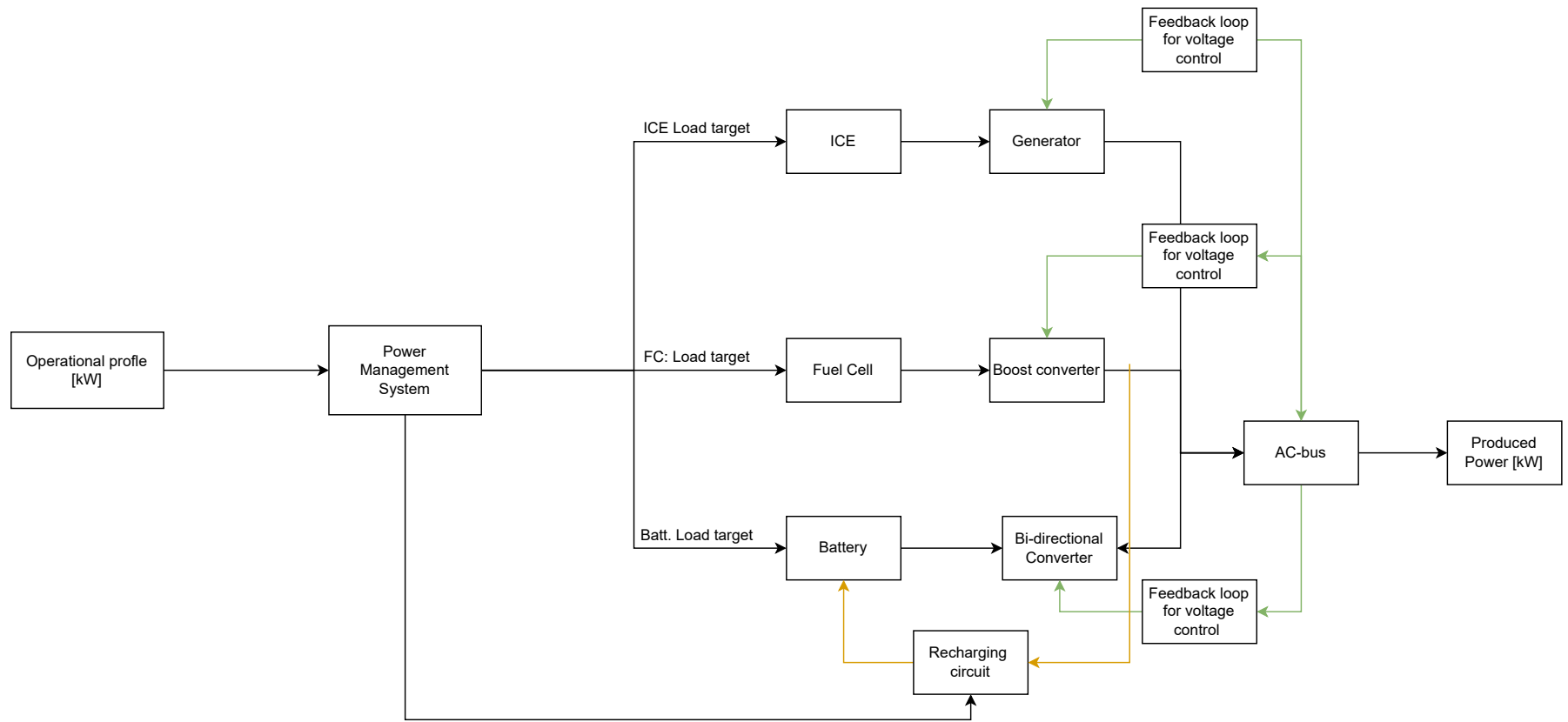


Figure 10.8: Power plant model depicting the integration of SOFC-battery modules.

10.5 Conclusion

In this concluding chapter, the engineering of the SOFC and battery modules is discussed. The approach involves scaling the model for three operational modes and choosing for conventional diesel engines for Transit due to their high fuel consumption and limited usage time. For the SOFC, due to a lack of information, a comparison of several manufacturers is undertaken to ascertain dimensions, weight, and TRL. Bloomenergy is selected as the reference fuel cell for efficiency assumptions, while the DFC@250 EU MCFC-Fuel Cell is chosen for dimensions and weight considerations. Despite limited technical data, an efficiency curve is constructed using a second-degree polynomial. Additionally, a degradation rate of 1% per 1000 hours is established. Consequently, the SOFC is sized at a net of 1082 kW and a gross of 1926 kW, ensuring a 5-year lifespan. However, it's noteworthy that these calculations, based on manufacturer information, reveal discrepancies from assumptions in existing literature, particularly in terms of volume energy density, which falls short by a factor of five.

Turning to the battery aspect, a similar approach is undertaken. Initially, a focused literature review is conducted to explore battery technologies. While considering the possibility of using existing engines to manage fluctuating demand, the decision is made to opt for batteries that offer emissions reduction. NMC technology is favored over LFP, primarily due to its higher volume energy density. The analysis involves assumptions regarding degradation rates, cycles, c-rate, and DoD. To size the battery module, the CDF method is employed, which helps gauge the proportion of time that power changes fall within specific thresholds, accounting for the maximum dynamic capability of an SOFC. Instances falling outside these limits necessitate the involvement of the battery system. Additionally, adhering to DP class regulations, a reserve capacity is incorporated, and a 10-year degradation timeline is factored in. This culminates in a required battery capacity of 1195 kWh. Employing this value, the battery pack's dimensions and weight are determined. Notably, the results indicate that battery packs deviate from literature assumptions, yet their power densities remain acceptable.

In the final analysis, the proposed power plant is presented, comprising two main diesel engines fueled by MGO, accompanied by two SOFC-battery systems fueled by methanol.

Ship design and Arrangement

Storing fuel on board a vessel presents challenges due to safety regulations, limited space, and the requirements of fuel cells. Efficient storage involves minimizing volume loss, considering cofferdams and tank shapes, and ensuring safe containment for fuel cells. Balancing safety and space limitations while optimizing fuel storage and consumption is crucial.

11.1 General storage considerations

Effective storage of methanol, used as fuel in SOFC systems on cable layers, is vital for the operation, reliability, and safety of these systems.

- **Safety:** Methanol, being flammable and harmful upon contact or ingestion, requires storage conditions that prevent combustion and leakage. The high vapor pressure of methanol and its corrosive nature towards certain materials further necessitates pressure-resistant and corrosion-resistant storage systems.
- **Space and Weight:** Designing a storage system on a cable layer demands optimization between methanol capacity and minimal weight and spatial footprint. It's crucial to maintain the ship's stability and balance and to consider ease of access for maintenance and emergencies.
- **Compatibility with SOFC:** Methanol storage systems must ensure purity and regulate the pressure and temperature of methanol to comply with the operational needs of SOFCs.
- **Environmental Impact:** Storage methods must be designed to prevent spills and leaks, minimize waste generation, and limit emissions. Sustainability in material selection for the storage system is also desirable.

11.2 Classification rules

Regulations governing methanol and ethanol fueled ships can be complex, covering a wide range of safety measures, design specifics, and operational procedures. Some of these important regulations, as suggested in the text provided, can be broadly categorized into the following areas. For a list of all rules see [23] or [64]

General Ship Arrangement: Ships using methanol or ethanol as fuel need to meet specific design and arrangement standards. This includes requirements regarding cofferdams (an empty space providing a second layer of protection) around fuel tanks, the positioning of the alcohol system, and escape routes not passing through hazardous areas.

Design and Arrangement of Methyl/Ethyl Alcohol Tanks: The rules the specific location and structural requirements of tanks containing fuel. For instance, these tanks should not be located within accommodation spaces or machinery spaces of category A. Also, they should be designed to withstand the strength requirements defined in NR467, Part B, Chapter 7.

Independent Fuel Tanks: Independent tanks may be located on open decks or in a fuel storage hold space and are to be fitted with specific protective measures and safety systems. These tanks should be secured to the ship's structure, designed to handle maximum expected static, dynamic inclinations, and accidental loads.

Portable Tanks: Portable fuel tanks must also meet certain requirements such as securing to the deck or hold space, consideration of the ship's strength, and the effect of the portable fuel tanks on the ship's

stability. Connections to the ship's fuel piping systems are to be made by means of approved flexible hoses suitable for methyl/ethyl alcohol.

Machinery Space: A single failure within the fuel system should not lead to a release of fuel into the machinery space. All fuel piping within machinery space boundaries are to be enclosed in gas and liquid tight enclosures.

Location and Protection of Fuel Piping: There are clear regulations on where fuel pipes can be located, including a minimum distance from the ship's side, restrictions on leading them through specific spaces, and requirements for mechanical protection.

Enclosed Spaces Design: There are also regulations on the design of enclosed spaces, including requirements for bilge systems, drip trays, and the arrangement of entrances and other openings. For example, bilge systems in areas where methyl/ethyl alcohol can be present must be segregated from other spaces.

Airlocks: Airlocks should be mechanically ventilated at an overpressure relative to the adjacent hazardous area or space, and should be fitted with an alarm system to give a warning if more than one door is moved from the closed position.

11.3 Fuel storage options

This section aims to identify and evaluate potential areas on the Nexus for storing methanol. The assessment will be based on classification rules that outline the advantages and disadvantages of three types of fuel tanks suitable for methanol storage. Furthermore in Appendix D a list is presented with used/unused ships tanks.

The three types of fuel tanks being investigated are as follows Figure 11.1:

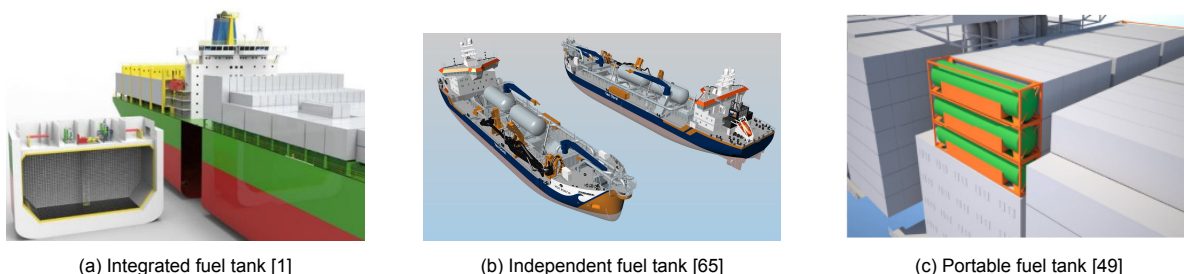


Figure 11.1: Storage options

Placement options are analysed per defined section (which are determined by the cofferdams) which are:

- Fore ship
- Mid ship
- Aft ship

11.3.1 Fore ship

In the fore ship section the following components are located:

- Engine room
- Accommodation

- Tanks

in Figure 11.2 illustrates the visualization of spaces using colored boxes. The engine room is represented by a red box, the accommodation by a orange box, and the tanks by a green box.

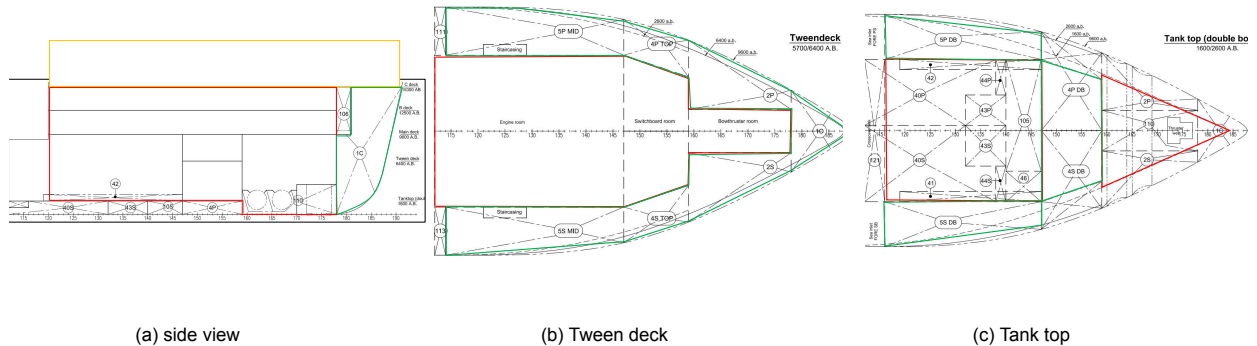


Figure 11.2: Fore ship

Table 11.1 provides an overview of the advantages and disadvantages of storing methanol in the fore ship, specifically focusing on the engine room, accommodation, and tanks.

Table 11.1: Advantages and disadvantages for storing methanol in fore ship

Engine Room		Accommodation		Tanks	
Advantages	Disadvantages	Advantages	Disadvantages	Advantages	Disadvantages
Shorter fuel lines, reducing risk of leaks	Increase the risk of fire hazards Require additional ventilation and safety measures Limited storage capacity	Leaks or spills can be better controlled and monitored	Not approved by class Increase fire risk in living space Decreases overall safety for crew	Tanks designed for methanol provide containment and control for fuel handling Can be located to optimize weight distribution and stability of the ship	Loss of ballast capacity Cofferdam needed

In terms of the engine room, storing methanol in the fore ship offers the advantage of shorter fuel lines, reducing the risk of leaks. However, it also increases the risk of fire hazards and requires additional ventilation and safety measures. For the accommodation area, one advantage is that leaks or spills of methanol can be better controlled and monitored. However, this approach is not approved by class and increases the fire risk in the living space, posing a safety concern for the crew. Regarding the tanks, those designed for methanol provide containment and control for fuel handling, optimizing weight distribution and stability of the ship. On the downside, using these tanks leads to a loss of ballast capacity and requires the use of a cofferdam

11.3.2 Mid ship

In the mid ship section the following components are located:

- Moonpool
- Double bottom tank
- Side tank
- MGO tank
- Work deck

in Figure 11.3 illustrates the visualization of spaces using colored boxes. The moonpool is represented by a purple box, the double bottom tanks by a Dark green box, the side tanks by a light green box, The MGO tanks by a brown box and the work deck by an orange box.

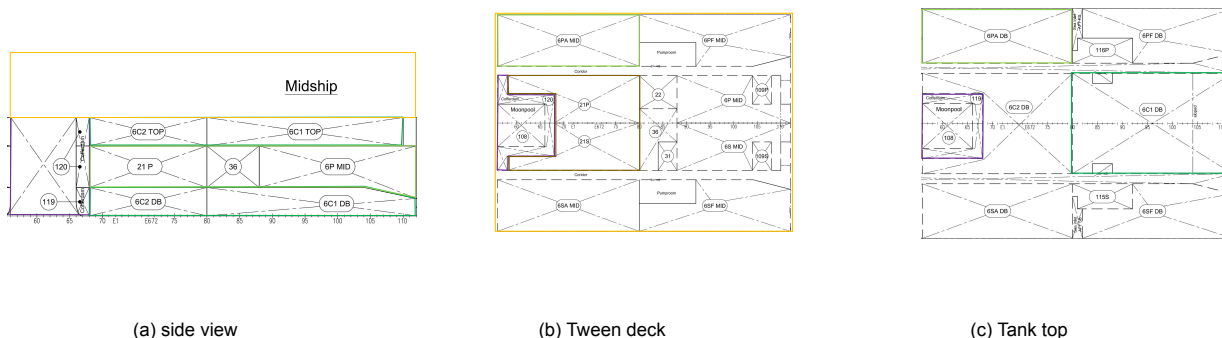


Figure 11.3: Mid ship

Table 11.2 provides an overview of the advantages and disadvantages of storing methanol in the fore ship, specifically focusing on the moon pool, double bottom tank, side tank, MGO tank and work deck.

Table 11.2: Advantages and disadvantages for storing methano mid ship

Moonpool		Double bottom tank		Side tank	
Advantages	Disadvantages	Advantages	Disadvantages	Advantages	Disadvantages
Cofferdam installed Good specifications for methanol storage Good stability influence	Limited storage available	Partly a cofferdam is need Large volume Good stability influence	Loss of ballast capacity	Partly a cofferdam is needed large volume Good stability influence	Loss of ballast capacity Above waterline cofferdam needed
MGO tank		Work deck			
Advantages	Disadvantages	Advantages	Disadvantages		
No loss of ballast Pre-existing aux. equipment	Decrease in range Deep cleaning and coating	Portable tanks available reduction of class regluations	negative stability influence limited space		

The Moonpool, with a pre-installed cofferdam, is one option that promotes stability. Despite its contribution to stability, the design and location of the Moonpool inherently limit the available storage space. The Double Bottom Tank is another potential choice, boasting a large storage volume which contributes positively to the ship's stability. Only a partial installation of a cofferdam is necessary, reducing the complexity of this option. It should be noted, however, that the use of the Double Bottom Tank may lead to a reduction in ballast capacity, which must be taken into account in the vessel's design and operation. Side Tanks situated on the sides of the ship offer large storage volumes, akin to the Double Bottom Tank, and necessitate only a partially installed cofferdam. These tanks do not pose concerns regarding stability. Nevertheless, they do lead to a reduction in ballast capacity and necessitate an above-waterline cofferdam, which may be disadvantageous under specific operational conditions. The MGO tank serves as an alternative solution for methanol storage. It is advantageous due to its lack of impact on ballast capacity and the presence of auxiliary equipment, simplifying operational considerations. However, the use of the MGO tank can result in a reduction in the vessel's range, a potential disadvantage for long-haul journeys. Furthermore, it would neces

Lastly, the Work Deck offers another possibility for methanol storage. It allows for the use of portable tanks, bringing flexibility to the table, and reduces the limitations imposed by class regulations. However, this method does influence stability negatively and might offer limited space, factors that can prove to be significant disadvantages.

11.3.3 Aft ship

In the aft ship section the following components are located:

- Propulsion room
- Double bottom tank
- Side tank
- MGO tank
- Work deck

in Figure 11.4 illustrates the visualization of spaces using colored boxes. The propulsion room is represented by a red box, the double bottom tanks by a Dark green box, the side tanks by a light green box, The MGO tanks by a brown box and the work deck by an orange box.

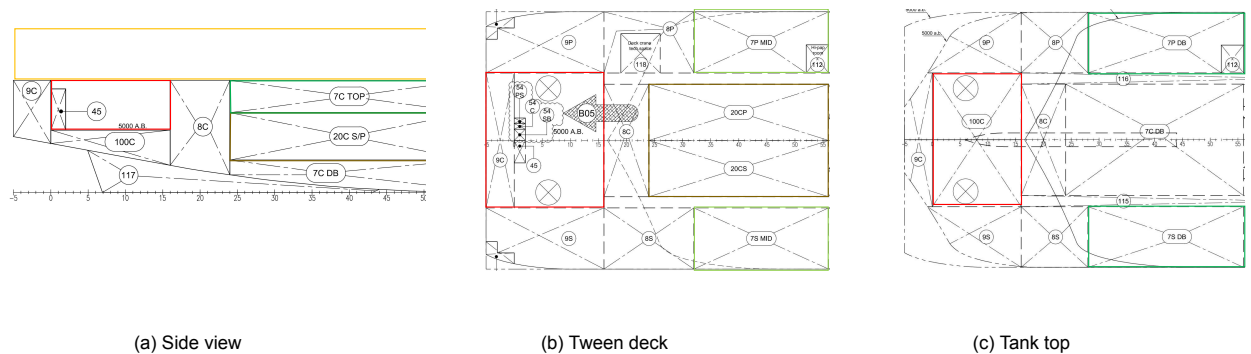


Figure 11.4: Aft ship

Table 11.3 provides an overview of the advantages and disadvantages of storing methanol in the fore ship, specifically focusing on the moon pool, double bottom tank, side tank, MGO tank and work deck.

Table 11.3: Advantages and disadvantages for storing methanol aft ship

Propulsion room		Double bottom tank		Side tank	
Advantages	Disadvantages	Advantages	Disadvantages	Advantages	Disadvantages
Pre-existing mechanical ventilation system in place	Limited storage available	Partly a cofferdam is need Large volume Good stability influence	Loss of ballast capacity	Partly a cofferdam is needed large volume Good stability influence	Loss of ballast capacity Above waterline cofferdam needed
MGO tank		Work deck			
Advantages	Disadvantages	Advantages	Disadvantages		
No loss of ballast Pre-existing aux. equipment	Decrease in range Deep cleaning and coating	Portable tanks available reduction of class regulations	negative stability influence limited space		

The propulsion room has an existing ventilation system but limited storage. The double bottom tank requires a partially installed cofferdam, offers a large storage volume, and improves stability but may result in a loss of ballast capacity. Similarly, the side tank requires a cofferdam, provides ample storage and stability, but also causes a loss of ballast capacity. The MGO tank avoids ballast loss, has installed equipment for ease of operation, but may decrease the vessel's range and requires cleaning and coating for methanol storage. Lastly, using the work deck allows flexibility with portable tanks, reduces class regulations, but negatively affects stability and offers limited space.

A design has been developed above the quadrant to accommodate potential container slots for the portable tanks as can be seen in Figure 11.5

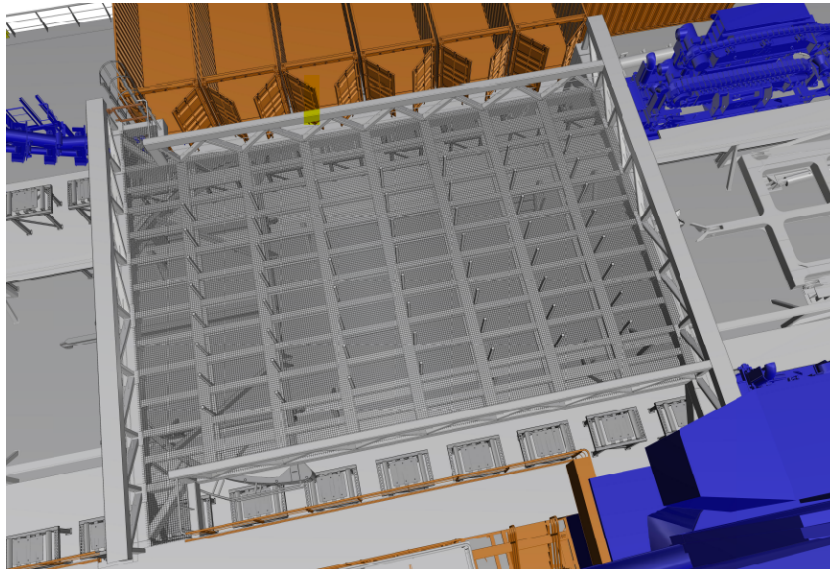


Figure 11.5: Container slots on the aft ship

11.4 Fuel cell and battery placement

This chapter provides the installation of SOFCs and batteries on the Nexus, guided by DNV rules for classification Section 1 'Electrical energy storage' and Section 3 'Fuel Cell Installations' of [23]. It outlines design parameters, fuel supply logistics, exhaust gas systems, and the use of reformers for hydrogen-rich gas production. Additionally, it discusses safety systems, as well as manufacturing and testing procedures. Given the absence of international conventions for fuel cells, case-by-case consideration for installation spaces and approval from flag authorities are emphasized.

11.4.1 Definition of Hazardous Zones

Understanding these zones is crucial when determining the placement of fuel cells, ensuring the safety of the ship and its crew. Additionally, the specific zone also influences the type of safety equipment and measures that need to be implemented in each area. In the context of safety, hazardous zones such as Zone 0, Zone 1, and Zone 2 are used to categorize areas where an explosive gas atmosphere is present. Each zone represents a different level of risk:

- **Zone 0:** The highest risk zone where an explosive gas atmosphere is present continuously or for long durations. This includes interiors of tanks, pipes, and equipment containing low flashpoint or reformed fuel. Only equipment and apparatus suitable for Zone 0 use, designed to prevent ignition, should be used here.
- **Zone 1:** Areas where an explosive gas atmosphere is likely to occur during normal operation. It includes fuel cell spaces and specific areas on open decks or semi-enclosed spaces on decks. The equipment used here needs to conform to safety standards that are typically less strict than Zone 0.
- **Zone 2:** The lowest risk zone, where an explosive gas atmosphere is unlikely to occur in normal operation and if it does occur, will only exist for a short time. This includes areas surrounding Zone 1 and airlocks.

11.4.2 Fuel cell placement

To establish the location of the fuel cell, several regulations must be taken into account. "Vessels complying with the FC Mandatory class notations are designed with specific requirements, particularly focusing on power. These vessels are equipped with fuel cell power installations that are specifically intended for electrical propulsion. Additionally, they are classified as hybrid vessels, capable of operating solely on fuel cells while keeping the other main power source in standby mode." Fuel cell compartments should be strategically situated away from accommodation, service and machinery spaces of

category A and control stations. Thereby if direct and independent access to fuel cell compartments from the open deck is not feasible, these compartments should be accessible through an air lock.

In light of the details provided in section 11.3 and the dimensions outlined in Table 10.12, an overview of potential methanol storage locations are presented. It is assumed that, despite power-to-weight and/or volume ratios, the methanol storage will have the given dimensions. To accommodate the necessary fuel cell components, certain tanks might need to be sacrificed. Taking spatial considerations into account, it appears that the aft section of the ship offers the most suitable space for accommodating methanol bunker tanks. Meanwhile, the fuel cell components are to be positioned in the midship section, adjacent to the engine room. This configuration optimizes the utilization of available space and ensures efficient integration of the fuel cell system within the ship's layout. In Appendix E a design is shown with the above requirements and safety measurements according [23] [86].

11.4.3 Battery storage

To establish the location of the battery system, several regulations must be taken into account. "Vessels that meet the requirements outlined in this section will be granted the class notation Battery (Power) or Battery (Safety), as indicated The Battery Mandatory: Power class notation is applicable to vessels where the Energy Storage System (EES) power is utilized for the electrical propulsion of the vessel. These vessels are classified as hybrid, utilizing the EES system as an additional source of power for main and/or supplementary class notations, such as dynamic positioning." Battery compartments should be strategically positioned, ambient temperature control, ventilation and fire fighting measurements.

Based on the information presented in the section titled section 11.3, several potential storage locations for batteries have been identified. To accommodate the battery components, adjustments may be necessary to allocate sufficient space. Following a thorough consideration of spatial factors, it is evident that the midship section of the ship is the most suitable area for both battery storage and auxiliary systems. The detailed design, coupled with the specified requirements and safety measures outlined in [23] and [86], can be accessed in Appendix E.

11.5 Conclusion

In conclusion, the design and arrangement considerations for fuel storage on a cable layer, with a focus on SOFC and battery systems, play a vital role in ensuring safety, efficiency, and regulatory compliance. Methanol storage, particularly for SOFC systems, demands paramount safety measures due to methanol's flammable and harmful properties. The design should include pressure-resistant and corrosion-resistant storage solutions, accounting for limitations and alignment with SOFC operational requirements. Three distinct storage possibilities are explored: Integrated, independent, and portable fuel tanks. Each option presents its own advantages and disadvantages. Furthermore, a tailored design is formulated for different sections of the ship, namely the fore, mid, and aft sections.

The fore ship emerges as the less favorable choice for methanol storage, whereas the aft section exhibits the highest potential. Consequently, the decision is made to retrofit the aft MGO bunker tanks into methanol bunker tanks. This adaptation results in a reduction of MGO bunker capacity from 1768 to 858 m^3 , while utilizing previously unused fresh water ballast tanks to achieve a total methanol bunker capacity of 1892 m^3 . Modifications to the surroundings are imperative to comply with ATEX requirements, which address the low flashpoint nature of the fuel. Classification rules exert a substantial influence on guiding the design and arrangement of fuel storage. These regulations contain diverse aspects such as cofferdams, tank placements, independent and portable tanks, fuel piping, enclosed space design, and airlocks. Conform to these rules guarantees compliance and elevates the safety and functionality of the storage system.

Turning to the positioning of fuel cell and battery systems, identifying the optimal location for the fuel cell involves strict to specific regulations, particularly for vessels subject to FC Mandatory class notations. Such vessels, designed for electric propulsion, possess the capability to operate exclusively on fuel cells while maintaining the main power source on standby. Compartments must be strategically situated away from critical areas and be accessible via an airlock if required. While power-to-weight considerations are important, the chosen methanol storage will conform to specified dimensions. In certain cases, repurposing existing tanks may be necessary to accommodate fuel cell components, which are ideally positioned midship and alongside the engine room.

Similarly, the placement of battery systems on a vessel is governed by regulations and various considerations. Vessels meeting specific criteria are eligible for battery storage of DNV based on EES power usage. Battery compartments necessitate careful positioning, temperature control, ventilation, and fire safety provisions. The chapter identifies potential sites for battery storage, necessitating adjustments to optimize available space. The midship section is deemed optimal for storage and auxiliary systems. For additional design details and safety information, please refer to [23] and [86], can be accessed in Appendix E.

Performance indicators

The new power- and energy systems have been fully characterized, enabling the establishment of a performance comparison. This section aims to evaluate how the introduction of a SOFC system impacts the design aspects and performance of the Nexus.

12.1 Fuel consumption

This section presents the results of the fuel consumption analysis for energy converters using both methanol and diesel as fuel sources. The comparison aims to provide valuable insights into the SFC of the respective converters.

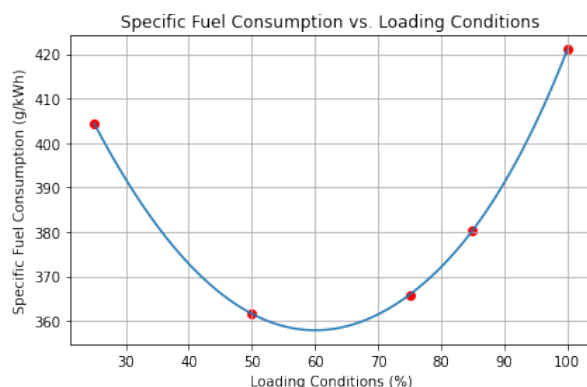


Figure 12.1: SFC (g/kWh)

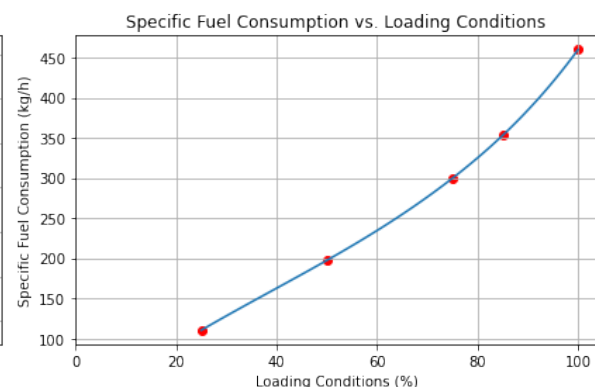


Figure 12.2: FC (kg/h)

In the Figure 12.2 the fuel consumption of the fuel cell on methanol is presented with a fuel utilization rate of 100%. It is evident that the specific fuel consumption (g/kWh SFC) is quite favorable.

It is essential to consider the Lower Heating Value (LHV) for both MGO and methanol. The LHV for MGO is 45.9 MJ/kg, whereas for methanol, it is 23.0 MJ/kg. This signifies that a factor of 2 needs to be added to account for the difference in energy content.

In Figure 12.3, these factors have been taken into account, and these are represented using 'kJ/kWh'. This metric quantifies the amount of fuel required to generate one kWh of energy. By utilizing this metric, a more straightforward comparison can be made regarding the increased efficiency between a diesel engine and a SOFC.

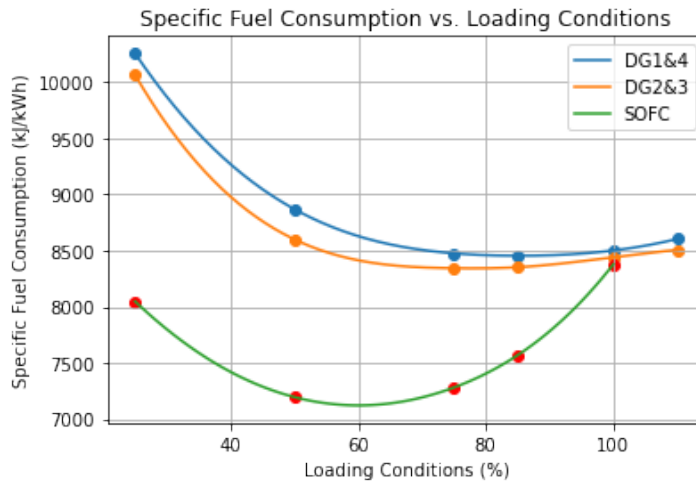


Figure 12.3: SOFC vs Diesel

Figure 12.4 below provides an overview of the fuel usage for the project 'Hollandse Kust Noord', illustrating the total fuel consumption.

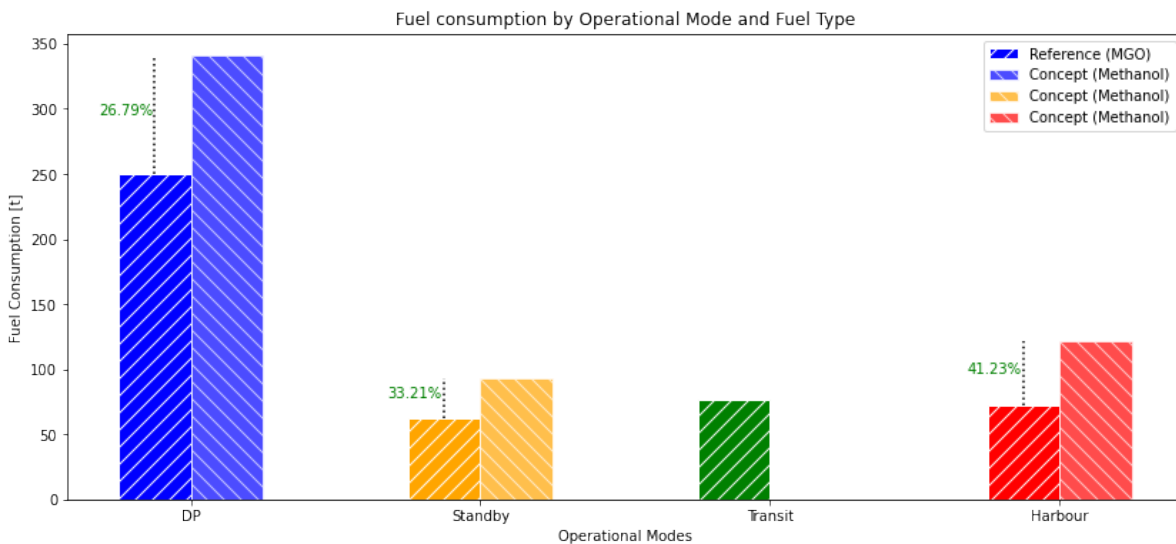


Figure 12.4: Fuel consumption by Operational Profile and Fuel Type

The fuel consumption increase is not as high as one might expect due to the difference in the LHV of the fuels. The significant factor contributing to this is the improved efficiency of the SOFC-battery system. Additionally, the battery system has been engineered with a sufficient level of reserve, eliminating the need for a second engine on standby. This decision has a considerable impact on reducing fuel consumption.

12.2 Emission indicator

In this section, the focus is on analyzing GHG for both methanol and diesel, which are equivalent – they both produce CO₂. However, for a correct assessment, it is crucial to consider the complete picture. Instead of solely measuring CO₂ emissions, the emissions are expressed in CO₂e, which includes other GHG as well.

Moreover, the efficiency of the energy converter is taken into account, which depends on the specific operational profile. By doing so, a better understanding is gained of the overall environmental impact of using methanol or diesel as a fuel. This approach allows consideration not only of the emissions per

energy content (kWh) but also the effectiveness of the energy conversion process based on how the vessel is operated.

Figure 12.5 provides a representation of the CO₂e emission index per operational profile and power-and energy system.

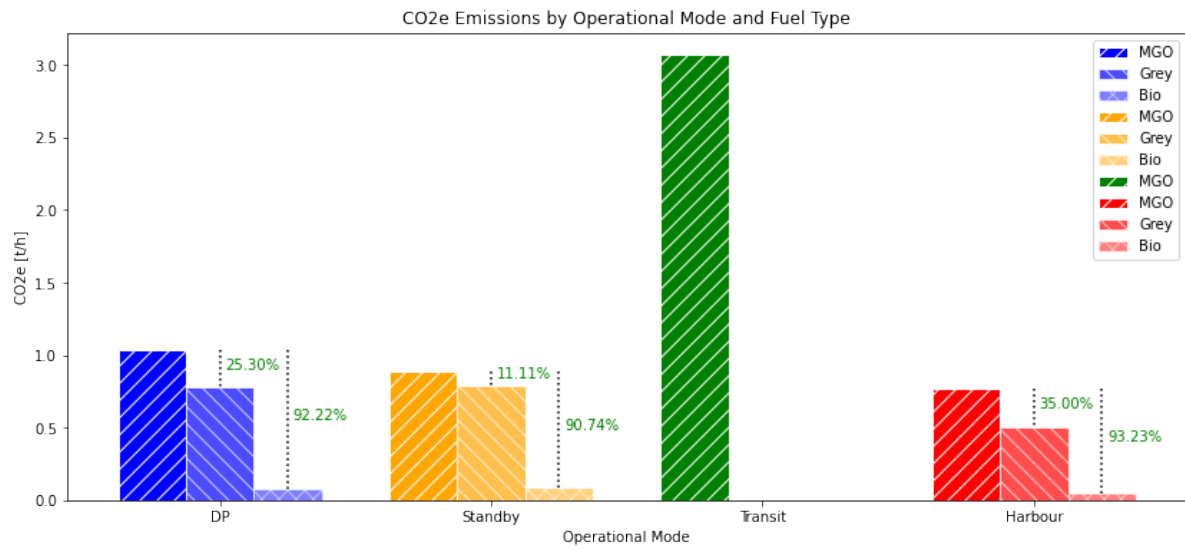


Figure 12.5: CO₂e Emissions by Operational Mode and Fuel Type

The figure displays four operational profiles, each represented by three bars. The intensity of color in each bar corresponds to the CO₂e of a specific fuel type. The most colored bar represents the CO₂e of MGO, the less colored bar represents the CO₂e of 'grey' methanol, and the least colored bar represents the emissions of bio-methanol.

To find the CO₂e values for 'grey' methanol, please refer to Table 12.1. For the CO₂e values of MGO, consult Table 9.3. It's important to note that the LHV for MGO is 45.9 MJ/kg, while the LHV for methanol is 23.0 MJ/kg.

Table 12.1: TTW emission grey and bio methanol

Fuel type	Emission type	Factor	Unit	Fuel type	Emission type	Factor	Unit
Grey Methanol	TTW CO ₂	1,3750	t/t	Bio Methanol	TTW CO ₂	0,0000	t/t
	TTW CH ₄	0,0001	t/t		TTW CH ₄	0,0001	t/t
	TTW N ₂ O	0,0022	t/t		TTW N ₂ O	0,0022	t/t
	TTW CO ₂ e	1,3773	t/t		TTW CO ₂ e	0,0023	t/t
	WTW CO ₂ e	2,0345	t/t		WTW CO ₂ e	0,212	t/t

In three out of the four profiles, there is a significant decrease in GHG emissions. The reasons behind this reduction can be attributed to both lower emissions factors and the use of a more efficient energy converter. However, the Transit profile does not show any decrease in GHG emissions. This will be elaborated on later in the discussion. The reduction in GHG emissions can be attributed to the utilization of more sustainable fuel sources. Specifically, the significant difference between 'grey' and bio-methanol emissions is due to their respective sources. 'Grey' methanol is collected from non-renewable sources, such as natural gas, while bio-methanol is entirely derived from renewable sources. Regarding the Transit profile, it has remained unchanged due to certain design considerations. Earlier, it was decided not to design the SOFC-battery system to cater to the demand in transit. This decision was based on factors such as efficiency considerations, fuel consumption, and the relatively short duration of transit activities in terms of the total profile.

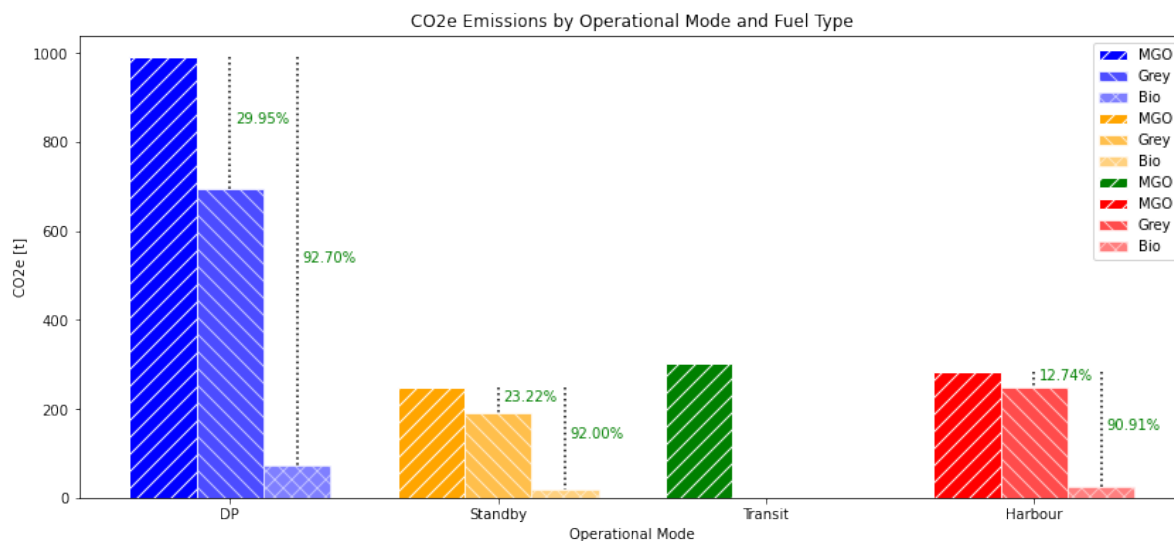


Figure 12.6: Total CO₂e Emissions by Operational Mode and Fuel Type

The total CO₂e emissions by operation profile for the Hollandse Kust Noord project Figure 12.6 show a significant reduction in GHG emissions. A reduction of 42.15% in DP mode is realistic, and this reduction is particularly significant because the ship spends most of its time in DP mode during offshore activities. Due to regulations, the ship operates with two different bus bars and two engines on standby, which negatively impacts efficiency and results in higher GHG emissions.

For the standby mode, a similar explanation applies, except that the ship may be in DP mode without the need for two engines on standby since it is not conducting offshore activities. This change improves efficiency and reduces emissions.

In contrast, the reduction in emissions is the lowest during harbor operations. This is primarily due to the efficiencies of the engines and bus bar layout used while in harbor, which are already quite good. By understanding and optimizing the ship's operational profiles, it becomes evident that significant reductions in GHG emissions can be achieved, particularly during DP mode and standby, contributing to a more environmentally friendly approach in maritime operations.

12.3 Weight and Volume

When considering energy installations on deck and carousel capacity, both weight and volume are critical factors that should not hinder workability. The 'SOFC + Batteries' module presents challenges in terms of weight and volume compared to the 'Genset,' which can impact stability and available space. In Figure 12.7, present a comparison of the weights and volumes for different energy converters.

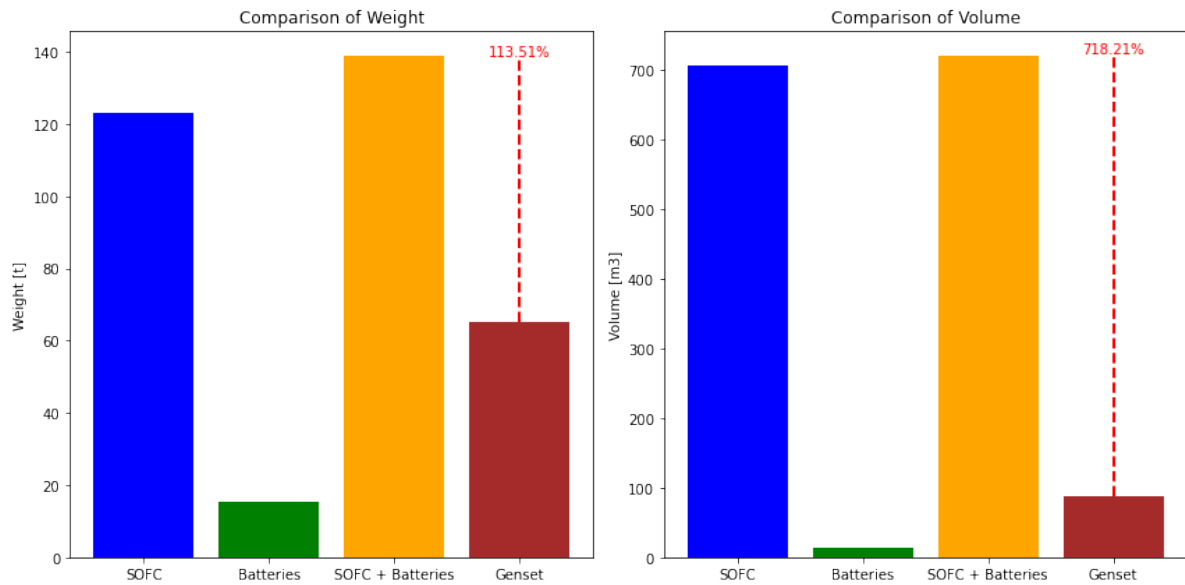


Figure 12.7: Comparison Weight vs. Volume

The weight increase of the 'SOFC + Batteries' module is more than doubled, reaching 138 tons, while the volume increase is even more significant. The volume increases by over 7 times, resulting in a volume of 706 m^3 compared to the Genset's 88 m^3 [56]. It's important to note that these numbers are based on scaling up a 250kW module, and in practice, the actual volume of the SOFC will likely be lower. Due to scale increases, the power ratios for the SOFC module are expected to be more favorable. Furthermore the numbers for SOFC + Batteries consist of the total BoP, where the Genset only consist of the ICE and generator. The auxiliary equipment like starting air, purifiers, LT and HT coolers are not included. Another important point to note is that the numbers for the 'SOFC + Batteries' module include the total BoP, while the Genset only includes the ICE and generator. The auxiliary equipment like starting air, separators, LT and HT coolers are not included in the Genset's numbers. This difference should be taken into account when comparing the two systems.

12.4 Conclusion

In conclusion, the new power- and energy systems enables a performance assessment, with specific emphasis on the integration of a SOFC and battery system within the Nexus design and operation.

The indicator of fuel consumption provides valuable insights into the efficiency of the methanol-SOFC configuration. Despite a higher g/kWh fuel consumption compared to diesel, the analysis highlights the efficiency of the system. This due energy content between MGO and methanol, where the LHV factor is 2. Consequently, a marginal increase in fuel consumption by a factor of two is anticipated. The assessment of fuel consumption across various operational modes, as exemplified by the 'Hollandse Kust Noord' project, emphasizes the significant impact of the improved efficiency of the SOFC-battery setup. This leads to only a 27% increase in fuel consumption in DP mode.

Taking into account the LHV and overall efficiency, there's potential for an even higher total efficiency. Moreover, the incorporation of a battery system reduces the number of diesel engines from 4 to 2, thanks to the engineered 'spinning reserve' within the battery pack. It's worth noting that the transit profile, which still relies solely on MGO, hasn't been compared with methanol.

Shifting the focus to emission indicators, the comparative analysis spans three fuels: MGO, grey methanol, and bio methanol. The assessment approaches this from a CO_2e perspective in the WTW

context, given the limited availability of bio methanol. The findings suggest that the proposed power plant configuration could potentially reduce CO₂e emissions by up to 35% for grey methanol, while bio methanol exhibits nearly negligible emissions. The overall emissions for the project demonstrate a potential reduction ranging from 12.7% to 29.9%, contingent on fuel choices. However, it is important to acknowledge the trade-off in terms of weight and volume to power density. The integration of SOFC and batteries necessitates approximately seven times the volume and twice the weight for the same power output compared to conventional systems.

Capital- and operating expenditures

The feasibility of the system relies not only on technical aspects but also on its economic viability. Therefore, a comprehensive and indicative economic assessment is conducted, with a specific focus on both Capital Expenditures (CAPEX) and Operational Expenditures (OPEX) for the case study. Ensuring economic feasibility is crucial to establish a successful and sustainable business model. Ultimately, the goal is to generate positive financial outcomes (green numbers) that support the transition. Given that the current market predominantly centers on fossil fuels, substantial subsidies may be necessary to compete effectively and make the sustainable business model financially viable.

13.1 CAPEX

CAPEX refers to funds utilized for acquiring the necessary power and energy systems. This economical assessment specifically focuses on the costs associated with energy converters and capital-intensive fuel systems required for the retrofit of the Nexus. The following components will be taken into account to calculate the CAPEX, and they are shown in the Table 13.1 below:

Table 13.1: Engine and storage system costs

Component	Cost	unit	Reference
SOFC stack	640	[€/kW]	[50]
SOFC system	1280	[€/kW]	[50]
Battery stack	500	[€/kW]	[50]
Battery system	1250	[€/kW]	[94]
ICE MGO	240	[€/kW]	[50]
Electric generator	250	[€/kW]	[52]
Methanol storage	50	[€/GJ]	[85]
MGO storage	25	[€/GJ]	[85]
Piping	200	[€/kW]	[52]
Shipyard	110	[€/kW]	[52]

By factoring in these components, the goal is to accurately evaluate the capital expenditures associated with the retrofit of the Nexus and ensure a comprehensive analysis of the project's financial aspects. It is important to note that the cost data presented in the table are obtained from scientific literature and represent some optimistic estimates. As with any complex project, real-world costs may vary based on several factors, such as market fluctuations, technological advancements, and implementation specifics. Thus, the figures provided serve as an initial guideline for assessing the economic feasibility of the retrofit, and they may be subject to further adjustments and refinements during the actual implementation process.

Table 13.2 and Table 13.3 present CAPEX for a SOFC batteries system and a comparative analysis with a conventional system. The system cost difference between the two configurations is a significant factor of 2.5. This notable cost disparity can be primarily attributed to the high expenses associated with the SOFC system itself and its auxiliary components. Notably, the storage of methanol is twice as expensive as MGO, primarily due to the requirement for extra volume for cofferdams, additional coating, and conform to safety regulations.

Similarly, the complexity of piping for the SOFC-batteries system is a notable factor. While the conventional system's piping is relatively negligible, the piping for methanol necessitates intricate design considerations. The use of connections must be minimized, requiring extensive welding, and a double-walled construction is mandatory to meet safety standards.

Table 13.2: CAPEX SOFC-batteries system

Component	Quantity	Cost	unit	CAPEX [€]	System cost
SOFC system	1926	1280	[€/kW]	2.465.280	2011€/kW
Battery system	1195	1250	[€/kW]	1.493.750	
Methanol storage	30099	50	[€/GJ]	1.504.935	
Piping	1926	200	[€/kW]	385.200	
Shipyard	3121	110	[€/kW]	332.907	

Table 13.3: CAPEX conventional system

Component	Quantity	Cost [€]	unit	CAPEX	System cost
ICE MGO	3820	240	[€/kW]	916800	691 €/kW
Electric generator	3820	250	[€/kW]	955000	
MGO storage	30716,4	25	[€/GJ]	767910	

13.2 OPEX

Operating expenditures are costs to run a company and in particular for this study, a vessel of which fuel is usually the largest expense. The OPEX includes more than only fuel costs, such as maintenance cost, crew and other ongoing company spends. It can be assumed that due to a more complex system and increased safety regulation and maintenance, OPEX would increase compared to a conventional diesel configuration. In order to verify the total increase in OPEX, more detailed economic analyses should be made which is out of the scope of this research.

OPEX analysis, the focus is on fuel consumption, as other factors have relatively minor impacts on the OPEX. Furthermore, the disparity between MGO and methanol in terms of fuel consumption is relatively limited. The determination of fuel consumption is based on the operational profile provided in Figure 8.12 and the corresponding efficiencies associated with the operational profiles.

In Table 13.4, the presented data includes the fuel used and the corresponding fuel prices as of 27th July 2023. It is evident from the data in Appendix G that fuel prices are subject to significant fluctuations. Notably, the methanol price aligns with the predictions in Figure 4.4.

Table 13.4: OPEX Conventional vs SOFC-batteries

Fuel	Cost [\$/MT]	System	Fuel usage	Volume [MT]	Fuel cost [\$]
MGO	810	Conventional	MGO	459,8	372.405,1
Methanol	392	SOFC-batteries	MGO + Methanol	76,1 + 556,3	279.716,1

An notable observation indeed is the significant difference in OPEX between the SOFC-batteries system and the conventional system, primarily attributed to the lower cost of methanol per metric ton. It's worth mentioning that the projected costs of alternative fuels like HVO and FAME are expected to be even higher. However, it's essential to note that the OPEX analysis shouldn't be based on fuel costs only, as there are other expenses involved. The short lifetime of approximately 10 years for the

SOFC-batteries system may lead to higher OPEX compared to the conventional system, considering the additional costs associated with maintenance, replacements, and potential technological advancements over time. Conducting an in-depth research, specifically focusing on the complete lifecycle and various operating expenses, would be necessary to gain a understanding of the economic feasibility of both systems. However, such an investigation is beyond the scope of the current study, and further more is this kind of technology so new that these cases in practice don't yet occur in order to make a good comparison for stack replacement of SOFC and battery system.

13.3 Conclusion

In conclusion, this chapter underscores the importance of economic viability alongside technical considerations in assessing the feasibility of transitioning to SOFC and batterie system CAPEX and OPEX play a crucial role in determining the success and sustainability of such solutions.

The CAPEX analysis delves into the costs associated with various components required for retrofitting a vessel with a SOFC-batteries system compared to a conventional system. The cost breakdown highlights the significant expense of the SOFC system itself, battery systems, methanol storage, piping complexity, and shipyard costs. These estimates provide a preliminary understanding of the financial outlay for such a project, but real-world costs could be influenced by various factors. With the assumption made, it will result in almost 3 times the CAPEX cost in comparison with conventional system.

On the OPEX side, the focus is on fuel cost, with the SOFC-batteries system demonstrating lower fuel costs due to the relatively cheaper price of methanol compared to MGO. However, it's important to note that a OPEX analysis should also contains maintenance, crew, and other ongoing expenses. Moreover, the shorter lifetime of the SOFC-batteries system may introduce additional OPEX in terms of maintenance and potential replacements over time.

Conclusion

The central goal is to evaluate the feasibility of a concept, considering its effects on design, operational capabilities, and GHG emissions in comparison to a standard reference design.

- **What is the impact of adding a methanol-fuelled SOFC and batteries to the power plant of the NEXUS on the emissions, design and performance of the ship?**

To answer the main question, this research is divided into two parts. The first part involves a literature review, while the second part delves into the subject and presents a case study.

The purpose of the current literature review is to identify the best method for integrating various fuel cell types and hydrogen carriers while also gaining insights into cable lay operations. Hydrogen fuel cells show great promise in improving Nexus performance, mainly because of their significantly higher efficiency compared to ICE. Moreover, these fuel cells offer added advantages such as reduced emissions, lower maintenance requirements, and a high degree of adaptability in design. Interestingly, cable laying vessels, which have relatively modest power demands, due to their operations, present an excellent opportunity for the application of fuel cell technology. There are various types of fuel cells to consider, including PEMFCs and SOFCs. PEMFCs operate at lower temperatures and require pure hydrogen, while SOFCs thrive at higher temperatures and even have the capability to reform their own fuel. After a thorough evaluation of these options, SOFCs emerge as the most suitable choice for medium-term integration. In terms of hydrogen carriers, a comprehensive assessment considering factors like flammability, toxicity, energy density, and emissions reveals ammonia and methanol as the most viable options. However, it's advisable to utilize these carriers in situations where vessel operations are less hazardous. Taking all these factors into careful consideration, the analysis supports the implementation of SOFC-powered systems utilizing methanol as the fuel of choice for the Nexus. This decision aligns with the specific attributes of the vessel and takes into account the availability of an existing reference design.

During the concept design phase in the second section of the report, the feasibility of the selected optimal combination was evaluated. This assessment enables us to address the following sub-questions:

- *What is the energy demand of the cable layer and how can methanol-fuelled SOFC and batteries technology be integrated into its power plant?*

The power setup on the Nexus cable layer ship is designed as diesel-electric. It has two bus bars, which are powered by four main diesel engines. The power requirements for the 'Hollandse Kust Noord' project were analyzed in four different operating modes: DP (1059 kW), harbor (638 kW), standby (1082 kW), and transit (4578 kW). Transit mode requires the most power, about three times more than the other modes. To address the challenge of reducing GHG emissions, a solution involves incorporating SOFC technology into the ship's power system. Embracing SOFC technology offers several advantages, including better efficiency compared to regular ICE, which leads to lower emissions for each unit of electricity generated. A 1926 kW SOFC has been developed, considering degradation, to meet the power requirements for all modes except transit. Additionally, a battery pack is being integrated due to the limitations of SOFCs in effectively

managing changes in power demand. This integration ensures the ability to handle fluctuating loads that could be problematic for a standalone fuel cell system. The capacity of the battery pack, determined through CDF analysis, is 1195 kWh. Furthermore, it serves as a 'level of reserve', allowing a reduction in the number of diesel engines from four to two. This reduction has a significant impact on both fuel consumption and GHG emissions. The transit mode is excluded from this setup due to its relatively high power demand and the relatively short duration for which the ship operates in this mode. Engineering a battery pack to handle this specific situation is not efficient.

- *How does the use of a methanol-fuelled SOFC and batteries affect the design and performance of the cable layer?*

The utilization of methanol within the SOFC system impacts various aspects of cable layer design and performance, including fuel storage, weight, space requirements, and operational efficiency. It is important to note that methanol is flammable and poses potential harm, necessitating stringent safety precautions during the design of methanol storage solutions. The storage design have materials that are both pressure-resistant and corrosion-resistant to ensure the secure containment of methanol. Special attention is essential to address the fuel's low flashpoint nature in line with ATEX requirements.

When designing methanol storage tanks, several critical factors come into play. The design considers three potential storage approaches: integrated, independent, and portable fuel tanks, each offering its own set of advantages and drawbacks. After thorough evaluation, the aft section serves as the most optimal location for methanol storage. A solution involves converting the existing MGO bunker tanks into methanol bunker tanks, utilizing existing cofferdams for the moonpool, effectively utilizing available space. This conversion results in a reduction of MGO bunker capacity from 1768 to 858 m^3 , while converting previously unused fresh water ballast tanks to achieve a combined methanol bunker capacity of 1892 m^3 . The weight of the methanol storage tanks and their associated systems contributes to the overall weight distribution of the vessel. To address this, the placement of the fuel cell stack is carefully selected amidships, adjacent to the engine room. This arrangement effectively utilizes two large ballast tanks. In the same manner, the battery stack and drive system are positioned at the aft, utilizing both the portside and starboard fresh water side tanks.

Though the integration of SOFC and battery technologies introduces trade-offs in terms weight and volume, Seven times in weight and twice in volume. Respectively when compared to conventional systems, these considerations must be weighed against the potential benefits of reduced emissions and increased fuel efficiency. In terms of regulatory compliance and class notations, it is that the design and arrangement of methanol storage, fuel cell, and battery systems conform to established regulatory standards and class notations. Specific regulations dictate the placement of fuel cell and battery system, especially the venting requirements of methanol brings challenges.

- *What are the economic and environmental benefits of using a methanol-fuelled SOFC and batteries?*

Integrating a SOFC and battery system into the design offers both economic and environmental benefits, aiming to reduce GHG emissions in cable laying operations. When it comes to fuel consumption in metric tons, it's important to highlight that the methanol-SOFC configuration falls short of surpassing diesel, showing a notable 27% increase of methanol consumption. This difference can be explained to the fuel's LHV, which was predicted to lead to a doubling of fuel consumption. However, the improved efficiency and the reduction of main engines from four to two have lead this increase to only a quarter of the original projection. So, the combination of the

SOFC and battery technologies presents a promising opportunity for enhancing overall efficiency. Moreover, a thorough comparison of emissions from three different fuels – MGO, grey methanol, and bio methanol – reveals substantial reductions in CO_{2e} (WTW) emissions. Noteworthy is the remarkable 35% potential reduction with grey methanol, while bio methanol exhibits minimal emissions. This potential for emission reduction extends throughout the entire operational profile modes spanning a range from 13% to 23%.

Economically, the initial estimated CAPEX of the SOFC-battery system (2011€/kW) is three times higher than that of conventional systems (691 €/kW). However, there's potential to optimize costs and gain long-term benefits from reduced fuel expenses and emissions, which positions the SOFC-methanol system as a strategic investment for sustained economic viability.

When considering the OPEX, the SOFC-battery system proves to be more cost-effective than the regular MGO. This is primarily due to the relatively lower cost of methanol compared to MGO. If the 'Hollandse kust noord' project were to be carried out again using the new system, there could be a fuel cost reduction of approximately \$92,689 (calculated as 372,405.1 - 279,716.1 = 92,689).

It's important to emphasize that this comparison focuses on the cost of fuel. The broader ongoing costs, which contains maintenance, crew salaries, and other continuous expenses, also align with the economic advantages of the system. Furthermore, the shorter lifespan of the SOFC-battery system could potentially lead to additional costs over time, including maintenance and replacement of components, only remain uncertain due to the innovative technology involved.

With the insights gained from the assessment of the selected optimal combination during the concept design phase, the answers to the main question can now be provided.

The integration of a methanol-fueled SOFC and batteries into the power plant of the Nexus has been demonstrated as technically feasible according to the concept design for the medium term. Showing acceptable operational capabilities and a significant reduction in GHG emissions with respect to the reference design. In the short term an implementation of only batteries as level of reserve will already gain an significant reduction of GHG emissions. On the short the implementation of SOFC technology is restrained by its power density and availability, which have not yet reached a competitive level when compared to alternative energy conversion methods. Looking at the economic aspect, in the medium term, the potential for lower fuel costs makes the integration of methanol-fueled SOFC and batteries financially viable. Nonetheless, in the short term, the high capital expenditure costs pose a significant economic hurdle to implementation.

14.1 Discussion

This section delves into certain aspects of the thesis that introduce uncertainty due to the innovation aspects of the technology. The primary source of uncertainty relates to the readiness of the components and the availability of bio fuels, particularly the SOFCs and methanol, required for this study.

SOFCs:

This study revolves around SOFC technology, focusing on its application in marine power plants. However, large-scale SOFCs of this magnitude have not yet been developed. While smaller 25 kW stacks have been employed in marine settings, projects to combine these stacks to meet the Nexus's power requirement are currently lacking. Notably, these combined modules are yet to undergo production or testing. For the SOFC module of 1980 kW, sized approximately as two 20-foot containers, faces technical constraints that hold back the short term feasibility. A comparison with a 250 kW DFC®250 EU MCFC-Fuel Cell Power Plant underscores the need for improvements in power density. Until these enhancements materialize, the conclusions presented in this thesis remain within the realm of theory.

Striving to adopt conservative assumptions, areas of uncertainty persist, including module efficiency, fuel consumption and utilization rate. The efficiency load curve, ranging from 53% to 65% for a SOFC module, is inferred from information furnished by manufacturers. Notably, this curve displays its highest efficiency under partial load conditions while demonstrating lower efficiency under full load conditions. Additionally, the dynamic load capabilities of SOFCs remain largely theoretical. Manufacturers and research entities such as TNO are actively exploring these capabilities, warranting critical assumptions in this regard. Should this figure deviate, adjustments in battery pack sizing become necessary, establishing a delicate interplay between these variables.

Methanol:

While the potential for methanol availability is indeed promising, a series of challenges demand careful consideration. Specifically, the current capacity for methanol production may require expansion to effectively address the escalating demands emerging from the shipping industry. As an increasing number of sectors, containing transportation and power generation, explore methanol as a feasible fuel alternative, the potential for resource competition threatens on the horizon. Efficient and reliable distribution for methanol delivery to ports and refueling stations is crucial. Adapting existing infrastructures to accommodate the specific storage and handling requisites of methanol might become an important step in this journey. In parallel, safeguarding an uninterrupted supply chain takes center stage to avert operational disruptions within the maritime sector.

Interestingly, methanol availability is tied to its cost. Higher demand might raise prices due to supply and demand. This leads us to explore other options like HVO or FAME to avoid fluctuating methanol costs. The energy sector's complexities, presenting both challenges and opportunities. It's important not to focus solely on methanol, as availability issues prompt consideration of alternative, potentially more cost-effective options. The future's fuel likely won't rely on just one choice, but could involve several.

Retrofitting:

Retrofitting ships to accommodate methanol storage demands a comprehensive overhaul of existing systems. Ensuring technical compatibility between ship design and methanol storage requirements necessitates precision engineering. Complexities arise from retrofitting storage tanks within spatial constraints, like the need of cofferdams, ventilation and FiFi while safeguarding the ship's structural integrity, stability, and performance. Furthermore the fuel piping is a big challenge, the methanol fuel piping needs to be double walled and must have welded connections, a big challenge when retrofitting a ship.

Range:

As highlighted in the conclusion, the transit mode is the most power demand aspect of the 'Hollandse kust Noord' project's operational profile. While currently only a fraction of the project operates in this mode, the escalating ambitions of the energy transition foresee the expansion of offshore wind farms. As these windmill parks move farther from the coastline, the distance between port and park increases, subsequently extending transit times and elevating emissions. To address this challenge, consideration should be given to the implementation of an EMS utilizing forward-looping strategies could optimize the utilization of SOFCs or explore the feasibility of a dual-fuel engine capable of running on both methanol and MGO. Such innovations hold potential to mitigate the elevated emissions associated with the expanding offshore energy landscape.

Design:

The layout and positioning of the fuel cell and battery modules have been thoughtfully planned to meet the rigorous class regulations, especially those set by DNV, known for their comprehensive standards. It's important to note that other class bureaus might have different viewpoints on these matters. It's worth mentioning that the existing regulations tend to be quite general, leaving room for interpretation, which also applies to this design. While important features like airlocks, piping, ventilation, FiFi equipment, and escape routes have been incorporated, there's potential to fine-tune and optimize these elements. In essence, while the design fully conform to the current regulations, there's an opportunity to make certain improvements through careful refinement.

A

Performance (6L48/60CR)

measurement-no: 47 0% shop test	Performance Data (L4860CR)																																		
03.03.2016, 11:53	BUREAU VERITAS engine power 1 % Stamped document, refer to 1st page																																		
engine type	6L48/60CR	air pressure	947	mbar																															
engine No.	1130881	ambient air temperature	21	°C																															
turbocharger type	TCA55/42132	abs. humidity	3,40	g/kg																															
turbocharger No.	7002447	luboil spec.	Shell Argina T40																																
attached pumps	2	fuel oil spec.	DMA																																
testbed No.	29	fuel NCV	43.061	kJ/kg																															
waterbrake type	Zöllner 16u160F	VVT position	part load																																
Power																																			
eng.speed	514	1/min																																	
engine power	71	kW	30	°C																															
force waterbrake	1,4	kN	12,5	bar																															
mean eff.pressure	0,3	bar	101	kg/h																															
Fuel																																			
s.f.o.c (42700kJ/kg,ISO)																																			
Governor																																			
fuel index	6,4	%																																	
Charge Air																																			
air temp.comp.inlet	21	°C	air press.comp.inlet	-0,52 mbar																															
air temp.comp.outlet	37	°C	air press.comp.outlet	62 mbar																															
charge air temp.	33,6	°C	charge air press.	50 mbar																															
			diff.press. intercooler	3 mbar																															
Peak Combustion Pressure																																			
peak comb.press. MV	52	bar	<table border="1"> <thead> <tr> <th>cyl.</th> <th>1</th> <th>2</th> <th>3</th> <th>4</th> <th>5</th> <th>6</th> <th>7</th> <th>8</th> <th>9</th> <th>10</th> </tr> </thead> <tbody> <tr> <td>bar</td> <td>52</td> <td>52</td> <td>52</td> <td>52</td> <td>51</td> <td>53</td> <td colspan="4"></td> </tr> </tbody> </table>							cyl.	1	2	3	4	5	6	7	8	9	10	bar	52	52	52	52	51	53								
cyl.	1	2	3	4	5	6	7	8	9	10																									
bar	52	52	52	52	51	53																													
Exhaust Gas																																			
exh gas temp.cyl.outlet MV	172	°C	<table border="1"> <thead> <tr> <th>cyl.</th> <th>1</th> <th>2</th> <th>3</th> <th>4</th> <th>5</th> <th>6</th> <th>7</th> <th>8</th> <th>9</th> <th>10</th> </tr> </thead> <tbody> <tr> <td>°C</td> <td>162</td> <td>177</td> <td>165</td> <td>173</td> <td>173</td> <td>182</td> <td colspan="4"></td> </tr> </tbody> </table>							cyl.	1	2	3	4	5	6	7	8	9	10	°C	162	177	165	173	173	182								
cyl.	1	2	3	4	5	6	7	8	9	10																									
°C	162	177	165	173	173	182																													
exh gas temp.turb.inlet	217	°C	exh gas press.turb.inlet	161	mbar																														
exh gas temp.turb.outlet	202	°C	exh gas press.turb.outlet	0	mbar																														
TC.speed	4.627	1/min																																	
Lubricating Oil																																			
lub.oil press.eng.inlet	4,9	bar	lub.oil temp.eng.inlet	55	°C																														
lub.oil press.turb.inlet	1,9	bar	lub.oil temp.eng.outlet	60	°C																														
			lub.oil temp.turb.outlet	59	°C																														
Cooling Water																																			
cw.press.eng.inlet	3,4	bar	cw.temp.eng.inlet	83	°C																														
cw.press.IC LT inlet	3,7	bar	cw.temp.eng.outlet	84	°C																														
cw.temp.IC HT inlet	84	°C	cw.temp.noz.inlet	59	°C																														
cw.temp.IC HT outlet	83	°C	cw.temp.noz.outlet	63	°C																														
cw.temp.IC LT inlet	32	°C	cw.press.noz.inlet	2,8	bar																														
cw.temp.IC LT outlet	36	°C																																	
Bearing																																			
mainbearing temp. MV	70	°C	<table border="1"> <thead> <tr> <th>No.</th> <th>01</th> <th>1</th> <th>2</th> <th>3</th> <th>4</th> <th>5</th> <th>6</th> <th>7</th> <th>8</th> <th>9</th> <th>10</th> <th>11</th> </tr> </thead> <tbody> <tr> <td>°C</td> <td>70</td> <td>69</td> <td>68</td> <td>69</td> <td>74</td> <td>70</td> <td>69</td> <td>73</td> <td colspan="4"></td> </tr> </tbody> </table>							No.	01	1	2	3	4	5	6	7	8	9	10	11	°C	70	69	68	69	74	70	69	73				
No.	01	1	2	3	4	5	6	7	8	9	10	11																							
°C	70	69	68	69	74	70	69	73																											
splash oil temp. MV	67	°C	<table border="1"> <tbody> <tr> <td>°C</td> <td></td> <td>66</td> <td>66</td> <td>66</td> <td>68</td> <td>68</td> <td>66</td> <td colspan="4"></td> </tr> </tbody> </table>							°C		66	66	66	68	68	66																		
°C		66	66	66	68	68	66																												
crankcase press.	0,6	mbar	smoke AVL				0,34																												
Abbreviations: CR: common rail LT/HT: low/high temperature IC: intercooler TC: turbocharger MV: mean value LHV: lower heating value																																			
Remarks: vol.flow main fuel leakage 375 ml/min																																			

sheet 15

R

C

CDF Code

```
In [ ]: from vessellog_io import VessellogIO
        from datetime import datetime
        import os
        import matplotlib.pyplot as plt
        import numpy as np
        from scipy.stats import norm
        import plotly.graph_objects as go
```

```
In [ ]: import logging

        # loglevel = "INFO"
        # loglevel = "WARNING"
        loglevel = "DEBUG"
        logging.basicConfig(level=loglevel)
        logger = logging.getLogger(__name__)
```

```
In [ ]: host_prod = 'https://vessellog.data.vanoord.com'
        host_dev = 'https://vessellog.data-dev.vanoord.com'
        host = host_prod
```

```
In [ ]: io = VessellogIO(host=host,
                        vessel_name='nexus',
                        datadirectory="/vessellog/vessels"
                    )
```

```
INFO:vessellog_io.vessellogio:Retrieving vessel ID from 'https://vessellog.data.vanoord.com'...
DEBUG:urllib3.connectionpool:Starting new HTTPS connection (1): vessellog.data.vanoord.com:443
DEBUG:urllib3.connectionpool:https://vessellog.data.vanoord.com:443 "GET /api/v1/vessel/search?name=nexus HTTP/1.1" 200 141
INFO:vessellog_io.vessellogio:Found vessel ID: '638684e5-cf5a-41d6-9d88-03da74bd9144'.
INFO:vessellog_io.vessellogio:Set vessel ID: '638684e5-cf5a-41d6-9d88-03da74bd9144'.
```

```
In [ ]: io = VessellogIO(host=host, vessel_name="nexus")
        io.clear_timeseries()
        # io.add_timeseries("trip_nr", "trip_number") # master label
        # io.add_timeseries("speed", "ship_velocity") # master label
        io.add_timeseries(" DP_in:_generator_1_power", "BOT867", vodas=True)
        io.add_timeseries(" DP_in:_generator_2_power", "BOT868", vodas=True)
        io.add_timeseries(" DP_in:_generator_3_power", "BOT869", vodas=True)
        io.add_timeseries(" DP_in:_generator_4_power", "BOT870", vodas=True)
        io.add_timeseries(" DP_in:_generator_5_power", "BOT871", vodas=True)
        io.get_recipe(datetime(2022,9,1), datetime(2022,9,30), resample=1)
```

```

In [ ]: # Calculate the number of rows and columns for subplots
num_rows = 3 # Adjust the number of rows
num_cols = int(np.ceil(len(generators) / num_rows))

fig, axes = plt.subplots(num_rows, num_cols, figsize=(15, 10))

# Flatten the axes array if necessary
if num_rows > 1 and num_cols > 1:
    axes = axes.flatten()

# Create a separate subplot for each generator
for i, (generator, search_string) in enumerate(zip(generators, search_strings)):
    ax = axes[i]

    # Calculate dP/dt and CDF
    deltaT_s = tmp.index.to_series().diff().dt.seconds
    dPdt = tmp[generator].diff() / deltaT_s
    x_fore = np.sort(dPdt)
    cdf = 1. * np.arange(len(dPdt)) / (len(dPdt) - 1)

    # Color code the plot based on generator
    if i == 0:
        ax.plot(x_fore, cdf, label=generator, color='green')
    elif i == 1:
        ax.plot(x_fore, cdf, label=generator, color='navy')
    elif i == 2:
        ax.plot(x_fore, cdf, label=generator, color='orange')
    elif i == 3:
        ax.plot(x_fore, cdf, label=generator, color='purple')
    elif i == 4:
        ax.plot(x_fore, cdf, label=generator, color='red')

    # Calculate percentiles
    percentile5 = np.percentile(x_fore[~np.isnan(x_fore)], 5)
    percentile95 = np.percentile(x_fore[~np.isnan(x_fore)], 95)

    ax.axvline(percentile5, color='r', linestyle='--', label='5th percentile')
    ax.axvline(percentile95, color='b', linestyle='--', label='95th percentile')

    ax.text(percentile5, -0.15, f'{percentile5:.2f}', ha='center', va='top', color='r')
    ax.text(percentile95, -0.15, f'{percentile95:.2f}', ha='center', va='top', color='b')

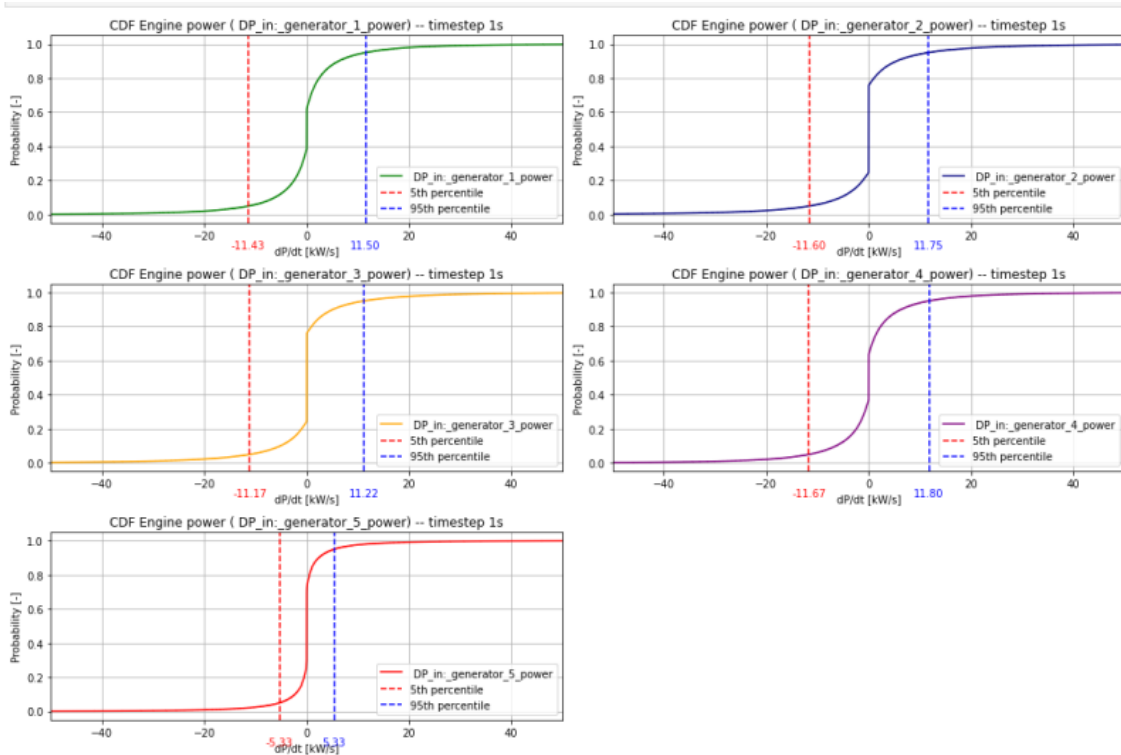
    ax.set_title(f'CDF Engine power ({generator}) -- timestep 1s')
    ax.set_xlabel('dP/dt [kW/s]')
    ax.set_ylabel('Probability [-]')
    ax.legend(loc='lower right')
    ax.grid(True)

    # Set the y-axis limits
    ax.set_xlim(-50, 50)

# Hide unused subplots if any
if len(generators) < len(axes):
    for j in range(len(generators), len(axes)):
        axes[j].axis('off')

plt.tight_layout()
plt.show()

```



```
In [ ]: battery_capacity = 0 # Initialize the battery capacity

for generator in generators:
    deltaT_s = tmp.index.to_series().diff().dt.seconds
    dPdt = tmp[generator].diff() / deltaT_s
    x_fore = np.sort(dPdt)

    # Filter power peaks outside 5th and 95th percentiles
    power_peaks = x_fore[(x_fore < percentile5) | (x_fore > percentile95)]

    # Calculate maximum power peak outside percentiles
    max_power_peak = np.max(np.abs(power_peaks))

    # Update the battery capacity if the current power peak is larger
    battery_capacity = max(battery_capacity, max_power_peak)

print(f"The required battery capacity to cope with loads outside the 5th and 95th percentiles is: {battery_capacity} kWh.")
```

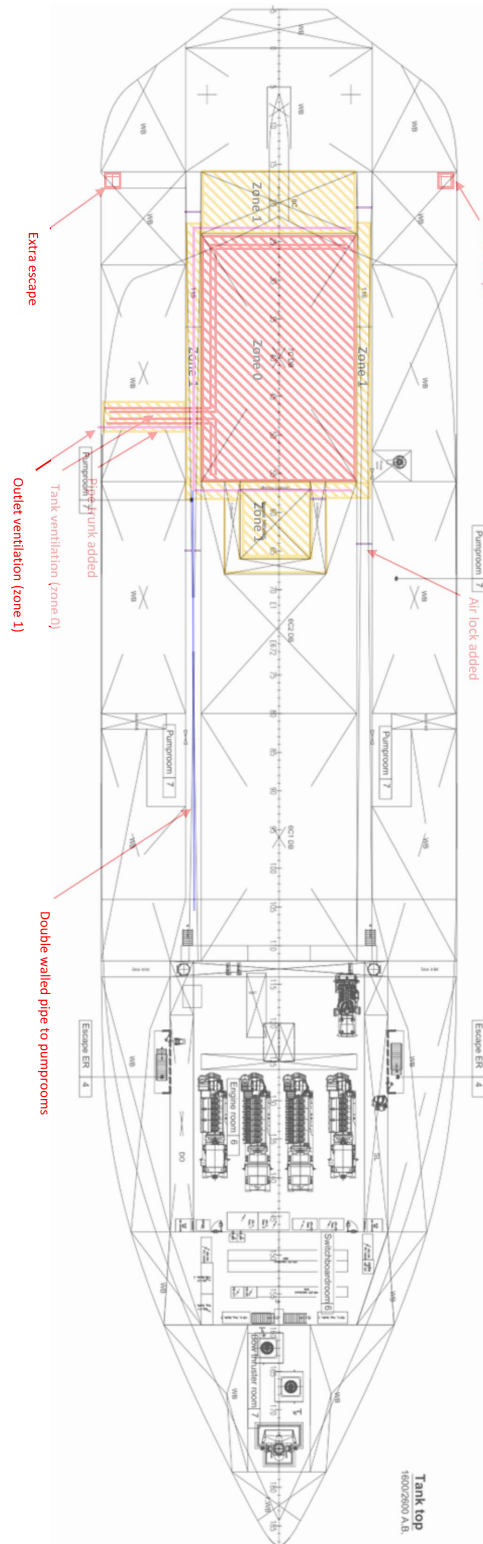
The required battery capacity to cope with loads outside the 5th and 95th percentiles is: 606.0 kWh.



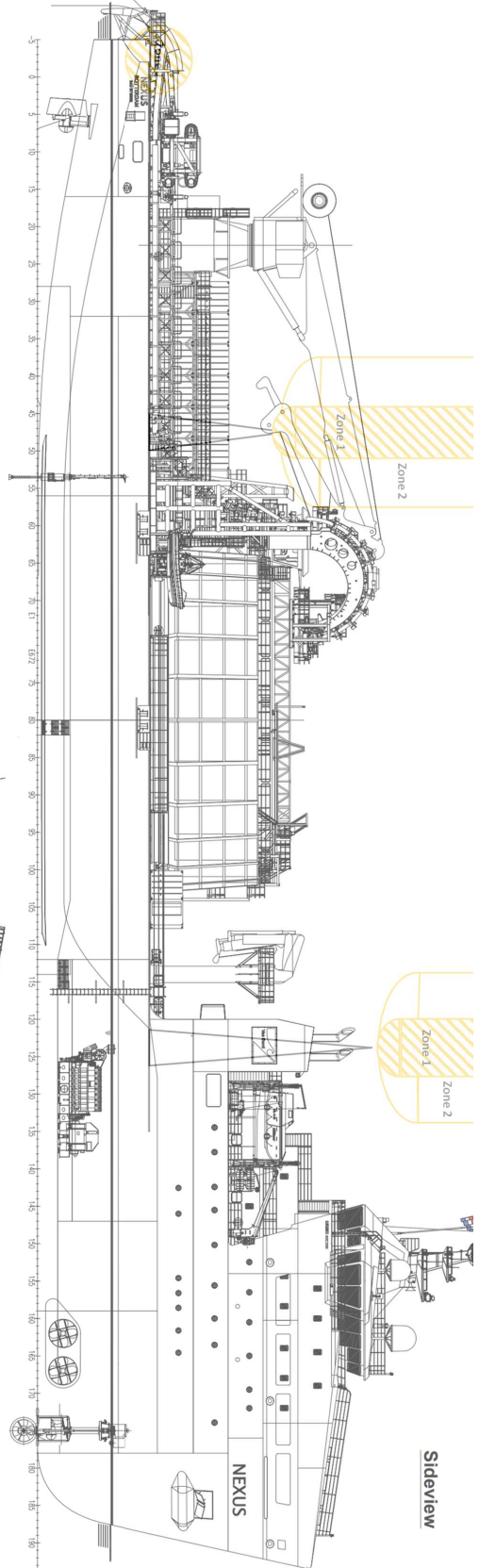
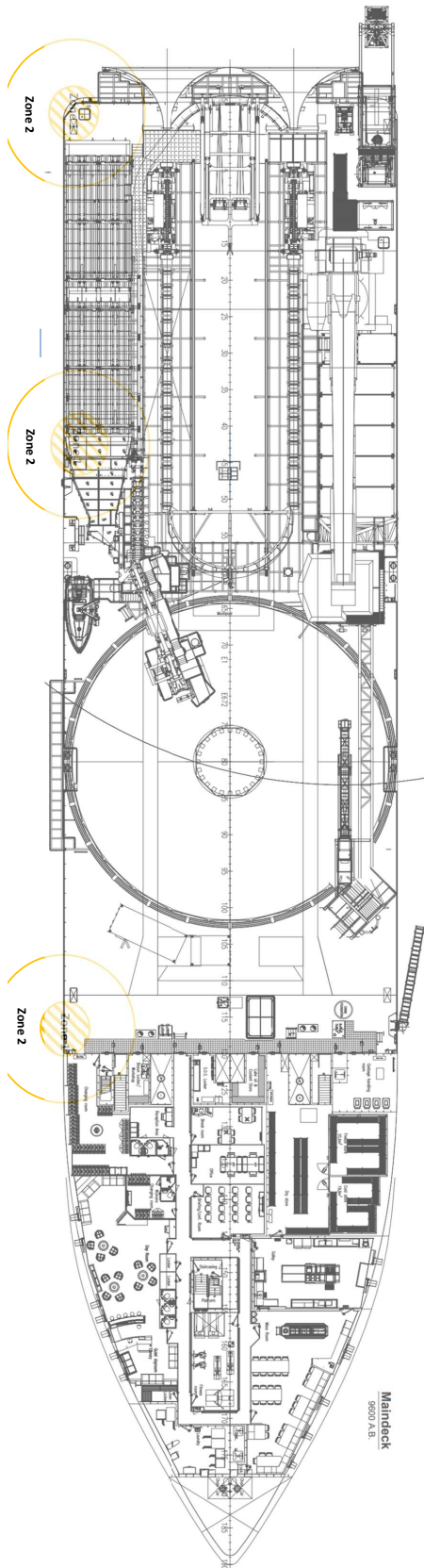
Ballast Tanks

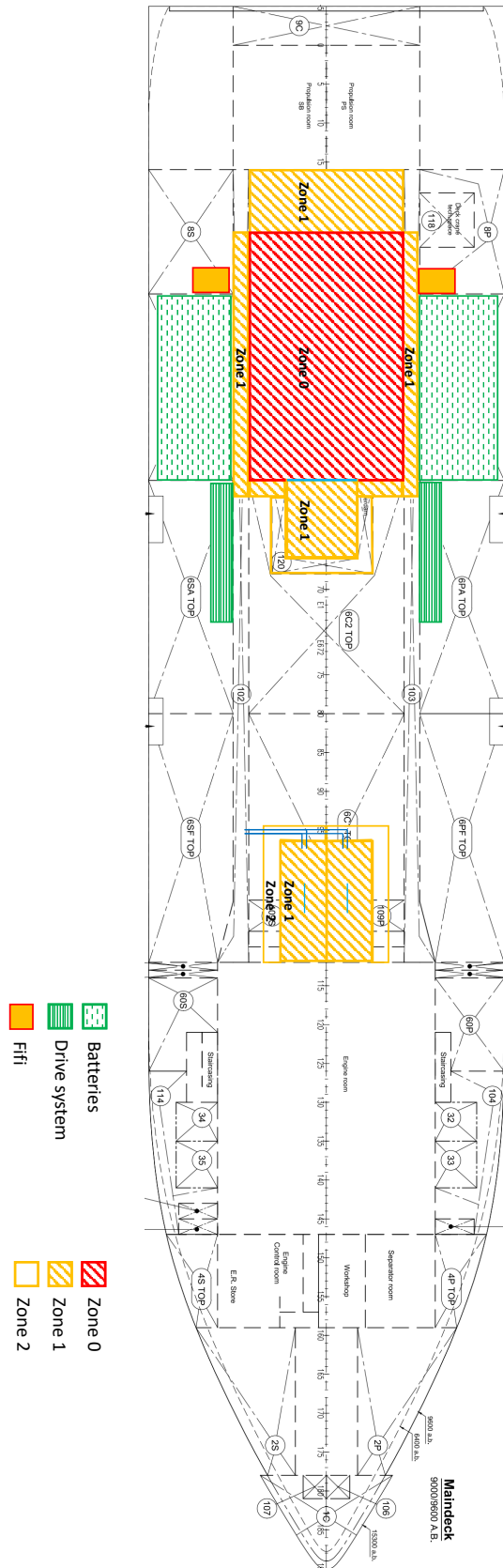
Ballast Tanks - Used/Unused - MOCs for measurement system

CAPACITY OF Water ballast tanks			Fresh Water ballast tanks		
#	Location	Comment	#	Location	Comment
1C	CL WB	Infrequently/Almost never	6PF TOP	PF TOP WB	Have never been used
2P	PS WB	Infrequently/Almost never	6C1 TOP	C1 TOP WB	Have never been used
2S	SB WB	Infrequently/Almost never	6SF TOP	SF TOP WB	Have never been used
4S TOP	SB WB	Infrequently/Almost never	6PA TOP	PA TOP PS	Have never been used
4P TOP	PS TOP WB Tank	Infrequently/Almost never	6C2 TOP	C2 TOP WB	Have never been used
4S DB	SB DB WB Tank	Infrequently/Almost never	6SA TOP	SA TOP SB	Have never been used
5P DB	PS WB	Infrequently/Almost never	7P TOP	PS TOP WB	Have never been used
5S DB	SB DB	Infrequently/Almost never	7C TOP	CL TOP WB	Have never been used
5P MID	PS MID WB	Infrequently/Almost never	7S TOP	SB TOP WB	Have never been used
5S MID	SB MID WB	Infrequently/Almost never	8P	PS WB	Are never used but could be used when you want to take a really heavy load with max stacking height
6PA DB	PA DB WB	Frequently	8C	CL WB	Are never used but could be used when you want to take a really heavy load with max stacking height
6SA DB	SA DB WB	Frequently	8S	SB WB	Have never been used
6C1 DB	C1 DB WB	Frequently	9C	CL WB	Have never been used
6PF DB	PF DB WB	Frequently			
6C2 WB	C2 DB WB	Most Frequently			
6SF DB	SF DB WB	Frequently			
6P MID	PS MID WB	Most Frequently			
6S MID	SB MID WB	Most Frequently			
6 PA MID	PA MID WB	Most Frequently			
6SA MID	SA MID WB	Most Frequently			
6PF MID	PF MID WB	Frequently			
6SF MID	SF MID WB	Most Frequently			
7P DB	PS DB WB	Most Frequently			
7C DB	CL DB WB	Frequently			
7S DB	SB DB WB	Most Frequently			
7P MID	PS MID WB	Fixed ballast			
7S MID	PS MID WB	Most Frequently			
9P	PS WB	Most Frequently			
9S	SB WB	Most Frequently			



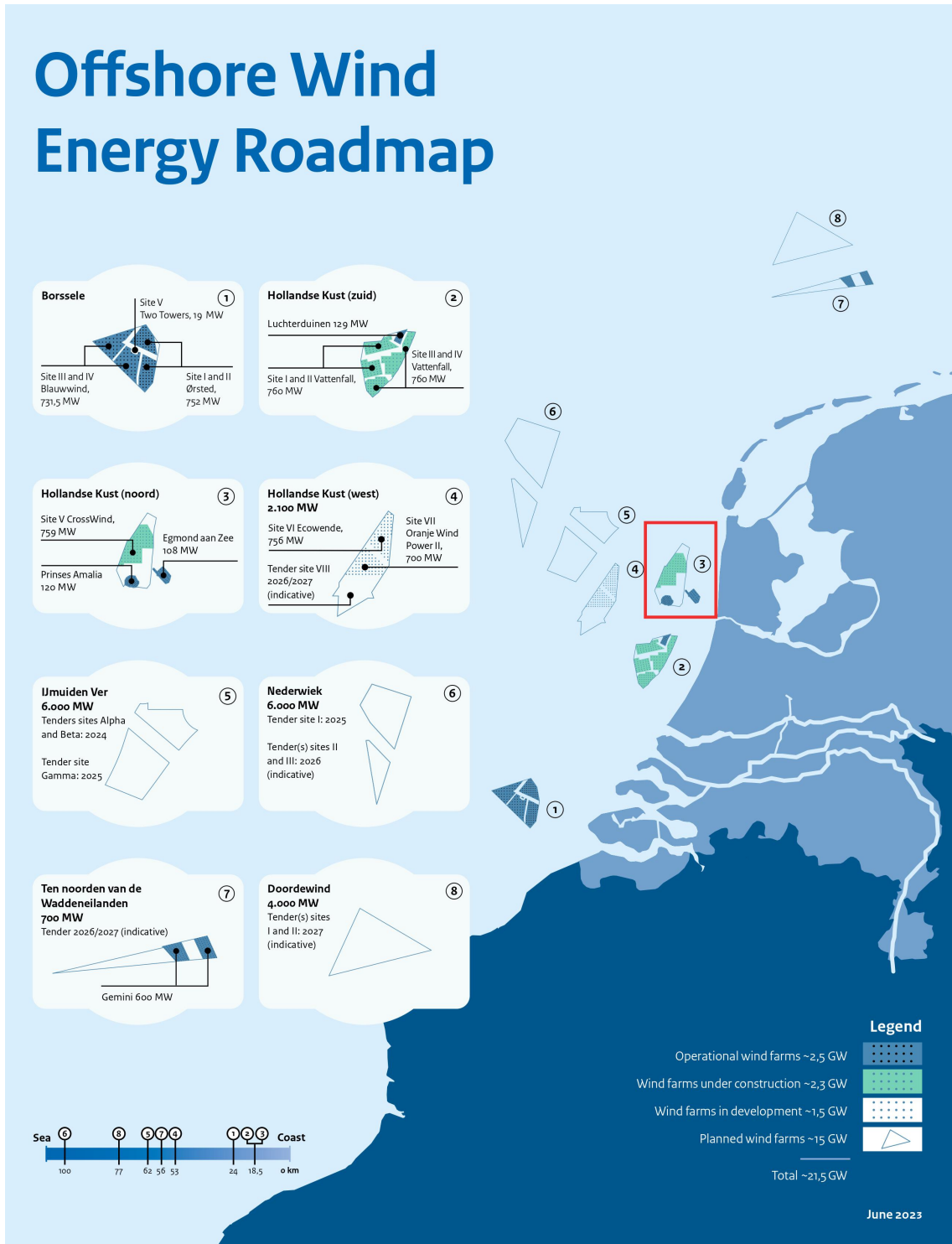
Tank top
1400/2000/140





Roadmap Offshore Wind Energy

Offshore Wind Energy Roadmap



Bunker Prices

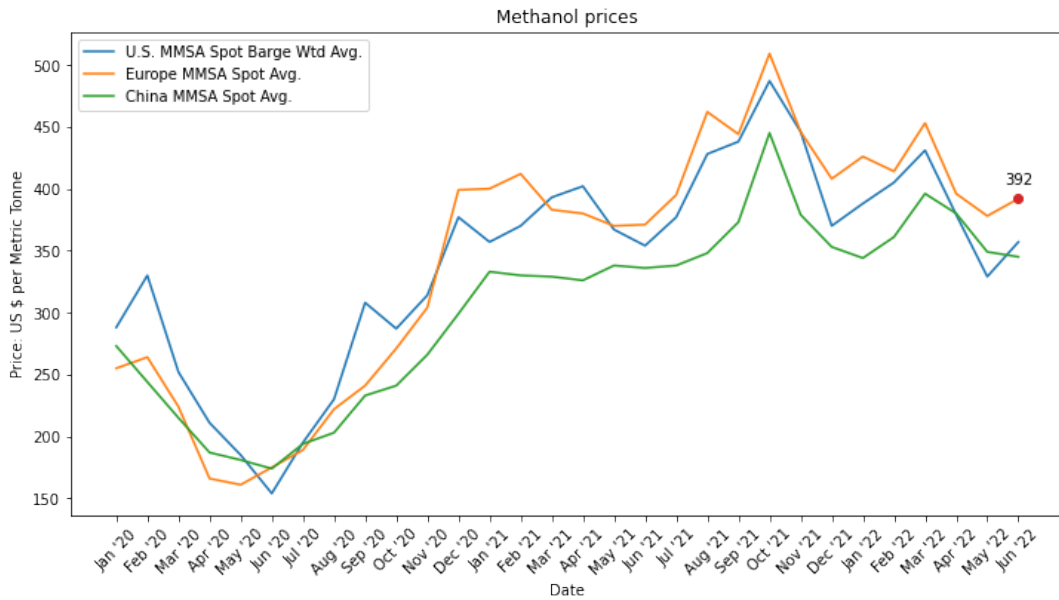


Figure G.1: Methanol prices [59]

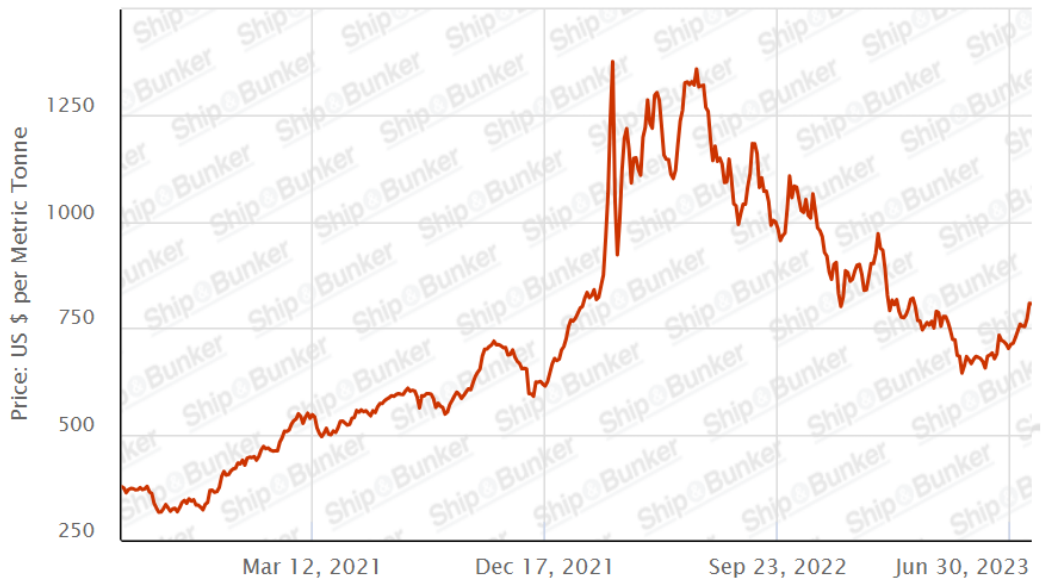


Figure G.2: MGO bunker price [81]

H Projects

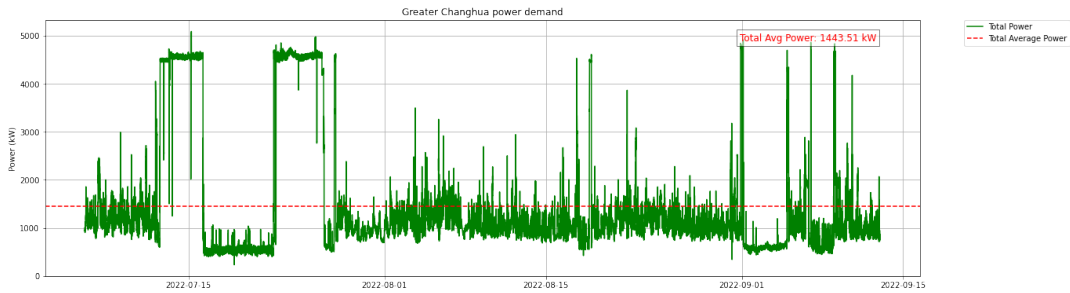


Figure H.1: Greater Changhua Power Demand

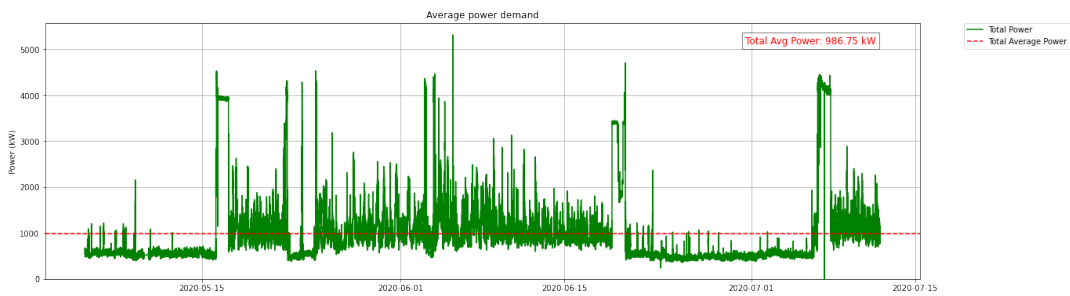


Figure H.2: Brossele 1 Power Demand

Table H.1: Similar projects executed by the NEXUS

Project	Date From	To	Total average power	Average power DG	Unit
Greater Changhua	6-7-2022	13-9-2022	1675	491,12	kW
Brossele 1	25-3-2020	12-7-2020	986,75	499,39	kW

Fuel Consumption

Table I.1: Calculation fuel consumption

Operational profiles	Power	N. of engines		g/kwh		kg/h		Fuel consumption	
		DG 1&4	DG 2&3	DG 1&4	DG 2&3	DG 1&4	DG 2&3	kg/h	g/kwh
DP	353	1	2	254,4	267,0	96,5	110,9	318,4	262,8
Waiting	541	1	1	233,9	245,1	132,1	141,0	273,1	239,5
Transit	1526	1	2	198,1	197,1	315,2	314,1	943,5	197,4
Harbour	638	1	0	225,7	150,0	235,8	156,8	235,8	225,7

DP System Requirements

Subsystems or components	Equipment	Minimum Requirements for each Class Notation		
		DP1	DP2	DP2+ DP3
POWER SYSTEM	Generators and Prime Movers	Non-redundant	Redundant	Redundant, in separate compartments.
	Main switchboard	1 See note (*)	1 with 2 busbars connected by normally closed 1 bus-tie	At least 2 with bus-ties arranged in separate compartments
	Bus-tie breaker	0 See note (*)	1	2 2 kept open, one in each main switchboard
	Distribution system	Non-redundant. See note (*)	Redundant arrangement	Redundant arrangement in separate compartments
THRUSTER SYSTEM	Power management system (PMS)	No	Yes	Yes
	Thrusters	Non-redundant	Redundant arrangement	Redundant arrangement in separate compartments
DP-CONTROL SYSTEM	Single levers for each thruster at main DP control centre	Yes	Yes	Yes
	Number of Control Computers	1	2	2
	Joystick with automatic heading	Required See note (**)	Required	Required
	Manual Thruster Control	Yes	Yes	Yes
REFERENCE SYSTEM	Position Reference system	2	3	3
	HMI for position reference systems required outside DP control system operator station(s)	No	No	Yes
	VRS/MRU	1	2	3
	Wind sensor	1	2	2
UPS UNIT	Gyro	1	3	3
	Printer	1	2	2 + 1 in backup control station
	Backup Control Station for Backup Unit	Yes	Yes	Yes
Loop monitoring emergency stop loop	N/A	N/A	N/A	Yes
Steering gear – additional monitoring requirements	No	No	Yes	No
Consequence Analyzer	No	Yes	Yes	Yes
FMEA	No	Yes	Yes	Yes

(*) According to Rules for Classification and Construction of the Sea-Going Ships, Part VIII. (**) Where provided failure of the joystick is to bring the system in a safe situation.

Figure J.1: Summary of DP System requirements [71].

Bibliography

- [1] . *LNG Fuel Tank Application* — *faparts.net*. <http://faparts.net/p/lng-fuel-tank-application-35653.html#>. [Accessed 05-Jul-2023].
- [2] 1. *Corvus Orca Energy - Corvus Energy* — *corvusenergy.com*. <https://corvusenergy.com/products/energy-storage-solutions/corvus-orca-energy/>. [Accessed 27-Jun-2023].
- [3] ABS ABS. *Sustainability methanol as marine fuel*. URL: <https://safety4sea.com/wp-content/uploads/2021/02/Sustainability-Methanol-as-Marine-Fuel.pdf>.
- [4] International Renewable Energy Agency. “Renewable Energy Technologies Cost Analysis Series: Biomass for Power Generation and CHP”. In: (2013). URL: https://www.irena.org/-/media/Files/IRENA/Agency/Publication/2013/RE_Technologies_Cost_Analysis-BIOMASS_Power_Generation.pdf.
- [5] *An energy carrier is a substance or phenomenon that stores and transports energy, like fuels, batteries, or fluids. They're crucial for efficient energy systems*. Online. 2023. URL: https://en.wikipedia.org/wiki/Energy_carrier.
- [6] Torstein I. B□, Anna Swider, and Eilif Pedersen. “Investigation of drivetrain losses of a DP vessel”. In: (2017), pp. 508–513. DOI: 10.1109/ESTS.2017.8069329.
- [7] Kiho Bae et al. “Recent advances in electrolyte materials for solid oxide fuel cells”. In: *Journal of Power Sources* 419 (2019), pp. 70–83.
- [8] Paul Balcombe et al. “Methanol as a marine fuel: Prospects and challenges”. In: *Applied Energy* 235 (2019), pp. 186–200. DOI: 10.1016/j.apenergy.2018.11.038.
- [9] Francesco Baldi and Andrea Coraddu. “Towards halving shipping GHG emissions by 2050: The imo introduces the CII and the EEXI”. In: *Sustainable Energy Systems on Ships (2022)*, pp. 513–517. DOI: 10.1016/b978-0-12-824471-5.00028-1.
- [10] Francesco Baldi et al. “The role of solid oxide fuel cells in future ship energy systems”. In: *Energy* 194 (Mar. 2020), p. 116811. DOI: 10.1016/j.energy.2019.116811.
- [11] L. Barelli, Gianni Bidini, and Andrea Ottaviano. “Solid oxide fuel cell modelling: Electrochemical performance and thermal management during load-following operation”. In: *Energy* 115 (Nov. 2016), pp. 107–119. DOI: 10.1016/j.energy.2016.08.107.
- [12] Lindert van Biert, Kamil Mrozewski, and Pieter 't Hart. *Public final report: Inventory of the application of Fuel Cells in the MARitime sector*. MIIP 007 - 2020 MIIP 007 - 2020. Maritime Knowledge Centre, TNO and TU Delft, Feb. 2021. URL: <https://www.koersenvaart.nl/files/MIIP%5C%20007-2020%5C%20FCMAR%5C%2003022021.pdf>.
- [13] Bloom Energy, Inc. *The Bloom Energy Server 5.5*. <https://www.bloomenergy.com/>. Data Sheet. Bloom Energy, Inc., 2023.
- [14] Roberto Bove, Pierluigi Leone, and Lidia Pino. “Materials and components for solid oxide fuel cells: A review”. In: *Journal of Power Sources* 356 (2017), pp. 205–233.
- [15] Selma Brynolf, Erik Fridell, and Karin Andersson. “Environmental assessment of marine fuels: liquefied natural gas, liquefied biogas, methanol and bio-methanol”. In: *Journal of Cleaner Production* 74 (2014), pp. 86–95. ISSN: 0959-6526. DOI: <https://doi.org/10.1016/j.jclepro.2014.03.052>. URL: <https://www.sciencedirect.com/science/article/pii/S0959652614002832>.
- [16] Annamaria Buonomano et al. “Hybrid solid oxide fuel cells–gas turbine systems for combined heat and power: A review”. In: *Applied Energy* 156.C (2015), pp. 32–85. DOI: 10.1016/j.apenergy.2015.0. URL: <https://ideas.repec.org/a/eee/appene/v156y2015icp32-85.html>.
- [17] Xiaonong Cheng et al. “Development of cathode materials for solid oxide fuel cells: A review”. In: *Journal of Power Sources* 439 (2019), p. 227032.

- [18] F. Curletti et al. "Large size biogas-fed Solid Oxide Fuel Cell power plants with carbon dioxide management: Technical and economic optimization". In: *Journal of Power Sources* 294 (2015), pp. 669–690. ISSN: 0378-7753. DOI: <https://doi.org/10.1016/j.jpowsour.2015.06.091>. URL: <https://www.sciencedirect.com/science/article/pii/S0378775315011258>.
- [19] Flavio D.F. Chuahy and Sage L. Kokjohn. "Solid oxide fuel cell and advanced combustion engine combined cycle: A pathway to 70% electrical efficiency". In: *Applied Energy* 235 (2019), pp. 391–408. ISSN: 0306-2619. DOI: <https://doi.org/10.1016/j.apenergy.2018.10.132>. URL: <https://www.sciencedirect.com/science/article/pii/S030626191831701X>.
- [20] Thorin Daniel et al. "Techno-economic Analysis of Direct Air Carbon Capture with CO₂ Utilisation". In: *Carbon Capture Science & Technology* 2 (2022), p. 100025. ISSN: 2772-6568. DOI: <https://doi.org/10.1016/j.ccst.2021.100025>. URL: <https://www.sciencedirect.com/science/article/pii/S2772656821000257>.
- [21] Andrew L Dicks and David A J Rand. *Fuel cell systems explained*. en. 3rd ed. Nashville, TN: John Wiley & Sons, Apr. 2018.
- [22] DNV. *The EU agrees on well-to-wake GHG limits to energy used on board ships from 2025*. https://www.dnv.com/news/the-eu-agrees-on-well-to-wake-ghg-limits-to-energy-used-on-board-ships-from-2025-243501?utm_campaign=MA_23Q2_GLOB_PROM_TRN%20on%20FuelEU%20to%20DCS%20Sales%20Campaign%20members&utm_medium=email&utm_source=Eloqua. Accessed: May 23, 2023. 2023.
- [23] *DNV Rules for Ships - July 2022 edition* — *dnv.com*. <https://www.dnv.com/news/dnv-rules-for-ships-july-2022-edition-227477>. [Accessed 05-Jul-2023].
- [24] Ahmed G. Elkafas et al. "Fuel Cell Systems for Maritime: A Review of Research Development, Commercial Products, Applications, and Perspectives". In: *Processes* 11.1 (Dec. 2022), p. 97. ISSN: 2227-9717. DOI: 10.3390/pr11010097. URL: <http://dx.doi.org/10.3390/pr11010097>.
- [25] *EMSA study on the use of fuel cells in shipping*. 2018. URL: <https://www.emsa.europa.eu/publications/item/2921-emsa-study-on-the-use-of-fuel-cells-in-shipping.html>.
- [26] Jasper Faber et al. "Fourth IMO GHG Study". In: *London, UK* (2020).
- [27] J Fleig. "Solid oxide fuel cell cathodes: Polarization mechanisms and modeling". In: *Chemical reviews* 107.10 (2007), pp. 3806–3806.
- [28] FuelCell Energy Solutions GmbH. *DFC250EU Product Sheet*. Online. Date Accessed. URL: https://www.energy-saxony.net/fileadmin/Inhalte/Downloads/Pressemitteilungen/Pressefaecher/FCES/alt/FuelCell_product_sheet_DFC250EU_en.pdf.
- [29] Christoph Gentner. "Einbindung von Brennstoffzellenanlagen in schiffstechnische Systeme". doctoralThesis. Technische Universität Hamburg, 2018. DOI: 10.15480/882.1712. URL: <http://tubdok.tub.tuhh.de/handle/11420/1715>.
- [30] Hossein Ghezal-Ayagh. *Progress in SOFC Technology Development at FuelCell Energy*. Presented at the 2021 SOFC Project Review Meeting on November 16, 2021. 2021. URL: https://netl.doe.gov/sites/default/files/netl-file/21SOFC_Ghezal-Ayagh16.pdf.
- [31] Hossein Ghezal-Ayagh. "Progress in SOFC Technology Development at FuelCell Energy". In: *SOFC Project Review Meeting*. Nov. 2021.
- [32] DNV GL. *Maritime Forecast to 2050*. <https://www.dnvgl.com/maritime/publications/maritime-forecast-to-2050-141266>. 2019.
- [33] Maria Grahn et al. "Review of electrofuel feasibility—cost and environmental impact". In: *Progress in Energy* 4.3 (June 2022), p. 032010. DOI: 10.1088/2516-1083/ac7937. URL: <https://dx.doi.org/10.1088/2516-1083/ac7937>.

- [34] Turgut M. Gür. “Comprehensive review of methane conversion in solid oxide fuel cells: Prospects for efficient electricity generation from natural gas”. In: *Progress in Energy and Combustion Science* 54 (2016), pp. 1–64. ISSN: 0360-1285. DOI: 10.1016/j.pecs.2015.10.004. URL: <https://www.sciencedirect.com/science/article/pii/S0360128515300496>.
- [35] HAMBURGISCHE SCHIFFBAU-VERSUCHSANSTALT GMBH. *HOLISHIP Project*. <https://cordis.europa.eu/project/id/689074>. Grant agreement ID: 689074. Brussels: European Union, Dec. 2020. DOI: 10.3030/689074.
- [36] A.D. Hawkes, D.J.L. Brett, and N.P. Brandon. “Fuel cell micro-CHP techno-economics: Part 2 – Model application to consider the economic and environmental impact of stack degradation”. In: *International Journal of Hydrogen Energy* 34.23 (2009), pp. 9558–9569. ISSN: 0360-3199. DOI: 10.1016/j.ijhydene.2009.09.095. URL: <https://www.sciencedirect.com/science/article/pii/S0360319909015353>.
- [37] Hans Otto Heiberg. “The merchant fleet: a facilitator of world trade”. In: *The Global Enabling Trade Report 2012* (2012), pp. 85–90.
- [38] Luc Henderik. “Solid Oxide Fuel Cell Propulsion System Fueled by Ammonia: Subjected to a vessel from the Watertaxi Rotterdam Company”. Embargoed until 2020-03-26. Master’s thesis. Delft University of Technology, Mar. 2020. URL: <http://resolver.tudelft.nl/uuid:42e5cf5d-454e-4e4f-a041-8419f9145597>.
- [39] Mohamed S. E. Houache et al. “On the Current and Future Outlook of Battery Chemistries for Electric Vehicles—Mini Review”. In: *Batteries* 8.7 (2022). ISSN: 2313-0105. DOI: 10.3390/batteries8070070. URL: <https://www.mdpi.com/2313-0105/8/7/70>.
- [40] Koen Houtkoop. “Nuclear reactors for marine propulsion and power generation systems”. Master’s thesis. Delft, Netherlands: Delft University of Technology, July 6, 2022.
- [41] Wei-Dong Huang and Y-H Percival Zhang. “Energy Efficiency Analysis: Biomass-to-Wheel Efficiency Related with Biofuels Production, Fuel Distribution, and Powertrain Systems”. In: *PLoS ONE* 6.7 (July 2011). Ed. by Valdur Saks, e22113. DOI: 10.1371/journal.pone.0022113. URL: <https://doi.org/10.1371/journal.pone.0022113>.
- [42] Weidong Huang and Yi-Heng P. Zhang. “Energy Efficiency Analysis: Biomass-to-Wheel Efficiency Related with Biofuels Production, Fuel Distribution, and Powertrain Systems”. In: *PloS one* 6 (July 2011), e22113. DOI: 10.1371/journal.pone.0022113.
- [43] Zhenyu Huang et al. “Transient response of performance in a proton exchange membrane fuel cell under dynamic loading”. In: *Energy Conversion and Management* 226 (2020), p. 113492. ISSN: 0196-8904. DOI: <https://doi.org/10.1016/j.enconman.2020.113492>. URL: <https://www.sciencedirect.com/science/article/pii/S0196890420310244>.
- [44] J.P.P Huijsmans et al. “An analysis of endurance issues for MCFC”. In: *Journal of Power Sources* 86.1-2 (2000), pp. 117–121. ISSN: 0378-7753. DOI: 10.1016/S0378-7753(99)00448-6. URL: <https://www.sciencedirect.com/science/article/pii/S0378775399004486>.
- [45] Iea. *Offshore wind outlook 2019 – analysis*. URL: <https://www.iea.org/reports/offshore-wind-outlook-2019>.
- [46] IMarEST. *Design of propulsion and electric power generation systems*. Witherby Seamanship International, Nov. 2019.
- [47] Methanol Institute. *Methanol: A Cost-Effective and Sustainable Marine Fuel*. <https://www.methanol.org/wp-content/uploads/2020/01/Methanol-Institute-Marine-Fuel-Brochure.pdf>. 2020.
- [48] Intergovernmental Panel on Climate Change (IPCC). *IPCC AR6 WG1 Chapter 7: Clouds and Aerosols*. 2021. URL: https://www.ipcc.ch/report/ar6/wg1/downloads/report/IPCC_AR6_WGI_Chapter_07.pdf (visited on 05/26/2023).
- [49] Tae-Woo Kim et al. “A Study and Design on Tank Container for Fuel Tank of LNG Fueled Ship”. In: *Journal of the Society of Naval Architects of Korea* 49 (Dec. 2012), pp. 504–511. DOI: 10.3744/SNAK.2012.49.6.504.

- [50] A.D. Korberg et al. "Techno-economic assessment of advanced fuels and propulsion systems in future fossil-free ships". In: *Renewable and Sustainable Energy Reviews* 142 (2021), p. 110861. ISSN: 1364-0321. DOI: <https://doi.org/10.1016/j.rser.2021.110861>. URL: <https://www.sciencedirect.com/science/article/pii/S1364032121001556>.
- [51] K.J. van Kranenburg-Bruinsma et al. *E-fuels - Towards a more sustainable future for truck transport, shipping and aviation*. <http://resolver.tudelft.nl/uuid:487a6a47-853d-4a1d-bc2e-dbe21d584cca>. other. Whitepaper. 2020.
- [52] Benjamin Lagemann et al. "Optimal ship lifetime fuel and power system selection". In: *Transportation Research Part D: Transport and Environment* 102 (Jan. 2022), p. 103145. DOI: 10.1016/j.trd.2021.103145.
- [53] N. Laosiripojana and S. Assabumrungrat. "Catalytic steam reforming of methane, methanol, and ethanol over Ni/YSZ: The possible use of these fuels in internal reforming SOFC". In: *Journal of Power Sources* 163.2 (2007), pp. 943–951. ISSN: 0378-7753. DOI: 10.1016/j.jpowsour.2006.10.006. URL: <https://www.sciencedirect.com/science/article/pii/S0378775306020581>.
- [54] Sven Los. "Concept design and feasibility study of an entirely battery powered naval submarine". [Online; accessed 27-June-2023]. MA thesis. Delft University of Technology, June 2017. URL: <https://repository.tudelft.nl/islandora/object/uuid:e51fa470-8742-4d90-9c41-fb2f8781cf79?collection=education>.
- [55] Andrew Lutz, Richard Larson, and Jay Keller. "Thermodynamic comparison of fuel cells to the Carnot cycle". In: *International Journal of Hydrogen Energy - INT J HYDROGEN ENERG* 27 (Oct. 2002), pp. 1103–1111. DOI: 10.1016/S0360-3199(02)00016-2.
- [56] MakMed. *M25C Propulsion*. Online. 2013. URL: <https://www.makmed.fr/moteurs/moteurs-mak/m-25-c-propulsion/>.
- [57] Vasileios A. Mamatsopoulos, Constantine Michailides, and Efstathios E. Theotokoglou. "An Analysis Tool for the Installation of Submarine Cables in an S-Lay Configuration Including "In and Out of Water" Cable Segments". In: *Journal of Marine Science and Engineering* 8.1 (2020). ISSN: 2077-1312. DOI: 10.3390/jmse8010048. URL: <https://www.mdpi.com/2077-1312/8/1/48>.
- [58] Charles J. McKinlay, Stephen R. Turnock, and Dominic A. Hudson. "Route to zero emission shipping: Hydrogen, ammonia or methanol?" In: *International Journal of Hydrogen Energy* 46.55 (2021), pp. 28282–28297. ISSN: 0360-3199. DOI: <https://doi.org/10.1016/j.ijhydene.2021.06.066>. URL: <https://www.sciencedirect.com/science/article/pii/S0360319921022175>.
- [59] Methanol Institute. *Monthly Methanol Spot Prices Worldwide from January 2020 to June 2022, by Region (in U.S. Dollars per Metric Ton)*. Statista. Accessed: July 27, 2023. 2022. URL: <https://www.statista.com/statistics/1323381/monthly-methanol-spot-prices-worldwide-by-region/>.
- [60] *Molten Carbonate Fuel Cells (MCFCs) - University of Babylon*. https://www.uobabylon.edu.iq/eprints/publication_12_2448_736.pdf. Accessed: 2023-02-09.
- [61] John Newman et al. "Review: An Economic Perspective on Liquid Solar Fuels". In: *Journal of The Electrochemical Society* 159.10 (Aug. 2012), A1722. DOI: 10.1149/2.046210jes. URL: <https://dx.doi.org/10.1149/2.046210jes>.
- [62] Xiaofei Niu et al. "Effect of pressure on performance of solid oxide fuel cell". In: *Journal of Power Sources* 398 (2018), pp. 185–191.
- [63] Xiaofei Niu et al. "Performance enhancement of anode-supported solid oxide fuel cell by infiltration of Sm_{0.2}Ce_{0.8}O_{1.9} electrolyte". In: *International Journal of Hydrogen Energy* 42.41 (2017), pp. 25904–25911.
- [64] *NR670 methanol ethanol fuelled ships — marine-offshore.bureauveritas.com*. <https://marine-offshore.bureauveritas.com/nr670-methanol-ethanol-fuelled-ships>. [Accessed 05-Jul-2023].

- [65] Van Oord. *Bereiken van Netto-nul-uitstoot: Van Oord/*. URL: <https://www.vanoord.com/nl/bereiken-van-netto-nul-uitstoot>.
- [66] International Maritime Organization. *Guidelines for vessels with dynamic positioning systems*. Technical report MSC/circ.645. 1994.
- [67] International Maritime Organization. *Initial GHG Strategy*. <https://www.imo.org/en/MediaCentre/HotTopics/Pages/Initial-GHG-strategy.aspx>. 2018.
- [68] Mehmet F. Orhan and Yuda Yurum. "Materials for solid oxide fuel cells: A review". In: *International Journal of Hydrogen Energy* 42.35 (2017), pp. 22323–22359.
- [69] Sung Park, Young Lee, and Kook Ahn. "Performance analysis of an SOFC/HCCI engine hybrid system: System simulation and thermo-economic comparison". In: *International Journal of Hydrogen Energy* 39 (Jan. 2014), pp. 1799–1810. DOI: 10.1016/j.ijhydene.2013.10.171.
- [70] Richard Payne, Jonathan Love, and Michael Kah. "Generating electricity at 60% electrical efficiency from 1 - 2 KWE SOFC products". In: *ECS Transactions* 25.2 (2009), pp. 231–239. DOI: 10.1149/1.3205530.
- [71] *Polski Rejestr Statków S.A.* <https://www.prs.pl/uploads/p120pen.pdf>. Centrala / Head Office: al. Józefa Hallera 126, 80-416 Gdańsk, Poland.
- [72] *Products - Convion — convion.fi*. <https://convion.fi/products/>. [Accessed 19-Jun-2023].
- [73] CM Rangel et al. "Fuel starvation: Irreversible degradation mechanisms in PEM fuel cells". In: *18th World Hydrogen Energy Conference 2010-WHEC 2010*. Forschungszentrum Jülich GmbH, Zentralbibliothek, Verlag. 2010, pp. 143–152.
- [74] Lloyd's Register and UMAS. *Zero emission marine fuels: Lifecycle GHG emissions study*. https://www.umas.amsterdam/wp-content/uploads/2019/11/Zero-Emission-Marine-Fuels-Lifecycle-GHG-Emissions-Study_LR_UMAS_FINAL.pdf. 2019.
- [75] Jeroen Reurings. "A modeling study to investigate performance of SOFC-ice hybrid systems for Marine Applications". Jan. 1970. URL: <http://resolver.tudelft.nl/uuid:7ff207b4-e7a8-4104-896a-91b27ceff34d>.
- [76] Harsh Sapra et al. "Integration of solid oxide fuel cell and internal combustion engine for maritime applications". English. In: *Applied Energy* 281 (2021). ISSN: 0306-2619. DOI: 10.1016/j.apenergy.2020.115854.
- [77] B.V. Sasank, N. Rajalakshmi, and K.S. Dhathathreyan. "Performance analysis of polymer electrolyte membrane (PEM) fuel cell stack operated under marine environmental conditions". In: *Journal of Marine Science and Technology* 21.3 (2016), pp. 471–478. DOI: 10.1007/s00773-016-0369-y.
- [78] Norazlianie Sazali et al. "New Perspectives on Fuel Cell Technology: A Brief Review". In: *Membranes* 10.5 (2020). ISSN: 2077-0375. DOI: 10.3390/membranes10050099. URL: <https://www.mdpi.com/2077-0375/10/5/99>.
- [79] Yangbin Shen et al. "Effect of the air electrode structure on the performance of a solid oxide fuel cell". In: *International Journal of Hydrogen Energy* 41.41 (2016), pp. 18680–18689.
- [80] Hiroyuki Shimada et al. "Effects of cathode microstructure on electrolyte/cathode interface of solid oxide fuel cell". In: *Solid State Ionics* 307 (2017), pp. 1–6.
- [81] Ship Bunker. *Rotterdam MGO Price*. Accessed: 27-7-2023. 2023. URL: <https://shipandbunker.com/prices/emea/nwe/nl-rtm-rotterdam#MGO>.
- [82] S.C Singhal. "Advances in solid oxide fuel cell technology". In: *Solid State Ionics* 135.1-4 (2000), pp. 305–313. ISSN: 0167-2738. DOI: 10.1016/S0167-2738(00)00452-5. URL: <https://www.sciencedirect.com/science/article/pii/S0167273800004525>.
- [83] Pontus Svens et al. "Evaluating Performance and Cycle Life Improvements in the Latest Generations of Prismatic Lithium-Ion Batteries". In: *IEEE Transactions on Transportation Electrification* 8 (Sept. 2022), pp. 1–1. DOI: 10.1109/TTE.2022.3158838.

- [84] SWZ|Maritime. *The AmmoniaDrive project explained: ammonia as a marine fuel done right*. Sept. 2022. URL: <https://swzmaritime.nl/news/2022/09/15/the-ammoniadrive-project-explained-ammonia-as-a-marine-fuel-done-right/> (visited on 10/11/2022).
- [85] Maria Taljegard et al. "Cost-effective choices of marine fuels in a carbon-constrained world: results from a global energy model". In: (). Department of Energy and Environment, Physical Resource Theory, and Department of Shipping and Marine Technology.
- [86] TNO. *Green Maritime Methanol. WP 5 - System Design for Short Sea Shipping*. report. 2021. URL: <http://resolver.tudelft.nl/uuid:b4ac3f8d-a06b-4dcc-b6a8-b23464d85f2b>.
- [87] American Journal of Transportation. "Transportation Costs for Alternative Fuels". In: (2018). URL: <https://www.ajot.com/whitepapers/download/transportation-costs-for-alternative-fuels>.
- [88] Hengyong Tu and Ulrich Stimming. "Advances, aging mechanisms and lifetime in solid-oxide fuel cells". In: *Journal of Power Sources* 127 (2004), pp. 284–293. DOI: 10.1016/j.jpowsour.2003.09.025.
- [89] Battery University. *BU-808: How to Prolong Lithium-based Batteries*. [Online; accessed 27-June-2023]. 2023. URL: <https://batteryuniversity.com/article/bu-808-how-to-prolong-lithium-based-batteries>.
- [90] L. Van Biert et al. "A review of fuel cell systems for maritime applications". In: *Journal of Power Sources* 327 (2016), pp. 345–364. ISSN: 0378-7753. DOI: 10.1016/j.jpowsour.2016.07.007. URL: <https://www.sciencedirect.com/science/article/pii/S0378775316308631>.
- [91] L. van Biert et al. "A thermodynamic comparison of solid oxide fuel cell-combined cycles". In: *Journal of Power Sources* 397 (2018), pp. 382–396. ISSN: 0378-7753. DOI: <https://doi.org/10.1016/j.jpowsour.2018.07.035>. URL: <https://www.sciencedirect.com/science/article/pii/S0378775318307432>.
- [92] Martijn Van Den Broek et al. *Ammonia as a fuel for internal combustion engines: Technical report*. Tech. rep. TNO Energy Transition, 2017. URL: <https://repository.tno.nl/islandora/object/uuid:7bccc026-6f42-4948-91b8-cd585f58d21c>.
- [93] Van Oord. *Equipment Leaflet: Cable-laying Vessel Nexus*. <https://www.vanoord.com/drupal/media//data/default/202012/Printed%20matters%20-%20Equipment%20leaflet%20-%20Cable-laying%20vessel%20-%20Nexus%20-%20LR%20-%20Clean.PDF>. December 2020.
- [94] Van Oord. *Inkoop - Afdeling SMD*. Internal Department Information. Company: Van Oord. Year of Publication.
- [95] Wolf Vielstich, Harumi Yokokawa, and Hubert A. Gasteiger. *Handbook of Fuel Cells: Advances in electrocatalysis, materials, diagnostics and durability: Volumes 5 & 6*. Wiley, 2009.
- [96] Shailesh D. Vora. "Overview of SOFC Program at DOE NETL". In: *Proceedings of the Conference/Event Name*. Technology Manager, Fuel Cells. Department of Energy's National Energy Technology Laboratory (DOE NETL). Location, Nov. 2021.
- [97] Eric D. Wachsman and Kang Taek Lee. "Lowering the Temperature of Solid Oxide Fuel Cells". In: *Science* 334.6058 (2011), pp. 935–939. DOI: 10.1126/science.1204090. eprint: <https://www.science.org/doi/pdf/10.1126/science.1204090>. URL: <https://www.science.org/doi/abs/10.1126/science.1204090>.
- [98] Bo Wang, Fanglin Chen, and Xiaofang Chen. "Materials and Technologies for Solid Oxide Fuel Cell Anode: A Review". In: *Materials* 13.3 (2020), p. 740.
- [99] Chad Wocken. "COAL SYNGAS CLEANUP FOR COMMERCIALY VIABLE SOFC PERFORMANCE". In: *Proceedings of the 22nd Annual Solid Oxide Fuel Cell Project Review Meeting*. Assistant Director, Clean Energy Solutions. Energy & Environmental Research Center (EERC). Location, Nov. 2021.
- [100] Xiaojuan Wu and Danhui Gao. "Fault tolerance control of SOFC systems based on nonlinear model predictive control". English. In: *International Journal of Hydrogen Energy* 42.4 (2017), pp. 2288–2308. DOI: 10.1016/j.ijhydene.2016.09.203.

- [101] Ming Xu et al. "Performance test of a 5 kW solid oxide fuel cell system under high fuel utilization with industrial fuel gas feeding". In: *International Journal of Coal Science & Technology* 8.3 (May 2021), pp. 394–400. DOI: 10.1007/s40789-021-00428-2. URL: <https://doi.org/10.1007/s40789-021-00428-2>.
- [102] Hiroyuki Yoshida et al. "Role of material and transport properties in the performance of solid oxide fuel cells: A review". In: *Journal of Power Sources* 397 (2018), pp. 103–118.
- [103] C. Zamfirescu and I. Dincer. "Using ammonia as a sustainable fuel". In: *Journal of Power Sources* 185.1 (Oct. 2008), pp. 459–465. DOI: 10.1016/j.jpowsour.2008.02.097. URL: <https://doi.org/10.1016/j.jpowsour.2008.02.097>.
- [104] Nikolas Zanetich. "Solid Oxide Fuel Cell Hybrid Systems as a Distributed Cogeneration Solution". ENG4111 and 4112 Research Project. Bachelor's Thesis. Toowoomba, Queensland, Australia: University of Southern Queensland, Oct. 2020.